

Abstract

Synthesis and Reactivity of Organometallic and Coordination Complexes of Mg and Ni

Louise M. Guard
2015

The first three chapters of this thesis summarize the synthesis and reactivity of a series of Mg complexes supported by both *meridinally* and *facially* binding neutral nitrogen based ligands. Chapter 1 is a review of Grignard reagents and covers both the history and preparation of these compounds, as well as their speciation in the solid state and in solution. Additionally, contemporary chemical applications of Grignard reagents are also discussed. Chapter 2 recounts the synthesis and characterization of a series of 2,2':6',2''-Terpyridine (terpy) Mg complexes. The selective reaction of terpy with MgX_2 over $RMgX$ and R_2Mg is rationalized computationally. Chapter 3 details the preparation of Mg complexes supported by Tris(2-dimethylaminoethyl)amine (Me_6tren). The reactivity of organometallic complex $(Me_6tren)MgMe_2$ is further investigated with a variety of small molecules.

Chapter 4 begins with a short review of Ni catalyzed Suzuki-Miyaura reactions and continues with the synthesis of a series of 1,1'-Bis(diphenylphosphino)ferrocene (dppf) supported Ni(0), (I) and (II) complexes. The catalytic activity of the compounds was tested and all precatalysts were found to be active at room temperature. The speciation of Ni during catalysis was investigated using both EPR and NMR spectroscopies and found to be predominantly Ni(I). Pathways to form Ni(I) from even electron Ni species were elucidated and found to involve comproportionation, which was also investigated computationally.

Synthesis and Reactivity of Organometallic and Coordination Complexes of
Mg and Ni

A Dissertation
Presented to the Faculty of the Graduate School
of
Yale University
In Candidacy for the Degree of
Doctor of Philosophy

by

Louise M. Guard

Dissertation Director: Nilay Hazari

May 2015

UMI Number: 3663446

All rights reserved

INFORMATION TO ALL USERS

The quality of this reproduction is dependent upon the quality of the copy submitted.

In the unlikely event that the author did not send a complete manuscript and there are missing pages, these will be noted. Also, if material had to be removed, a note will indicate the deletion.

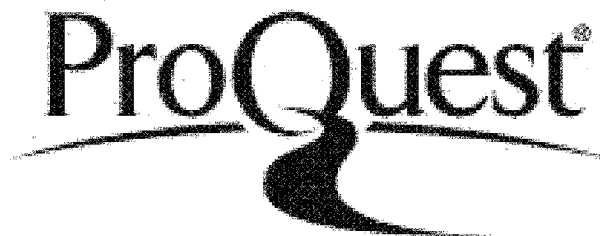


UMI 3663446

Published by ProQuest LLC 2015. Copyright in the Dissertation held by the Author.

Microform Edition © ProQuest LLC.

All rights reserved. This work is protected against unauthorized copying under Title 17, United States Code.



ProQuest LLC
789 East Eisenhower Parkway
P.O. Box 1346
Ann Arbor, MI 48106-1346

© 2015 by Louise M. Guard
All rights reserved

This work is dedicated to:
Granny and Grandad North
Granny and Grandad Seaside
Mother and Daddio...
...and I guess Simon

Acknowledgements

There are a number of people that I want to thank. Firstly to my academic advisors: Michael Vaughn, Tim Storr, Mike Whittlesey and Nilay Hazari. Mr Vaughn taught me so much as a secondary school student and encouraged the whole class to 'follow the path of true enlightenment that is Chemistry'. Perhaps unfortunately for him, I was the only one who listened. Working for Tim and Mike as an undergraduate was excellent. Mike in particular has always been very friendly, supportive (and sarcastic), and it was in working in his lab that I decided to pursue Graduate school. In fact, if it wasn't for his New Haven background check and mention that Nilay was at Yale, then maybe I wouldn't have ended up here. Lastly, I would like to thank Nilay. Aside from all the obvious, boring things like being supportive and encouraging and enthusiastic, I'd like to thank him for the little things; lending me books that he thinks I would like, and listening to me talk about hockey (go Bulldogs!), and ordering the eggplant pizza at group events because he knows it's my favourite.

Throughout my time at Yale Chemistry, I have been incredibly lucky with the people I have had the chance to interact and spend my time with. The Hazari group has seen some amazing people come and go, and I'd like to mention a few (in vague chronological order). Will and Eric (Sweet Bros), Joy (lover of too strong coffee), Eddie (fixer of all things), Matt (disgustingly logical), Amymarie (super shifty), Damian (joint longest-running housemate), Liz (please send me some slides so I don't miss you too much), Hee Won (chicken stock fan), Megan (one day you will be Katy Perry) and Patrick (#1 funniest in lab, average joke rating is 8.9). Outside of the group, I'd like to acknowledge Bob Crabtree and Gary Brudvig for being extremely valuable members of my thesis committee. They've both had very positive impacts on my time here, and have directly helped me in my research a number of times. Additionally: James Blakemore, Laura Jo Sunshine Allen, Graham Dobereiner, Nate Schley, Jeremy Praetorius, Uli Hintermair, Simon Bonyhady, Richard Lewis, Cory Macleod, Ann Valentine, Jim Mayer, Pat Holland, Kurt Zilm I thank them for their help (lots of help), guidance and good humour!

I would like to highlight some of people who have made my time here wonderful, but I'll change the names to protect the innocent: Kphos, Mr and Mrs Rumpy, Bboo, Beaver, #2, Geebs, Fang, Kimdrews, Short British Alex and Team Thanksgiving, Dunk, Papaya, Paedo, Spurs guy and Erin and Lauren, because apparently I don't have nicknames for them (alas).

Lastly, I'd like to thank my family. They're pretty great, I won't lie. Thank you for talking to me. And for everything else.

Table of Contents

List of Figures, Schemes and Tables	viii
Chapter One: The Grignard Reagent	1
I. Background	1
II. Complex Speciation	2
a. Solution-State Characterization	2
b. Solid-State Characterization	4
III. Chemical Applications	6
IV. Conclusions	11
V. References	12
Chapter Two: Synthesis and Computational Studies of Mg Complexes Supported by 2,2':6',2''-Terpyridine Ligands	15
I. Introduction	15
II. Results and Discussion	17
a. Synthesis and Structure of Mg Terpy Complexes	17
b. Computational Studies on the Coordination of Terpy to Mg	23
III. Conclusions	29
IV. Experimental Section	29
a. General Methods	29
b. X-ray Crystallography	30
c. Computational Procedures	31
d. Synthesis and Characterization of Compounds	32
e. Acknowledgements	37
V. References	37
Chapter Three: Synthesis and Reactivity of Magnesium Complexes Supported by Tris(2-dimethylaminoethyl)amine (Me₆tren)	39
I. Introduction	40
II. Results and Discussion	43
a. Synthesis and Characterization of Mg Compounds	43
b. Reactivity of Mg Complexes	53
III. Conclusions	56
IV. Experimental	57
a. General Methods	57
b. X-ray Crystallography	59
c. ESI-MS	59
d. Synthesis and Characterization of Compounds	60
e. Acknowledgements	67
V. References	67

Chapter Four: Comparison of a Series of dppf Supported Ni Precatalysts for the Suzuki-Miyaura Reaction: The Importance of Ni(I)	69
I. Introduction.....	69
II. Results and Discussion	78
a. Synthesis.....	78
b. Catalysis	81
c. Speciation During Catalysis.....	84
d. Stoichiometric Experiments	87
e. Disproportionation/Comproportionation of Ni(0)/Ni(II) to Ni(I)	93
f. Catalytic Implications	95
III. Conclusions.....	97
IV. Experimental.....	98
a. General Methods	98
b. X-ray Crystallography.....	99
c. Computational Details.....	100
d. Synthesis and Characterization of Compounds.....	100
e. Acknowledgements	108
V. References.....	108

List of Figures, Schemes and Tables

Chapter One: The Grignard Reagent	1
Figure 1.01: Synthesis and mechanism of formation of Grignard reagents	1
Figure 1.02: A generic example of the Schlenk equilibrium	3
Table 1.01: Equilibrium constants for various Grignard reagents in Et ₂ O and THF	4
Figure 1.03: Examples of a dimeric Grignard (left) and a tetrameric Grignard (right)	6
Scheme 1.01: A small selection of the organic transformations for which Grignard reagents are used	7
Scheme 1.02: Diagram depicting a generic catalytic cycle for the Kumada coupling	8
Figure 1.04: Generic examples of a) Li-halogen exchange and, b) Mg-halogen exchange	8
Figure 1.05: General synthesis using Turbo Grignard Reagents	10
Scheme 1.03: Examples of products synthesized using Turbo Grignard reagents	10
Figure 1.06: General synthesis using the Knochel-Hauser (K-H) base	11
Chapter Two: Synthesis and Computational Studies of Mg Complexes Supported by 2,2':6',2''-Terpyridine Ligands	15
Figure 1.01: The reaction of 1 eq. R-terpy and 1 eq. MeMgBr in Et ₂ O	18
Figure 1.02: The reaction of 0.5 eq. R-terpy and 1 eq. MeMgBr in Et ₂ O or THF	19
Figure 1.03: Theoretical equilibrium between (R-terpy)MgMeX, (R-terpy)MgX ₂ , Me ₂ Mg and terpy	20
Figure 1.04: ORTEP of 1a at 30% probability	22
Figure 1.05: ORTEP of 1b at 30% probability	23
Figure 1.06: Orientation of dipole moments in different isomers of terpy	24
Figure 1.07: Phenylterpy π -stacking from DFT calculations at the wB97XD level with the 6-31+G(d,p) basis set	25
Figure 1.08: Computed reaction between a disolvated Grignard reagent and free mesitylterpy ligand	26
Table 1.01: Thermodynamic energies for the coordination of mesitylterpy to Mg species starting from a dimeric mesitylterpy starting material	26
Figure 1.09: Computed equilibrium between dihalide and mixed halide alkyl Mg species	28
Table 1.02: Thermodynamic energies for the equilibrium between mixed alkyl halide Mg mesitylterpy species and dihalide and dialkyl Mg complexes	28
Table 1.03: Crystallographic data for 1a and 1b.	36
Chapter Three: Synthesis and Reactivity of Magnesium Complexes Supported by Tris(2-dimethylaminoethyl)amine (Me₆tren)	39
Figure 2.01: Tris(aminoethyl)amine (H ₆ tren) and tris(2-dimethylaminoethyl)amine (Me ₆ tren)	41
Figure 2.02: Group I and II complexes of H ₆ tren and Me ₆ tren	42
Figure 2.03: The reaction of Me ₆ tren with one equiv. PhMgBr	43
Figure 2.04: The reaction of Me ₆ tren with two equiv. PhMgX	43
Figure 2.05: Simulated (left) and recorded (right) ESI-MS spectra of compound 1	44
Figure 2.06: ORTEP of 1 at 30% probability	45
Figure 2.07: The reaction of Me ₆ tren with 1 equiv. MeMgBr	47
Figure 2.08: ORTEP of 4 at 30% probability	49
Figure 2.09: Overlaid ¹ H NMR spectra of 1 (blue) and 4 (red)	49
Figure 2.10: ORTEP of 5 at 30% probability	50
Figure 2.11: The reaction of Me ₆ tren with 1 equiv. Me ₂ Mg	50
Figure 2.12: ORTEP of 6 at 30% probability	52
Scheme 2.01: Summary of the reactivity of (Me ₆ tren)MgMe ₂ (6)	54

Table 2.01: Crystallographic data for 1, 4, 5 and 6	66
---	----

Chapter Four: Comparison of a Series of dppf Supported Ni Precatalysts for the Suzuki-Miyaura Reaction: The Importance of Ni(I).....69

Scheme 4.01: Diagram depicting a generic catalytic cycle for the Pd catalyzed Suzuki-Miyaura reaction.	70
Scheme 4.02: First reports of Ni catalysts for the Suzuki-Miyaura reaction	71
Scheme 4.03: Previously reported room temperature Ni precatalysts for the coupling of aryl halides and boronic acids	73
Figure 4.01: Common Ni precatalysts	73
Scheme 4.04: Substrate scope and conditions for the Suzuki-Miyaura reaction using Ni(dppf)(Cin)(Cl) ..	74
Scheme 4.05: Previously reported Ni(I) precatalysts for the Suzuki-Miyaura reaction.....	75
Scheme 4.06: a) Stoichiometric reactions to test Ni(I) viability and b) Ni(I) methyl complex, top, and Ni(II) alkyl cation, bottom	76
Scheme 4.07: The reaction of Ni(0) and Ni(I) precatalysts with aryl halides and/or boronic acids	77
Figure 4.02: Ni precatalysts studied in this work	79
Figure 4.03: ORTEP of 1	79
Figure 4.04: ORTEP of 5.....	80
Figure 4.05: Synthesis of 5.....	81
Table 4.01: Yields of product for the Suzuki-Miyaura reaction catalyzed by complexes 1-5.....	82
Figure 4.06: Equilibrium between 1 and 2	82
Figure 4.07: Activation pathway for Ni(II) precatalysts	83
Figure 4.08: (a) $^{31}\text{P}\{^1\text{H}\}$ NMR spectra taken before and after a catalytic reaction using 1 as the precatalyst. (b) EPR spectra of a catalytic reaction mixture(left, black) and a pure sample of 5 (blue, right)	85
Table 4.02: Percentage 5 formed at various time points during catalysis.....	86
Figure 4.09: Stoichiometric reactivity of 1.....	87
Figure 4.10: Stoichiometric reactivity of 2.....	88
Figure 4.11: ORTEP of $[\text{Ni}(\text{dppf})(\text{Cl})]_2(\mu\text{-dppf})$	88
Figure 4.12: Stoichiometric reactivity of 3.....	89
Figure 4.13: Transmetallation-reductive elimination pathway for the formation of 5 and Ni(dppf)(Ar) from 3.....	90
Figure 4.14: Comproportionation of 3 and 1 to form 5	90
Figure 4.15: Stoichiometric reactivity of 4.....	91
Scheme 4.08: Quantification of Ni(I) with varying boronic acid equivalents	92
Figure 4.16: Reaction of 5 with CO	93
Figure 4.17: Reaction of 5 with 0.5 equivalents of dppf	94
Table 4.03: Computational results for the disproportion of 5 with ethene as the L ligand.....	94
Table 4.04: Computational results for the disproportion of 5 with dmpf as the L type ligand	95
Figure 4.18: Comproportionation of 2 with Ni(dppf)(Cl) $_2$	95
Scheme 4.09: Possible products of catalysis when a radical clock substrate is used	97
Table 4.05: Crystallographic data for 1, 5 and 6	107

The Grignard Reagent

I. Background

The Grignard reagent was discovered 100 years ago by Victor Grignard at the University of Lyon, France.^{1,2} Much of the initial work was included in his doctoral thesis on 'Mixed Organomagnesium Compounds and their Applications to Synthesis'.^{1,2} The reagent's obvious relevance to organic synthesis, and facile preparation, led to its widespread application, and Grignard was promptly awarded the Nobel Prize in Chemistry in 1912 for his discovery.³

The current synthesis⁴ of the Grignard reagent has not been significantly altered from Grignard's original report, and is detailed in Figure 1.01.⁵

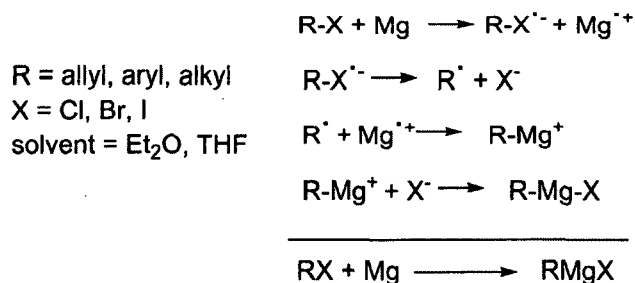


Figure 1.01: Synthesis and mechanism of formation of Grignard reagents.

Generally, the reaction of Mg metal with the appropriate aryl, alkyl or allyl halide under an inert atmosphere (to avoid oxidation^{6,7}) and in ethereal solvent yields the corresponding Grignard reagent.^{5,8,9} The reaction is proposed to proceed via a single electron transfer from the Mg to the halide.⁹⁻¹⁴ Subsequently, the R-X bond undergoes homolytic cleavage to yield an organic radical and a halide anion. The organic radical then combines with the radical Mg ion, and this resulting cation associates with the halide to yield RMgX (Figure 1.01). The reaction is believed to occur at the metal-solution interface^{9,10} and, as such, the

slow rate of initiation in the preparation of Grignard reagents is often attributed to unreactive layers of MgO blocking the active metal from reaction with RX. Numerous methods have been reported to remove this layer and therefore speed up the reaction. Most commonly an I₂ initiator is used,¹⁵ although mechanical methods, such as rapid stirring,¹⁶ crushing¹⁶ or sonication¹⁷ are also employed. The use of Rieke Mg, a highly reactive form of Mg powder, also circumvents this induction period.^{8,15} In addition, the activation of Mg can facilitate reaction with less reactive organic halides, allowing a wider range of reagents to be prepared.¹⁵

II. Complex Speciation

Several in-depth studies on both the solid-state and solution properties of Grignard reagents, both experimentally and computationally, have been conducted.¹⁸⁻²⁶ However, since the composition of the solution is highly dependent on concentration, solvent, and the identity of both the R and X groups, the exact nature of the species present are unknown except in the specific systems studied.

a. Solution-State Characterization

The instant adoption of Grignard reagents in organic synthesis prompted much study into the properties and identity of these compounds in solution. Around 30 years after Grignard's initial report, Wilhelm Schlenk and his son, Wilhelm Schlenk, Jr, proposed that there was more than one Mg containing species present in a diethyl ether solution of the reagent.¹⁸ The redistribution of ligands they suggested - now called the Schlenk equilibrium - afforded both R₂Mg and MgX₂ from RMgX, along with halide bridged dimers (Figure 1.02).^{8,18}

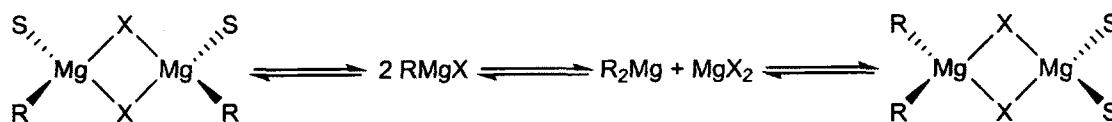


Figure 1.02: A generic example of the Schlenk equilibrium (where s = solvent).

Support for this hypothesis is provided by the fact that the addition of 1,4-dioxane to a Grignard solution results in the immediate precipitation of (1,4-dioxane) MgX_2 as a highly insoluble white solid, leaving R_2Mg in solution.^{18,27} Here, the solvent causes an extreme perturbation of the equilibrium, and allows the isolation of pure binary Grignard reagents which can be used as potent alkylating, arylating or allylating agents.²⁸ In addition, it has been observed that upon mixing a sample of MgBr_2 enriched with radioactive ^{28}Mg with an ether solution of RMgX , the radioactive label is quickly scrambled between the species R_2Mg , RMgBr and MgBr_2 .⁸

One of the most direct ways of determining speciation in solution is using NMR spectroscopy, which provides evidence to support the equilibria described above. Both the ^1H and ^{25}Mg nuclei have been probed using NMR spectroscopy,^{19,20,29} and the field has been reviewed in great detail by Bonesteel.²¹ The ^1H NMR spectrum of MeMgBr displays only one peak at room temperature, suggesting rapid exchange between Me_2Mg and MeMgBr . However, at temperatures lower than -100°C , two peaks are observed. A study of EtMgBr using ^{25}Mg NMR spectroscopy revealed three peaks in the ^{25}Mg NMR spectrum at room temperature in THF, which coalesced into one resonance at 67°C .^{8,22}

The general trend is that THF solutions of Grignard reagents tend to exist as solvated monomers of the form $(\text{solvent})_2\text{MgRX}$ over a wide range of concentrations. In Et_2O they exist as higher order species (dimers, trimers etc.) at concentrations greater than 1 M,^{23,24,30} whereas at low concentrations, less than 0.3 M, it is generally accepted that di-

and polymeric structures are either not present or comprise a very small amount of the mixture.⁴ The equilibrium constants for MeMgBr and EtMgBr have been measured in both Et₂O and THF and illustrate the non-innocent role of the solvent in the Schlenk equilibrium (Table 1.01). This drastic solvent effect is rationalized by both the increased Lewis basicity of THF^{25,29} as well as its size; four THF molecules can solvate a monomeric fragment, for example MgBr₂, but only two Et₂O molecules can solvate the same fragment.²⁶ In addition, a comparison between EtMgBr and EtMgCl reveals that there is also a halide effect.⁴

$$2 \text{RMgX} \xrightleftharpoons{K} \text{R}_2\text{Mg} + \text{MgX}_2$$

Grignard	Solvent	K
MeMgBr	THF	3.5
MeMgBr	Et ₂ O	~320
EtMgBr	Et ₂ O	428
EtMgBr	THF	5.09
EtMgCl	THF	5.52

Table 1.01: Equilibrium constants for various Grignard reagents in Et₂O and THF.^{4,26}

Over 80 years of research since the publication of the Schlenk's seminal work has shown that the speciation may be more complicated than originally suggested, as many higher order aggregates^{19,31} (trimers, tetramers and beyond) have been proposed and observed in various Grignard reagent solutions.⁸ Further evidence for the presence of these species comes from solid state studies on Grignard reagents.

b. Solid-State Characterization

The crystallization of Grignard reagents has been an active area of research for many years.³² Although the solid-state structures do not necessarily pertain to species present in

solution, they at least give an indication as to the vast number of ways the simple monomer RMgX can form higher order structures.

There are numerous examples of monomeric Grignard reagents which have been characterized by X-ray crystallography with varying coordination numbers.^{31,33-37} In the late 1960's Toney and Stucky elucidated the nature of dimeric Grignard reagents.³⁸ Solution based molecular weight studies had indicated that species of the type [RMgX·solvent]₂ were present, but no information on the structure, i.e. which groups were occupying the terminal or bridging positions, had been obtained.³⁹ The addition of EtMgBr in ⁿBu ether to 2 eq. NEt₃ afforded crystals of [EtMgBr·NEt₃]₂ in which the Br atoms were bridged between two Mg centers (Figure 1.03, left). The inclusion of only one molecule of NEt₃ per Mg atom in the molecule is rationalized by steric factors, as a disolvated monomeric species is certainly more sterically crowded.^{38,40} The *trans* orientation in the dimer is also presumably to minimize steric clash. This finding supports the idea that speciation is not only solvent dependent, but also R group dependent. A bulky organic group can impose a steric restraint, which may influence both the number of solvent molecules coordinated and the extent of association between Mg monomers. Other dimeric Grignard reagents have been since reported.^{32,41}

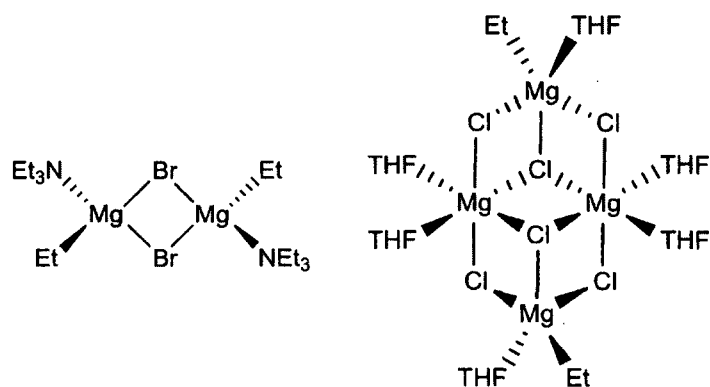
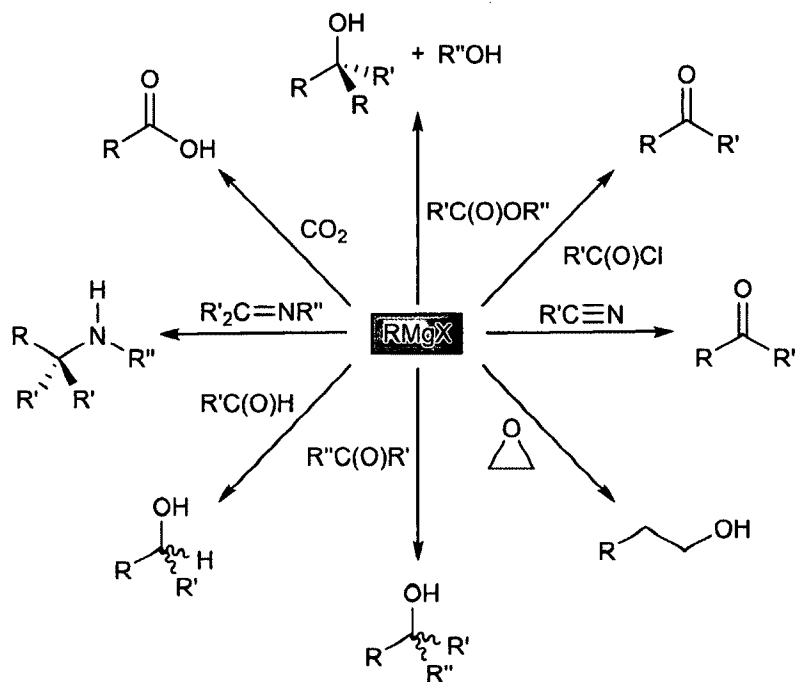


Figure 1.03: Examples of a dimeric Grignard³⁸ (left) and a tetrameric Grignard³⁸ (right).

Higher order aggregates have also been isolated from solutions containing Grignard reagents. Toney and Stucky were able to obtain a crystal structure of a tetrameric Grignard reagent ($[\text{EtMg}_2(\text{THF})_3]_2$) by slow evaporation of solvent from a THF solution of EtMgBr (Figure 1.03 right).⁴⁰ The structure contains four Mg atoms, all bridged by Cl atoms with two Mg atoms capped by two solvent molecules, and two by one ethyl group and one THF, although as previously mentioned, the degree of solvation in solution is likely higher and aggregates of this type are probably disassembled.⁴⁰ At this stage clusters containing more than four Mg atoms have not been crystallized from a Grignard reagent.

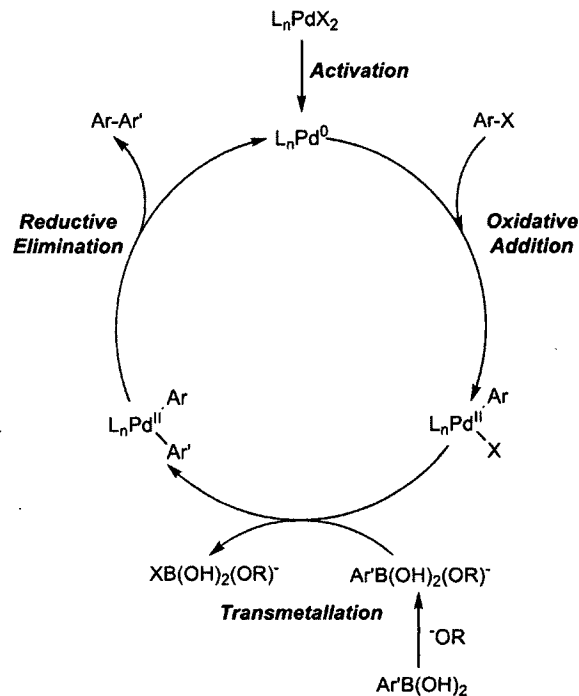
III. Chemical Applications

A major use of Grignard reagents is as nucleophiles in organic transformations. Indeed, there are a plethora of known reactions between these reagents and carbonyl compounds and other electrophiles, and a selection are represented in Scheme 1.01. Reactions of this type are well documented and will not be covered in any more detail in this chapter, however more information on this topic can be found here.^{8,42-45}



Scheme 1.01: A small selection of the organic transformations for which Grignard reagents are used.^{8,42,44} Organic products depicted are the result of acid work-up.

Another area in which Grignard reagents have found utility is the Pd-catalyzed Kumada coupling reaction where an Mg reagent is coupled to an aryl or alkenyl halide (Scheme 1.02). Interestingly, this reaction was known for many years using other metals^{4,46-50} such as Cu, Fe, Ni, Co and Cr until it was reported using Pd in 1975.⁵¹⁻⁵³ The latter has proven to be the most effective and as a result this topic has been widely chronicled and expanded to include synthetically important sp^3 hybridized organic halide coupling partners. More information on this reaction can be found here.^{51,54-56}



Scheme 1.02: Diagram depicting a generic catalytic cycle for the Kumada coupling

Grignard reagents have also found use in the preparation of other organometallic reagents using metal-halogen exchange reactions.⁵⁷⁻⁵⁹ This is often considered a milder alternative to another common example of this type of metathesis, Li-halogen exchange (Figure 1.04).^{57,58}

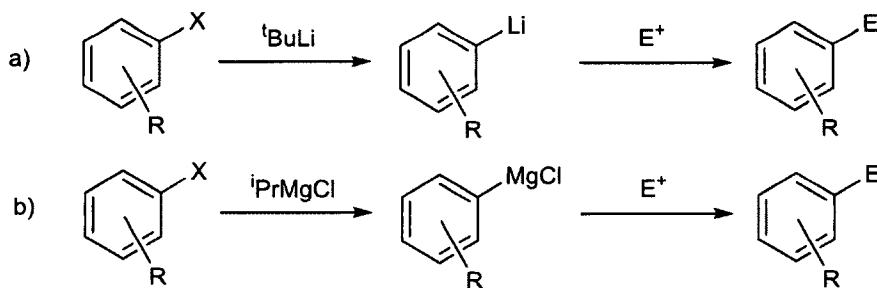


Figure 1.04: Generic examples of a) Li-halogen exchange and, b) Mg-halogen exchange.

There are several major drawbacks associated with using Li-halogen exchange reactions in organic synthesis: (i) low temperatures, usually around -78°C are required, (ii) the functional group tolerance is poor due to the high reactivity of R^- in RLi , (iii) organolithium

reagents can participate in a variety of side reactions; and (iv) it is experimentally difficult to handle these extremely sensitive and pyrophoric materials.

While being safer to prepare and handle, there are also problems associated with using traditional organomagnesium reagents. Due to the comparatively less reactive nature of R^- in $RMgX$, the reaction is slower. Furthermore different competing side reactions can occur compared with organolithium reagents due to the slower rate of reaction.^{58,60} Finally, Mg-halogen exchange reactions require higher temperatures to proceed, which further limits compatibility with other functional groups present in the molecule.⁵⁸⁻⁶⁰

In the last ten years, the Knochel group has made substantial progress in this area, through their development of 'Turbo Grignards'.⁶⁰ These reagents are comprised of $RMgCl$ ($R = ^iPr, ^sBu$) and 1 eq. of $LiCl$. The salt additive is proposed to increase the rate and efficiency of the reaction by breaking up the polymeric aggregates present in Grignard solutions and enduing a negative charge on the Mg species formed, thereby decreasing the negative charge on the alkyl fragment, making it less nucleophilic.⁶¹ As a consequence, there are fewer side reactions and increased functional group tolerance. In fact, reagents containing ester,^{60,62} cyano,^{60,61} ether,⁶⁰ halogen,⁶⁰ triazenes⁶³ alkene^{61,64,65} and heteroaryl^{60,65} functionality have been accessed (Figure 1.05, Scheme 1.02). These have been used with great success in various organic applications including the synthesis of functionalized furans,⁶⁶ cyclopentenes,⁶⁷ unprotected imidazoles,⁶⁸ pyridines^{60,65} and carbazoles⁶³ (a small selection is illustrated in Scheme 1.03).

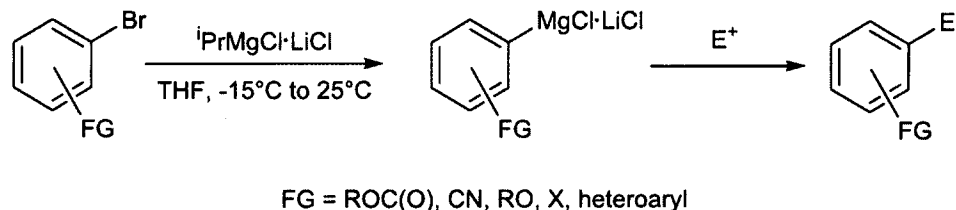
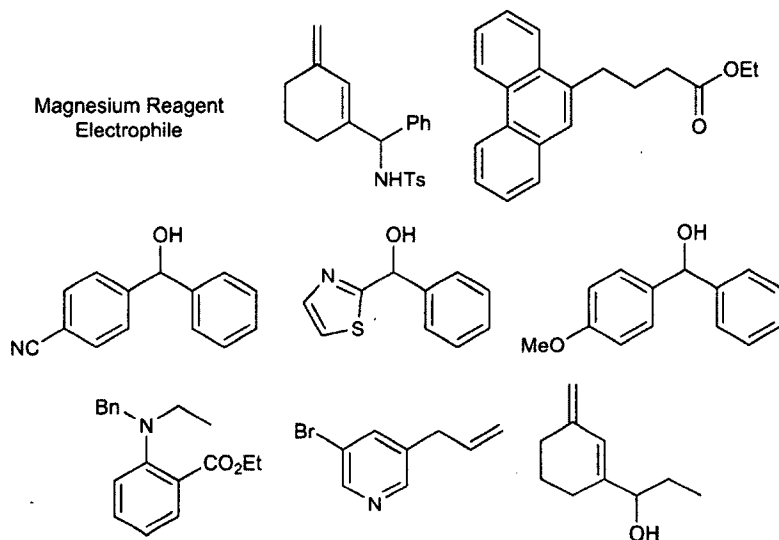


Figure 1.05: General synthesis using Turbo Grignard Reagents.



Scheme 1.03: Examples of products synthesized using Turbo Grignard reagents. The fragment of the molecule originally from the Magnesium reagent is in blue, while the fragment from the electrophile is in red.^{60,62,64} The bond that is formed is shown in black.

An additional use of this chemistry is the adoption of related Mg compounds with LiCl additives in the selective deprotonation of aromatics. Again, the commonly used strong bases (alkyl lithiums, lithium amides) have significant drawbacks, namely competing addition reactions and the requirement for low temperatures (-78 to -90°C).⁶⁹ In addition, many amides are not stable in solution for extended periods of time and therefore must be generated *in situ*.⁶⁹ To this end, Knochel and coworkers have also added LiCl to a Mg amide base⁷⁰ (Hauser base) [(TMP)MgCl, TMP = 2,2,6,6-tetramethylpiperidino] to generate the Knochel-Hauser base [(TMP)MgCl·LiCl], which retains many of the benefits

of Turbo Grignards, namely functional group tolerance and fewer side reactions.^{69,71} Additionally, their increased THF solubility and basicity are superior to common bases used for this transformation.^{69,71} In the presence of a directing group, arenes can be selectively deprotonated to form highly functionalized Grignard reagents, which can undergo further derivitization by reaction with electrophiles. As before, ester, cyano, ether, halogen and heteroaryl substrates are tolerated (Figure 1.06). Again, the high activity is proposed to be due to the dispersion of aggregates present before the addition of LiCl,⁶⁹ and indicates that the addition of LiCl to Mg solutions could be used to enhance reactivity elsewhere.

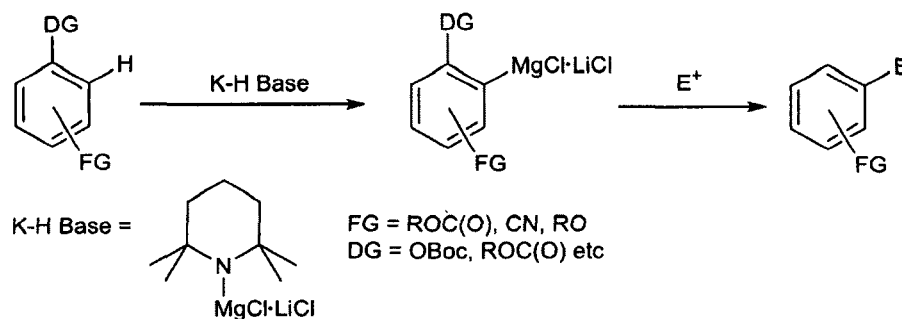


Figure 1.06: General synthesis using the Knochel-Hauser (K-H) base.

IV. Conclusions

Despite the universal use of Grignard reagents across all types of preparative chemistry, even today relatively little is known about their nature in solution. Although this has not significantly hindered progress in Grignard chemistry thus far, it is clear that in the contemporary cases presented here, an increase in the understanding of the speciation of the solution both prior and after LiCl addition could advance understanding of this phenomenon and ascertain exactly what role the salt additive plays. Specifically, this could result in more improved reagents for important functionalization reactions. More broadly

a deeper understanding of these reagents could lead to the discovery of new applications for Grignard reagents, where their use has previously been deemed too harsh, and allow for the fine-tuning of known reactions by informing the choice of Grignard reagent and solvent used.

V. References

- (1) *Nobel Lectures, Chemistry 1901-1921*; Elsevier Publishing Company: Amsterdam, 1966.
- (2) Nobelprize.org. Victor Grignard - Biographical. http://www.nobelprize.org/nobel_prizes/chemistry/laureates/1912/ (accessed 6th Dec 2014).
- (3) Nobelprize.org. The Nobel Prize in Chemistry 1912. http://www.nobelprize.org/nobel_prizes/chemistry/laureates/1912/ (accessed 6th Dec 2014).
- (4) Orchin, M. *J. Chem. Educ.* **1989**, *66*, 586.
- (5) 'Common Methods for Grignard Reagent Preparation'. G. S. Silverman in *Handbook of Grignard Reagents*, Eds G. S. Silverman and P. E. Rakita, Marcel Decker, New York, 1996, 9-22.
- (6) Goebel, M. T.; Marvel, C. S. *J. Am. Chem. Soc.* **1933**, *55*, 1693.
- (7) Slough, W.; Ubbelohde, A. R. *J. Chem. Soc.* **1955**, 108.
- (8) Elschenbroich, C.; Salzer, A. *Organometallics: A Concise Introduction*; 2 ed.; VCH, 1992.
- (9) Walborsky, H. M. *Acc. Chem. Res.* **1990**, *23*, 286.
- (10) Rogers, H. R.; Deutch, J.; Whitesides, G. M. *J. Am. Chem. Soc.* **1980**, *102*, 226.
- (11) 'Mechanism of Grignard Reagent Formation'. J. F. Garst and F. Ungvary in *Grignard Reagents: New Developments*, Ed H. G. Richey, John Wiley & Sons, New York, 2000, 185-275.
- (12) 'Mechanism of Grignard Reagent Formation'. C. Hamdouchi and H. W. Walborsky in *Handbook of Grignard Reagents*, Eds G. S. Silverman and P. E. Rakita, Marcel Decker, New York, 1996, 145-218.
- (13) Garst, J. F. *Acc. Chem. Res.* **1991**, *24*, 95.
- (14) Walling, C. *Acc. Chem. Res.* **1991**, *24*, 255.
- (15) Lai, Y. H. *Synthesis* **1981**, 585.
- (16) 'Magnesium Activation'. R. D. Rieke and M. S. Sell in *Handbook of Grignard Reagents*, Eds G. S. Silverman and P. E. Rakita, Marcel Decker, New York, 1996, 53-78.
- (17) Smith, D. H. *J. Chem. Educ.* **1999**, *76*, 1427.
- (18) Schlenk, W.; Schlenk, W. *Ber. Dtsch. Chem. Ges.* **1929**, *62*, 920.
- (19) Ashby, E. C.; Parris, G.; Walker, F. *J. Chem. Soc., Chem. Commun.* **1969**, 1464.
- (20) Parris, G. E.; Ashby, E. C. *J. Am. Chem. Soc.* **1971**, *93*, 1206.
- (21) 'Nuclear Magnetic Resonance Analyses of Grignard Reagents'. J.-A. K. Bonesteel in *Handbook of Grignard Reagents*, Eds G. S. Silverman and P. E. Rakita, Marcel Decker, New York, 1996, 103-116.
- (22) Simeral, L.; Maciel, G. E. *J. Phys. Chem.* **1976**, *80*, 552.
- (23) Walker, F. W.; Ashby, E. C. *J. Am. Chem. Soc.* **1969**, *91*, 3845.

- (24) 'The Composition of Grignard Reagents in Solution: The Schlenk Equilibrium and its Effect on Reactivity'. K. C. Cannon and G. R. Krow in Handbook of Grignard Reagents, Eds G. S. Silverman and P. E. Rakita, Marcel Decker, New York, 1996, 271-289.
- (25) Tammiku-Taul, J.; Burk, P.; Tuulmets, A. *J. Phys. Chem. A* **2004**, *108*, 133.
- (26) Smith, M. B.; Becker, W. E. *Tetrahedron* **1967**, *23*, 4215.
- (27) Weiss, E. *J. Organomet. Chem.* **1964**, *2*, 314.
- (28) Andersen, R. A.; Wilkinson, G. *Inorg. Synth.* **1979**, *19*, 262.
- (29) Lehmkuhl, H.; Mehler, K.; Benn, R.; Rufinska, A.; Kruger, C. *Chem. Ber. Recl.* **1986**, *119*, 1054.
- (30) Seyferth, D. *Organometallics* **2009**, *28*, 1598.
- (31) Ashby, E. C. *Bull. Soc. Chim. Fr.* **1972**, 2133.
- (32) 'Crystal Structures of Grignard Reagents'. H. L. Uhm in Handbook of Grignard Reagents, Eds G. S. Silverman and P. E. Rakita, Marcel Decker, New York, 1996, 117-144
- (33) Stucky, G.; Rundle, R. E. *J. Am. Chem. Soc.* **1964**, *86*, 4825.
- (34) Guggenberger, L. J.; Rundle, R. E. *J. Am. Chem. Soc.* **1964**, *86*, 5344.
- (35) Zerewitinoff, T. *Ber. Dtsch. Chem. Ges.* **1908**, *41*, 2244.
- (36) Vallino, M. *J. Organomet. Chem.* **1969**, *20*, 1.
- (37) Perucaud, M. C.; Lebihan, M. T. *Acta Crystallogr., Sect. B: Struct. Sci.* **1968**, *B 24*, 1502.
- (38) Toney, J.; Stucky, G. D. *Chem. Commun.* **1967**, 1168.
- (39) Wakefield, B. J. *Organometallic Chem. Rev.* **1966**, *1*, 131.
- (40) Toney, J.; Stucky, G. D. *J. Organomet. Chem.* **1971**, *28*, 5.
- (41) Marsch, M.; Harms, K.; Massa, W.; Boche, G. *Angew. Chem. Int. Ed.* **1987**, *26*, 696.
- (42) 'Nucleophilic Substitution with Electrophilic Organic, Main Group, and Transition Metal Species'. G. S. Silverman in Handbook of Grignard Reagents, Eds G. S. Silverman and P. E. Rakita, Marcel Decker, New York, 1996, 307-354.
- (43) 'Nucleophilic Addition to Unconjugated C-C Multiple Bonds'. P. E. Rakita in Handbook of Grignard Reagents, Eds G. S. Silverman and P. E. Rakita, Marcel Decker, New York, 1996, 355-360.
- (44) 'Nucleophilic Addition to Carbon-Heteroatom Multiple Bonds: O, S, N, P.'. L. Miginiac in Handbook of Grignard Reagents, Eds G. S. Silverman and P. E. Rakita, Marcel Decker, New York, 1996, 361-372.
- (45) 'Nucleophilic Addition to Conjugated Carbon-Carbon Multiple Bonds'. P. E. Rakita in Handbook of Grignard Reagents, Eds G. S. Silverman and P. E. Rakita, Marcel Decker, New York, 1996, 381-390.
- (46) Corriu, J. P.; Masse, J. P. *J. Chem. Soc., Chem. Commun.* **1972**, 144.
- (47) Kharasch, M. S.; Fields, E. K. *J. Am. Chem. Soc.* **1941**, *63*, 2316.
- (48) Smith, R. S.; Kochi, J. K. *J. Org. Chem.* **1976**, *41*, 502.
- (49) Elson, I. H.; Morrell, D. G.; Kochi, J. K. *J. Organomet. Chem.* **1975**, *84*, C7.
- (50) Tamao, K.; Sumitani, K.; Kumada, M. *J. Am. Chem. Soc.* **1972**, *94*, 4374.
- (51) Seechurn, C. C. C. J.; Kitching, M. O.; Colacot, T. J.; Snieckus, V. *Angew. Chem. Int. Ed.* **2012**, *51*, 5062.
- (52) Murahashi, S. I.; Yamamura, M.; Yanagisawa, K.; Mita, N.; Kondo, K. *J. Org. Chem.* **1979**, *44*, 2408.
- (53) Yamamura, M.; Moritani, I.; Murahashi, S. I. *J. Organomet. Chem.* **1975**, *91*, C39.
- (54) Terao, J.; Kambe, N. *Acc. Chem. Res.* **2008**, *41*, 1545.
- (55) Adrio, J.; Carretero, J. C. *ChemCatChem* **2010**, *2*, 1384.
- (56) Mphahlele, M. J.; Lesenyehlo, L. G. *J. Heterocycl. Chem.* **2013**, *50*, 1.
- (57) Boudier, A.; Bromm, L. O.; Lotz, M.; Knochel, P. *Angew. Chem. Int. Ed.* **2000**, *39*, 4414.
- (58) Boymond, L.; Rottlander, M.; Cahiez, G.; Knochel, P. *Angew. Chem. Int. Ed.* **1998**, *37*, 1701.

- (59) Knochel, P.; Dohle, W.; Gommermann, N.; Kneisel, F. F.; Kopp, F.; Korn, T.; Sapountzis, I.; Vu, V. A. *Angew. Chem. Int. Ed.* **2003**, *42*, 4302.
- (60) Krasovskiy, A.; Knochel, P. *Angew. Chem. Int. Ed.* **2004**, *43*, 3333.
- (61) Ren, H. J.; Krasovskiy, A.; Knochel, P. *Org. Lett.* **2004**, *6*, 4215.
- (62) Sinha, P.; Knochel, P. *Synlett* **2006**, 3304.
- (63) Liu, C. Y.; Knochel, P. *Org. Lett.* **2005**, *7*, 2543.
- (64) Ren, H. J.; Krasovskiy, A.; Knochel, P. *Chem. Commun.* **2005**, 543.
- (65) Ren, H. J.; Knochel, P. *Chem. Commun.* **2006**, 726.
- (66) Melzig, L.; Rauhut, C. B.; Knochel, P. *Chem. Commun.* **2009**, 3536.
- (67) Despotopoulou, C.; Bauer, R. C.; Krasovskiy, A.; Mayer, P.; Stryker, J. M.; Knochel, P. *Chem. Eur. J.* **2008**, *14*, 2499.
- (68) Kopp, F.; Wunderlich, S.; Knochel, P. *Chem. Commun.* **2007**, 2075.
- (69) Krasovskiy, A.; Krasovskaya, V.; Knochel, P. *Angew. Chem. Int. Ed.* **2006**, *45*, 2958.
- (70) Hauser, C. R.; Walker, H. G. *J. Am. Chem. Soc.* **1947**, *69*, 295.
- (71) Lin, W. W.; Baron, O.; Knochel, P. *Org. Lett.* **2006**, *8*, 5673.

Synthesis and Computational Studies of Mg Complexes

Supported by 2,2':6',2''-Terpyridine Ligands

This work has been previously published.¹ All computational work was conducted by Dr. Julio Palma (Batista Group, Yale) and a more detailed discussion of the calculations can be found in reference 1. This project, including the initial synthesis and crystallographic characterization of (mesitylterpy)MgBr₂, was started by William Stratton (Hazari Group, Yale).

I. Introduction

Since the first metal complexes containing the 2,2':6',2''-terpyridine (terpy) ligand were prepared in the 1930s,²⁻⁶ this generally κ^3 -N *meridional* tridentate ligand has been used extensively to support a range of different coordination compounds.^{7,8} In part, this is because terpy is fairly easy to synthesize, inexpensive, oxidation resistant and stable to harsh reaction conditions.^{7,8} Electronically, terpy is both a powerful σ -donor, due to its relatively hard nitrogen lone pairs, and a reasonable π -acceptor, as a result of the low lying unfilled π^* -orbitals of the aromatic rings.⁷ Therefore, because terpy can support complexes in both low and high oxidation states, terpy-containing species have been utilized in a wide variety of applications.⁹ These include applications as dye molecules¹⁰ and water oxidation catalysts¹¹ in solar energy conversion schemes, as metal containing scaffolds for supramolecular¹² and nanoscale¹³ chemistry, as reagents for facilitating and studying the kinetics and mechanism of electron transfer in biochemical, inorganic and organic processes¹⁴⁻¹⁶ and as dyes for luminescent sensors¹⁷ and molecular photonic devices.^{18,19}

In contrast to the plethora of transition metal complexes containing terpy ligands, examples of s-block species containing these ligands are very rare.⁷ The majority of complexes of this type are either homoleptic species containing two terpy ligands, or species containing one terpy ligand and a variable number of water molecules as the remaining ligands.²⁰⁻²⁴ Given the importance of s-block organometallic compounds (in particular Li and Mg) as reagents in organic synthesis,^{25,26} we were interested in preparing organometallic Mg complexes supported by terpy ligands. The synthesis of monomeric derivatives of this type could assist in increasing our mechanistic understanding of organic reaction pathways involving Grignard reagents, which are currently difficult to study due to the complex speciation of Grignard reagents in solution. Here, we show that the reaction of a number of different Grignard reagents (R_2Mg or $RMgX$) in either Et_2O or THF with substituted terpy ligands, results in either no reaction or disproportionation to give exclusively non-organometallic products of the form $(terpy)MgX_2$ ($X = Cl$ or Br); these are some of the first Mg complexes supported by terpy ligands. Our results are in direct contrast to reactions between Grignard reagents, such as $MeMgBr$, and other tridentate nitrogen ligands, which form either mixed halide alkyl complexes, or dihalide and bis(alkyl) complexes depending on whether Et_2O or THF is used as the solvent.^{27,28} Density functional theory (DFT) is used to understand the binding of the terpy ligand to Mg and explain our experimental observations. Surprisingly, we find that it is crucial to model π -stacking of the terpy ligands in solution to accurately model the energetics of terpy binding to Mg.

II. Results and Discussion

a. Synthesis and structure of Mg terpy complexes

In a series of seminal articles, Parkin and co-workers demonstrated that the treatment of Grignard reagents with protonated tris(pyrazolyl)hydroborates led to a metathesis reaction, in which an alkane was released from the Grignard reagent and a four coordinate Mg species with the tridentate ligand coordinated in a *facial* geometry was formed.²⁹⁻³³ To the best of our knowledge, there are only two examples of the use of Grignard reagents as Mg precursors for the preparation of Mg complexes with chelating tridentate neutral ligands.^{27,28} Both Steinborn and co-workers and Viebrock and Weiss prepared a mixture of (pmdta)MgBrMe (pmdta = *N,N,N',N'',N'''*-pentamethyldiethylenetriamine), (pmdta)MgMe₂ and (pmdta)MgBr₂ through the reaction of pmdta with MeMgBr.^{27,28} The ratio of the products varied depending on whether the reaction was performed in THF or Et₂O.²⁸ Given this limited prior work, we were interested in preparing organometallic Mg complexes supported by terpy ligands. Initially, unsubstituted terpy was treated with MeMgBr in Et₂O at room temperature and a solid immediately precipitated. Unfortunately, this solid was insoluble in all common solvents and it was impossible to obtain a ¹H NMR spectrum. We postulated that organic-soluble, Mg-containing products could be generated by adding hydrophobic substituents to the 2,2':6',2''-terpyridine framework. The coordination chemistry of three different terpy ligands was explored; 4'-mesityl-2,2':6',2''-terpyridine (mesitylterpy), commercially available 4,4',4''-tri-*tert*-butyl-2,2':6',2''-terpyridine (tri-*t*Buterpy) and 4'-phenyl-2,2':6',2''-terpyridine (phenylterpy), which was prepared using a literature route.³⁴

As in the analogous reaction with unsubstituted terpy, when MeMgBr in Et₂O was treated with mesitylterpy or tri-^tBu terpy a solid immediately precipitated out of the reaction mixture. However, after the solid was isolated by filtration, it was soluble in both chlorinated solvents and THF, which allowed for full characterization. Surprisingly, the reaction of one equivalent of substituted terpy ligands with one equivalent of MeMgBr produced half an equivalent of (R-terpy)MgBr₂ (R = mesityl (**1a**), or tri-^tBu (**1b**)), which was insoluble in the Et₂O solution, and half an equivalent of Me₂Mg, which was soluble in Et₂O. In addition, an unidentified terpy-containing product was present in low yield (Figure 1.01).

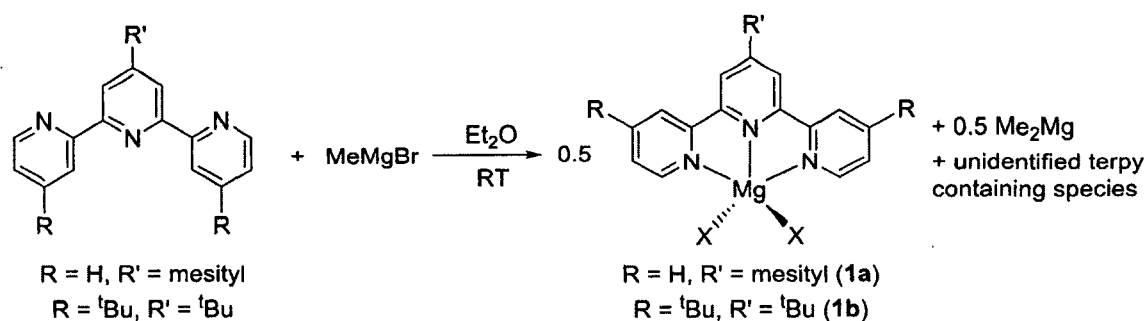


Figure 1.01: The reaction of 1 eq. R-terpy and 1 eq. MeMgBr in Et₂O

When half an equivalent of mesitylterpy or tri-^tButerpy was treated with MeMgBr, the only products were **1a** or **1b** and Me₂Mg (Figure 1.02). There was no evidence to indicate that mixed halide, alkyl complexes of the type (R-terpy)MgMeBr or dialkyl species such as (R-terpy)MgMe₂ were being formed. In fact, when one equivalent of our substituted terpy ligands was added to one equivalent of Me₂Mg³⁵ in Et₂O or THF, no products containing terpy bound to Mg were isolated and it appeared that if any coordination was occurring, the equilibrium strongly favored free terpy and Me₂Mg.

Changing the Grignard reagent from MeMgBr to PhMgBr had no effect on reactivity. Again, the only product with terpy coordinated to Mg was (R-terpy)MgBr₂, which precipitated from the reaction mixture. There was no evidence for complexes of the type (R-terpy)MgPhBr or (R-terpy)MgPh₂, although free Ph₂Mg was observed using ¹H NMR spectroscopy. Similarly, when the halide on the Grignard reagent was changed from Br to Cl, the dichloride species **2a** or **2b** was formed (Figure 1.02). Complexes **2a** and **2b** were fully characterized. In contrast to reactions with mesitylterpy and tri-^tButerpy, phenylterpy was too insoluble to give reactions in pure Et₂O. Adding THF to an Et₂O solution solubilized the phenylterpy, and it appeared that the (phenylterpy)MgBr₂ (**1c**) was formed from the reaction of phenylterpy with MeMgBr. However, compound **1c** was highly insoluble and was only characterized by ¹H NMR spectroscopy. The ¹H NMR spectrum indicated that a small amount of an unknown impurity was present which could not be removed, and as such **1c** was not isolated in its pure form.

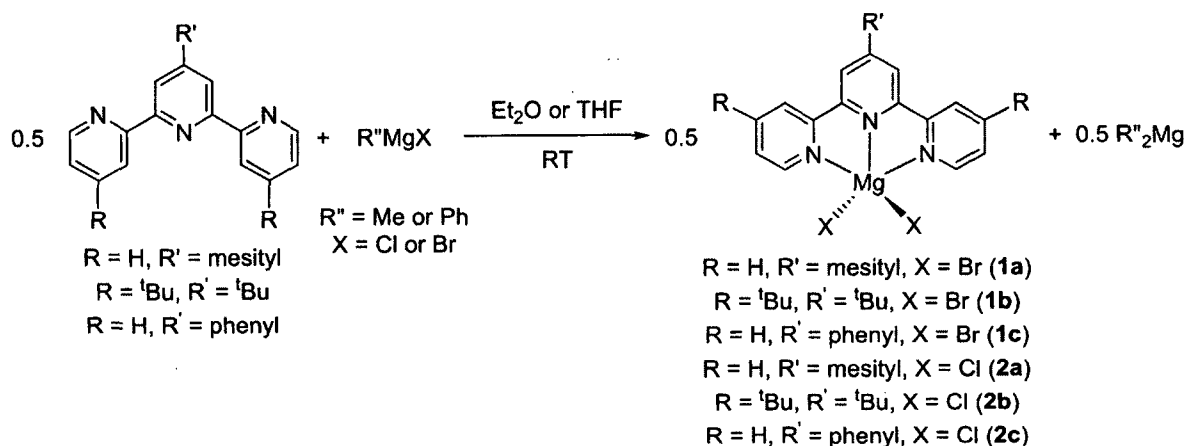


Figure 1.02: The reaction of 0.5 eq. R-terpy and 1 eq. MeMgBr in Et₂O or THF

One possible explanation for the selective formation of the dihalide species is that there is an equilibrium between (R-terpy)MgR'X and 0.5 equivalents of (R-terpy)MgX₂ and R'₂Mg (Figure 1.03). If this equilibrium occurs, presumably the insolubility of the dihalide species

drives the equilibrium, and as a result only the dihalide species is observed (along with the unligated bis(alkyl) species in solution). In order to test this hypothesis, the reaction between half an equivalent of the terpy ligands and the Grignard reagents was performed in THF, because in this solvent the terpy-coordinated dihalide species, **1a**, **1b**, **2a** and **2b**, are completely soluble.

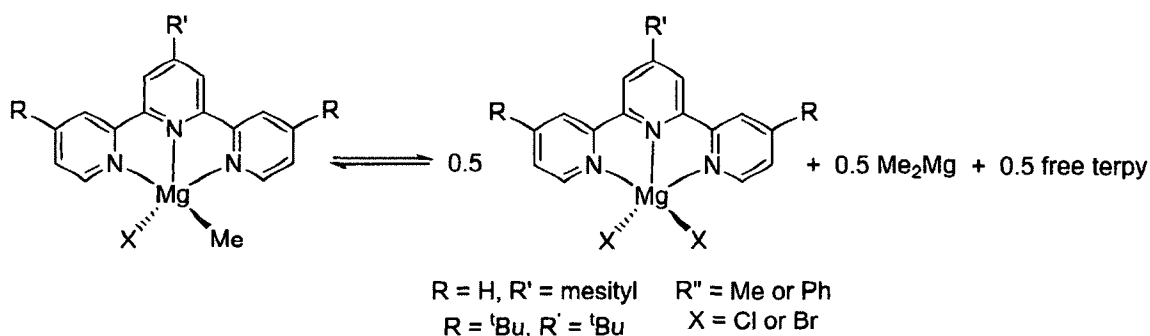


Figure 1.03: Theoretical equilibrium between (R-terpy)MgMeX, (R-terpy)MgX₂, Me₂Mg and uncoordinated terpy

Surprisingly, this reaction also only led to formation of the ligated dihalide species and the unligated bis(alkyl) species (Figure 1.02). In this case, isolation of the terpy Mg dihalide species could be achieved by removing the THF from the reaction mixture and then extracting the bis(alkyl) by-product with Et₂O.

The most likely explanation for the selectivity of the reactions between Grignard reagents and mesitylterpy and tri-^tButerpy is that the terpy Mg dihalide species and the uncoordinated bis(alkyl)Mg species are thermodynamically preferred over the mixed ligand alkylmagnesium halide species. Thus, if any of the terpy alkylmagnesium halide species forms, it rapidly undergoes disproportionation. This is explored further using DFT calculations (*vide infra*). Our results are in direct contrast to Steinborn's finding that with pmdta as the chelating tridentate nitrogen ligand, the products of the reaction with MeMgBr

are influenced by whether the reaction is performed in Et₂O or THF.²⁸ In Steinborn's case, the lack of solubility of (pmdta)MgBr₂ in Et₂O drives the reaction to the dihalide and bis(alkyl) products, whereas in THF, where there are no solubility issues, (pmdta)MgMeBr is formed.

The compounds **1a** (Figure 1.04) and **1b** (Figure 1.05) were characterized by X-ray crystallography. Unsurprisingly, the structures are closely related and in both species the geometry around Mg is distorted trigonal bipyramidal, with the terpy ligand occupying two axial sites and one equatorial site. The bond angle formed by the two nitrogen atoms occupying the axial positions and the Mg center is 146.18(15)° (N(1)-Mg(1)-N(3)) in **1a** and 147.57(11)° (N(1)-Mg(1)-N(1A)) in **1b**. The τ parameter is a value which places the structure on a scale of 0 to 1, where 0 is idealized square pyramidal (SP) and 1 idealized trigonal bipyramidal (TPB).³⁶ τ for **1a** is 0.52 and 0.56 for **1b** indicating that both structures are slightly distorted towards TBP over SP. To the best of our knowledge, there are only two other Mg complexes supported by a terpy ligand, Mg(terpy)₂²⁺ and Mg(terpy)(H₂O)₃²⁺, and these are both six coordinate species with distorted octahedral geometries around Mg.^{21,23} Despite the differences in charge and coordination number in **1a** and **1b**, the bond lengths and angles associated with the binding of terpy are comparable with those of the previous two complexes.^{21,23} In general, the geometry around the metal center in most five coordinate monomeric Mg complexes is square pyramidal, and examples of trigonal bipyramidal complexes are relatively rare.³⁷ The structures of **1a** and **1b** are quite different from the structure of (pmdta)MgBr₂ which adopts a square pyramidal geometry with one of the Br ligands in the axial position.²⁸ The difference in geometry may

be due to the fact that the pmdta ligand has less in-plane bulk and, thus, allows another ligand to coordinate in the plane.

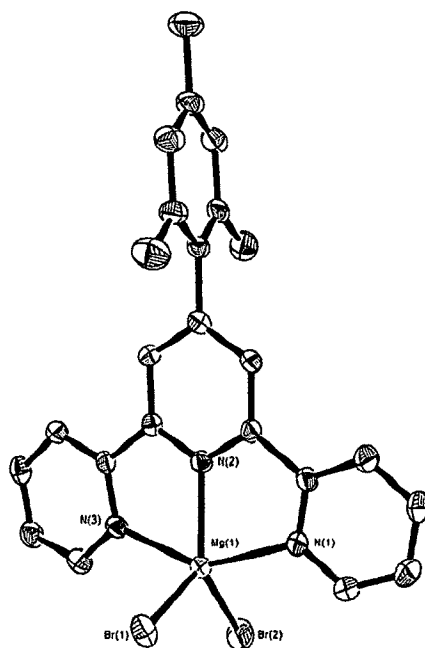


Figure 1.04: ORTEP³⁸ of **1a** at 30% probability (hydrogen atoms and solvent in crystal lattice have been omitted for clarity). Selected bond lengths (Å) and angles (°): Mg(1)-N(1) 2.183(4), Mg(1)-N(2) 2.098(4), Mg(1)-N(3) 2.170(4), Mg(1)-Br(1) 2.4653(18), Mg(1)-Br(2) 2.4435(17), N(1)-Mg(1)-N(2) 73.60(15), N(1)-Mg(1)-N(3) 146.18(15), N(1)-Mg(1)-Br(1) 100.41(13), N(1)-Mg(1)-Br(2) 97.65(12), N(2)-Mg(1)-N(3) 74.06(14), N(2)-Mg(1)-Br(1) 111.22(13), N(2)-Mg(1)-Br(2) 133.96(14), N(3)-Mg(1)-Br(1) 100.23(12), N(3)-Mg(1)-Br(2) 97.62(12), Br(1)-Mg(1)-Br(2) 114.81(6).

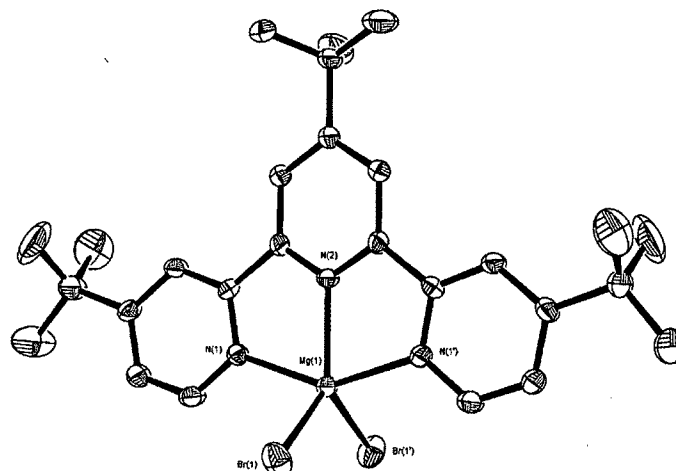


Figure 1.05: ORTEP of **1b** at 30% probability (hydrogen atoms and solvent in crystal lattice have been omitted for clarity; only one conformation of disordered 'Bu group shown). A mirror plane is present along the N(2)-Mg(1) axis. Selected bond lengths (Å) and angles (°): Mg(1)-N(1) 2.156(3), Mg(1)-N(2) 2.110(4), Mg(1)-Br(1) 2.4571(14), N(1)-Mg(1)-N(1') 147.57(11), N(1)-Mg(1)-N(2) 73.78(14), N(1)-Mg(1)-Br(1) 97.97(13), N(1)-Mg(1)-Br(1') 99.48(9), N(2)-Mg(1)-Br(1) 122.88(4), Br(1)-Mg(1)-Br(1') 114.24(8).

b. Computational studies on the coordination of terpy to Mg

In order to accurately calculate the energy associated with terpy binding to various Grignard reagents, the thermodynamics of rotation of the pyridine-based rings in terpy was determined. Previously, it has been shown that the low energy configuration occurs when the N atoms are mutually *anti* (Figure 1.06, a),^{39,40} but for coordination to a metal to occur, rotation of the two rings are required to give a *syn* arrangement (Figure 1.06, c). The energy associated with these rotations, calculated to be 18.5 kcal/mol, was included in our calculations for the binding of terpy to Mg.

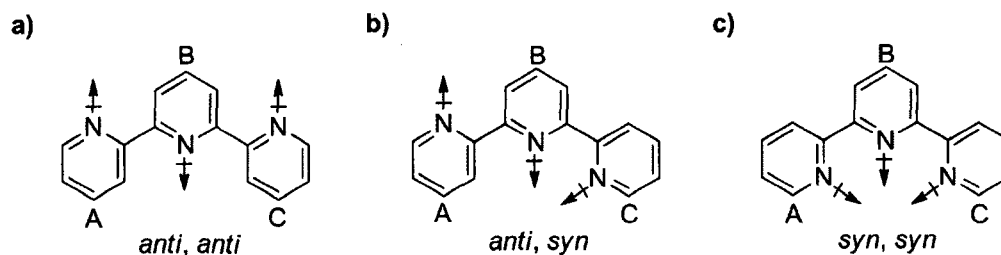


Figure 1.06: Orientation of dipole moments in different isomers of terpy. **a)** *anti, anti* conformation with dipole moment of rings A and C oriented opposite to B and aligned with each other; **b)** *anti, syn* conformation with dipole moment of ring A oriented partially opposite rings B and C and dipole moments of B and C almost aligned; **c)** *syn, syn* conformation with all dipole moments partially aligned.

In addition, we found that to obtain good agreement with our experimental observation of no reaction occurring between $\text{Me}_2\text{Mg}/\text{Ph}_2\text{Mg}$ and any terpy ligands, we had to include a correction factor accounting for the presence of π -stacking in solutions containing free terpy. Calculations were performed on phenylterpy and two stable dimeric conformations were found (phenylterpy was used as a model for mesitylterpy because at this higher level of theory it is computationally expensive to calculate two mesitylterpy units). In one conformer, there is π -stacking between the phenyl ring of one monomer and one of the nitrogen rings of the other monomer (Figure 1.07, a). This is the same conformation as observed in the crystal structure of mesitylterpy, and the stacking energy correction was found to be -17.5 kcal/mol. However, the most stable conformation of two phenylterpy dimers was when both monomers were stacked directly on top of each other so that there was an interaction between two of the three nitrogen containing rings (Figure 1.07, b). In this case, the stacking energy correction was -19.6 kcal/mol. Presumably, crystal packing effects result in the first conformation being observed by X-ray crystallography.

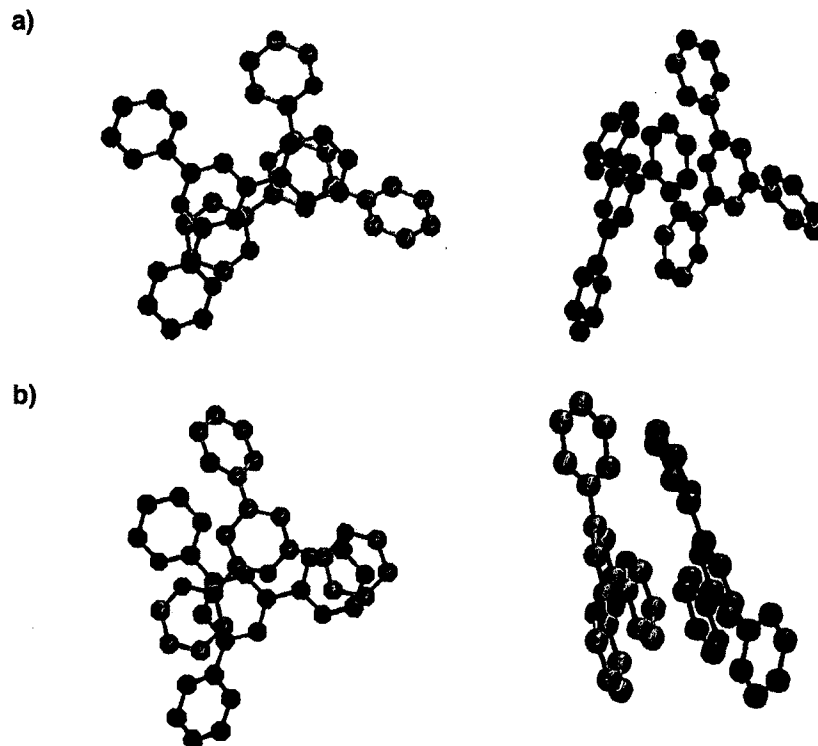


Figure 1.07: Phenylterpy π -stacking from DFT calculations at the wb97XD level with the 6-31+G(d,p) basis set. **a)** Conformation with interactions between a phenyl group and a nitrogen containing ring with stacking energy correction of -17.5 kcal/mol and **b)** conformation with interactions between two nitrogen containing rings with stacking energy correction of -19.6 kcal/mol.

The thermodynamic energies for the coordination of mesitylterpy to a variety of different Mg species were calculated based on the assumption that the starting Mg species had two molecules of Et₂O coordinated to them (Figure 1.08). This assumption is consistent with the results of Kato and Mori, who found that the lowest energy structure, for a variety of Grignard reagents in Et₂O, was a tetrahedral monomer with two molecules of Et₂O coordinated.⁴¹ In our case, the two molecules of Et₂O are released when mesitylterpy coordinates. The free terpy was modeled as a π -stacked dimeric species. The crystal structures of the Mg complexes supported by terpy show no π -stacking and, therefore, it

was not necessary to make any corrections to the product energies. The calculated energies of formation of various bis alkyl/bis halide/mixed alkyl halide are given in Table 1.01.

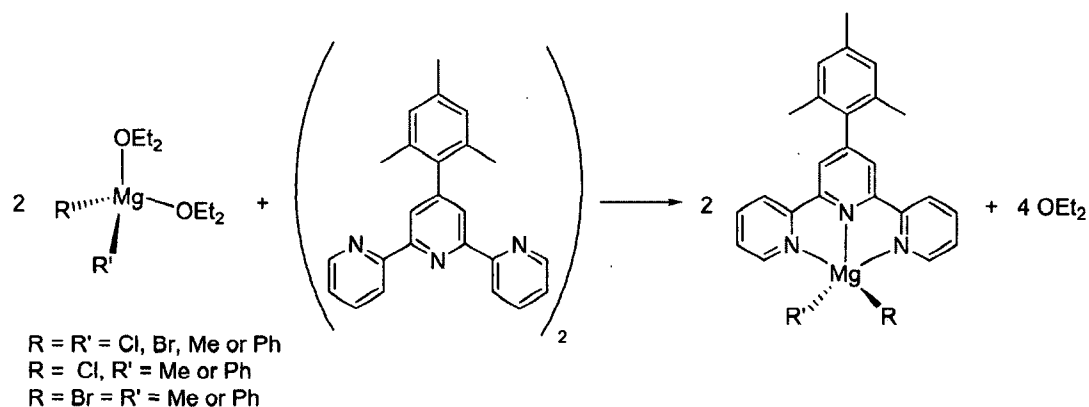


Figure 1.08: Computed reaction between a disolvated Grignard reagent and free mesitylterpy ligand

Product	$\Delta G^\circ_{(\text{ether})}$
(mesitylterpy)MgBr ₂	-9.38
(mesitylterpy)MgBrMe	-3.99
(mesitylterpy)MgBrPh	-6.53
(mesitylterpy)MgCl ₂	-7.68
(mesitylterpy)MgClMe	-3.82
(mesitylterpy)MgClPh	-4.71
(mesitylterpy)MgMe ₂	-1.33
(mesitylterpy)MgPh ₂	-1.76

Table 1.01: Thermodynamic energies for the coordination of mesitylterpy to Mg species starting from a dimeric mesitylterpy starting material (Figure 1.07). All energies are in kcal/mol relative to the starting materials.

Although the Gibbs free energy with solvent corrections is still favorable for the binding of mesitylterpy to Me₂Mg(OEt₂)₂ and Ph₂Mg(OEt₂)₂, these reactions are now favored by

only around 1.5 kcal/mol, and it is probable that our calculated values lie within the DFT error in calculating thermodynamic properties.⁴²

One of the most intriguing findings from our experimental results is the selective observation of terpy-coordinated dihalide species and the absence of any mixed alkyl halide complexes when terpy is reacted with Grignard reagents. In order to investigate this selectivity, calculations were performed on the equilibrium shown in Figure 1.09 in both Et₂O and THF. The calculated energy differences and equilibrium constants are summarized in Table 1.02. It can be seen that in almost all cases the mixed alkyl halide species is preferred; however, the energy differences between the two sides are very small. In fact, within the DFT error of calculating thermodynamic properties,⁴² it is not possible to say whether the starting material or the product is preferred, and the computational results are consistent with the experimental result of only observing the dihalide product (although, in the case of reactions in Et₂O, the precipitation of the dihalide is presumably an important factor). When the alkyl group on the Grignard is changed from methyl to phenyl, it becomes more favorable to form the mixed alkyl halide species, and this is also true when the solvent is changed from Et₂O to THF. This suggests that in order to promote the formation of organometallic Mg complexes supported by terpy ligands, electron deficient alkyl groups may be required. Perhaps the most remarkable aspect of our work is comparing the calculated value of K for the reaction of MeMgBr with mesitylterpy in THF with Steinborn's result for the reaction of MeMgBr with pmdta.²⁸ Whereas our calculated value is 0.12 (and from experiment it has to be greater than 1), with pmdta Steinborn calculates a value of 1.2×10^{-3} .²⁸ The difference in equilibrium constant between the two systems is probably related to the change in geometry and indicates that a relatively small

change in the nature of the tridentate chelating ligand can cause a large change in the preferred speciation of Mg. Hence, it may be possible to change the nature of the ligand to control the speciation of the Grignard reagent, in the same way that solvent is currently used.

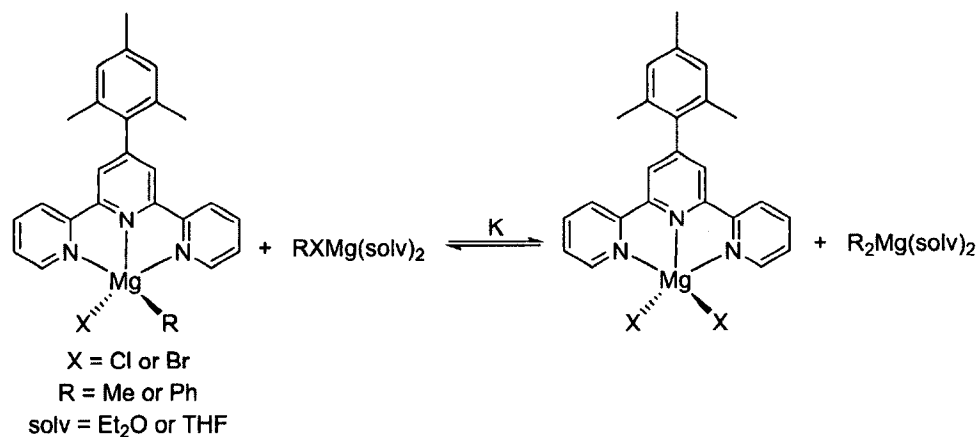


Figure 1.09: Computed equilibrium between dihalide and mixed halide alkyl Mg species

X	R	Solvent	$\Delta G^\circ_{(\text{solv})}$	$K_{(298)}$
Cl	Me	Et ₂ O	0.24	0.66
Cl	Me	THF	1.20	0.13
Cl	Ph	Et ₂ O	0.51	0.42
Cl	Ph	THF	0.41	0.50
Br	Me	Et ₂ O	-0.20	1.4
Br	Me	THF	1.24	0.12
Br	Ph	Et ₂ O	0.57	0.38
Br	Ph	THF	1.81	0.05

Table 1.02: Thermodynamic energies for the equilibrium between mixed alkyl halide Mg mesitylterpy species and dihalide and dialkyl Mg complexes (Figure 1.09). All energies are in kcal/mol relative to the starting materials.

III. Conclusions

Through the reactions of substituted terpy ligands with Grignard reagents, we have prepared rare examples of Mg complexes supported by terpy ligands. Surprisingly, the reactions of terpy ligands with RMgX ($\text{R} = \text{Me}$ or Ph ; $\text{X} = \text{Cl}$ or Br) are selective and lead exclusively to products of the type $(\text{terpy})\text{MgX}_2$ and R_2Mg . The solid state structures of $(\text{mesitylterpy})\text{MgBr}_2$ and $(\text{tri-}^t\text{Buterpy})\text{MgBr}_2$ show that the coordination geometry around Mg is distorted trigonal bipyramidal, which is unusual for five coordinate Mg species. A series of DFT calculations, performed to understand the preferential formation of $(\text{terpy})\text{MgX}_2$ and R_2Mg over $(\text{terpy})\text{MgRX}$, indicated that the reaction could only be modeled accurately if π -stacking effects associated with free terpy were explicitly included. Our combined experimental and theoretical studies suggest that preference for the formation of $(\text{terpy})\text{MgX}_2$ and R_2Mg is related to thermodynamic factors. Given that mixed halide alkyl species are the preferred thermodynamic product from the reaction of other tridentate nitrogen containing ligands, such as pmdta with Grignard reagents, this suggests that these types of ligands can be used to control the speciation of Grignard reagents.

IV. Experimental

a. General methods

Experiments were performed under a dinitrogen atmosphere in an M-Braun dry box or using standard Schlenk techniques, unless otherwise noted. (Under standard glovebox conditions, purging was not performed between uses of pentane, Et_2O , benzene, toluene and THF; thus, when any of these solvents were used, traces of all these solvents were in

the atmosphere and could be found intermixed in the solvent bottles.) Moisture- and air-sensitive liquids were transferred by stainless steel cannula on a Schlenk line or in a dry box. Solvents were dried by passage through a column of activated alumina followed by storage under dinitrogen. All commercial chemicals were used as received, except where noted. PhMgCl in THF, 2,2':6',2''-terpyridine, and 4,4',4''-tri-tert-butyl-2,2':6',2''-terpyridine (**1b**) were purchased from Aldrich, MeMgBr in THF and PhMgBr in both Et₂O and THF were purchased from Acros Organics, and MeMgCl in THF from Alfa Aesar. Deuterated solvents were obtained from Cambridge Isotope Laboratories. CD₂Cl₂ was dried using CaH₂ and C₆D₆ using sodium metal. Both were vacuum-transferred prior to use. NMR spectra were recorded on Bruker AMX-400 and -500 spectrometers at ambient probe temperatures. Chemical shifts are reported in ppm with respect to residual internal protio solvent for ¹H and ¹³C{¹H} NMR spectra; *J* values are given in Hz. Robertson Microlit Laboratories, Inc., performed the elemental analyses. Literature procedures were utilized to synthesize phenylterpy^{34,43} and mesitylterpy.¹

b. X-ray crystallography

The diffraction experiments were carried out on a Rigaku Mercury275R CCD (SCX mini) diffractometer with a sealed tube at 223 K using graphite-monochromated Mo K α radiation ($\lambda = 0.71073 \text{ \AA}$). The software used was SMART for collecting frames of data, indexing reflections, and determination of lattice parameters, SAINT for integration of intensity of reflections and scaling, SADABS for empirical absorption correction, and SHELXTL for space group determination, structure solution, and least-squares refinements on $|F|$. The crystals were mounted at the end of glass fibers and used for the diffraction experiments.

Anisotropic thermal parameters were refined for the rest of the non-hydrogen atoms. Hydrogen atoms were placed in their ideal positions.

c. Computational Procedures

All calculations were performed using the Gaussian 09 Revision A.02 package. Electronic structure calculations were performed with density functional theory (DFT) using the Becke3-Lee-Yang-Parr (B3LYP) functional. The TZV basis set was used for Mg, C, O, and H atoms while the 6-311++g(d,p) was used for the halogen atoms, Cl and Br. This level of theory and the basis sets were selected after comparing bond lengths and angles in the crystal structure of (mesitylterpy)MgBr₂ with the optimized structures from calculations using a number of different functionals and basis sets. Electronic structure calculations consisted of geometry optimizations, frequency calculations and solvent effect calculations to obtain enthalpies and free energies of reactions in gas phase and in solution. Free energies of reactions were obtained using the Born-Haber thermodynamic cycle where the optimized structures in gas phase were used to calculate the zero-point correction energy and entropic contribution via a vibrational frequency calculation. Solvation free energies were obtained with the self-consistent reaction field (SCRF) for the standard continuum solvation model (CPCM) using the optimized structures and the thermodynamic correction from the gas phase calculations. Stacking energies of the phenylterpy were performed with the wB97XD level of DFT and 6-31+G(d,p) basis set. Benchmark calculations were performed on pyridine where π -stacking interactions have been widely studied and reported.

d. Synthesis and characterization of compounds

(mesitylterpy)MgBr₂ (1a)

Mesitylterpy (0.10 g, 0.29 mmol) was added to a Schlenk flask, dissolved in Et₂O (25 ml) and a solution of PhMgBr in Et₂O (2.8 M, 0.21 ml, 0.57 mmol) added. The immediate precipitation of a pale green solid was observed and the mixture stirred for one hour at RT. The reaction mixture was filtered and the solid dried under reduced pressure to yield **1a** as an off white solid. Yield: 0.125 g (82 %). Diffraction-quality crystals were grown by diffusion of Et₂O into a concentrated dichloromethane solution. This reaction could also be performed using MeMgBr as the Grignard reagent or using THF as the solvent.

¹H NMR (CD₂Cl₂, 400.0 MHz): δ 9.13 (2H, d, ArH, J = 4.81 Hz), 8.14 (4H, m, ArH), 8.09 (2H, s, ArH), 7.73 (2H, m, ArH), 7.06 (2H, s, ArH), 2.38 (3H, s, ArCH₃), 2.10 (6H, s, ArCH₃). ¹³C-¹H NMR (CD₂Cl₂, 125.8 MHz): δ 158.1 (s), 152.3 (s), 151.4 (s), 150.1 (s), 140.9 (s), 139.6 (s), 135.4 (s), 135.1 (s), 129.3 (s), 127.6 (s), 123.5 (s), 122.0 (s), 21.39 (s), 21.0 (s). Anal. found (calcd for C₂₄H₂₁Br₂MgN₃•CH₂Cl₂): C 48.4 (48.4), H 4.2 (3.8), N 6.3 (6.7) %. Note one molecule of CH₂Cl₂ was found in the crystal structure and in the ¹H NMR spectrum.

(tri-^tButerpy)MgBr₂ (1b)

A PhMgBr solution in Et₂O (2.8 M, 0.18 ml, 0.50 mmol) was added to a Schlenk flask containing a solution of tri-^tButerpy (0.10 g, 0.25 mmol) in Et₂O (25 ml), causing instantaneous precipitation of a blue solid. The suspension was then stirred for one hour at RT. After filtering, the solid was dried under vacuum to afford **1b** as a pale blue powder. Yield: 0.136 g (93 %). Diffraction-quality crystals were grown by diffusion of pentane into

a dichloromethane solution. This reaction could also be performed using MeMgBr as the Grignard reagent or using THF as the solvent.

^1H NMR (CD_2Cl_2 , 500.0 MHz): δ 8.98 (2H, dd, ArH, $J = 5.52, 0.62$ Hz), 8.20 (2H, s, ArH), 8.16 (2H, dd, ArH, $J = 1.68, 0.57$ Hz), 7.69 (2H, dd, ArH, $J = 5.54, 1.77$ Hz), 1.55 (9H, s, ArC(CH₃)), 1.46 (18H, s, ArC(CH₃)). ^{13}C - $\{^1\text{H}\}$ NMR (CD_2Cl_2 , 125.8 MHz): δ 168.5 (s), 165.6 (s), 152.1 (s), 150.9 (s), 150.31 (s), 124.6 (s), 118.9 (s), 118.6 (s), 36.7 (s), 36.1 (s), 30.8 (s), 30.7 (s). Anal. found (calcd for C₂₇H₃₅Br₂MgN₃): C 55.1 (55.4), H 5.9 (6.0), N 7.0 (7.2) %.

(phenylterpy)MgBr₂ (1c)

Phenylterpy (0.10 g, 0.32 mmol) was dissolved in THF (25 ml) and a solution of PhMgBr in THF (1 M, 0.65 ml, 0.65 mmol) added. The solution was initially yellow and turned green after 3 minutes of stirring, followed by precipitation of a light green solid. The mixture was stirred for 2 hours at RT and filtered. The solid residue was washed with 2 x 25 ml Et₂O, though an impurity remained and the product was not cleanly isolated due to its insolubility. This reaction could also be performed using MeMgBr as the Grignard reagent or using a mixture of Et₂O and THF as the solvent.

^1H NMR (CD_2Cl_2 , 400.0 MHz): δ 9.14 (2H, d, ArH, $J = 4.51$ Hz), 8.41 (2H, s, ArH), 8.32 (2H, d, ArH, $J = 8.02$ Hz), 8.16 (2H, td, ArH, $J = 7.73, 1.62$), 7.85 (2H, m, ArH), 7.74 (2H, ddd, ArH, $J = 7.44, 4.94, 0.59$), 7.63 (3H, m, ArH).

(mesitylterpy)MgCl₂ (2a)

A solution of PhMgCl in THF (2.0 M, 0.14 ml, 0.29 mmol) was added to a solution of mesitylterpy (0.05 g, 0.14 mmol) in THF (20 ml). The yellow solution turned green within minutes. After 1 hour of stirring at RT, the solvent was removed *in vacuo* to give a green

oil. The oil was washed with 2 x 15 ml Et₂O, to give **2a** as a light yellow solid. Yield: 0.049 g (78 %). This reaction could also be performed using MeMgCl as the Grignard reagent.

¹H NMR (CD₂Cl₂, 400.0 MHz): δ 9.08 (2H, d, ArH, J = 5.08 Hz), 8.14 (4H, m, ArH), 8.07 (2H, s, ArH), 7.72 (2H, m, ArH), 7.06 (2H, s, ArH), 2.37 (3H, s, ArCH₃), 2.09 (6H, s, ArCH₃). ¹³C-¹H NMR (CD₂Cl₂, 125.8 MHz): δ 157.9 (s), 152.5 (s), 151.2 (s), 150.4 (s), 140.8 (s), 139.5 (s), 135.4 (s), 135.2 (s), 129.3 (s), 127.5 (s), 123.4 (s), 121.8 (s), 21.39 (s), 21.0 (s). Anal. found (calcd for C₂₄H₂₁Cl₂MgN₃): C 61.2 (64.5), H 3.8 (4.7), N 8.6 (9.4) %. Note despite repeated attempts a satisfactory elemental analysis could not be obtained for this compound.

(tri-^tButerpy)MgCl₂ (2b)

Tri-^tButerpy (0.10 g, 0.25 mmol) was dissolved in THF (25 ml) and a solution of PhMgCl in THF (2.0 M, 0.25 ml, 0.50 mmol) added via syringe. After one hour stirring at RT, the solvent was removed to give a blue oil which was washed with 1 x 15 ml Et₂O. The resulting solid was dried in vacuo to give **2b** as a light blue powder. Yield: 0.124 g (90 %). This reaction could also be performed using MeMgCl as the Grignard reagent.

¹H NMR (CD₂Cl₂, 500.0 MHz): δ 8.92 (2H, dd, ArH, J = 5.42, 0.32 Hz), 8.19 (2H, s, ArH), 8.16 (2H, dd, ArH, J = 1.75, 0.32 Hz), 7.68 (2H, dd, ArH, J = 5.48, 1.75 Hz), 1.55 (9H, s, ArC(CH₃)), 1.46 (18H, s, ArC(CH₃)). ¹³C-¹H NMR (CD₂Cl₂, 125.8 MHz): δ 168.3 (s), 165.4 (s), 152.3 (s), 150.8 (s), 150.6 (s), 124.5 (s), 118.9 (s), 118.5 (s), 36.6 (s), 36.1 (s), 30.8 (s), 30.7 (s). Anal. found (calcd for C₂₇H₃₅Cl₂MgN₃•0.5CH₂Cl₂): C 60.8 (61.3), H 6.4 (6.7), N 7.5 (7.8) %. Note half a molecule of CH₂Cl₂ was observed in the ¹H NMR spectrum after recrystallization from a Et₂O/dichloromethane solution.

(phenylterpy)MgCl₂ (2c)

A solution of PhMgCl in THF (2.0 M, 0.32 ml, 0.65 mmol) was added to a solution of phenylterpy (0.10 g, 0.32 mmol) in THF (25 ml). The initially yellow solution turned green within minutes, followed by precipitation of a green solid. After filtration, the solid was washed with 2 x 25 ml THF though an unknown impurity remained and the product was not cleanly isolated due to its insolubility. This reaction could also be performed using MeMgCl as the Grignard reagent.

¹H NMR (CD₂Cl₂, 500.0 MHz): δ 9.08 (2H, d, ArH, J = 4.63 Hz), 8.39 (2H, s, ArH), 8.30 (2H, d, ArH, J = 7.99 Hz), 8.14 (2H, td, ArH, J = 7.43, 1.65), 7.85 (2H, m, ArH), 7.72 (2H, m, ArH), 7.63 (3H, m, ArH).

Table 1.03: Crystallographic data for **1a** and **1b**.

	1a	1b
Empirical formula	Br ₂ MgN ₃ C ₂₅ H ₂₃ Cl ₂	Br ₂ MgN ₃ C ₂₇ H ₃₅
Formula weight	620.50	585.71
Temperature/K	223	223
Crystal system	monoclinic	trigonal
Space group	C2/c	P3 ₂ 21
a/Å	20.815(3)	12.5029(20)
b/Å	15.326(3)	12.5029(20)
c/Å	16.421(3)	15.991(3)
α/°	90.0000	90.0000
β/°	100.713(7)	90.0000
γ/°	90.0000	120.0000
Volume/Å ³	5147.3(15)	2164.9(6)
Z	8	3
ρ _{calc} /cm ³	1.601	1.348
μ/mm ⁻¹	3.410	2.857
F(000)	2480.0	900.0
Crystal size/mm ³	0.20 × 0.15 × 0.15	0.20 × 0.20 × 0.20
Radiation	Mo Kα (λ = 0.71075)	Mo Kα (λ = 0.71075)
2θ max/deg	54.96	48.8
Index ranges	-23 ≤ h ≤ 26, -18 ≤ k ≤ 19, -21 ≤ l ≤ 21	-14 ≤ h ≤ 14, -14 ≤ k ≤ 14, -18 ≤ l ≤ 18
Reflections collected	17383	13546
Independent reflections	6108 [R _{int} = 0.0660]	2392 [R _{int} = 0.0590]
Data/restraints/parameters	6108/0/298	2392/0/171
Goodness-of-fit on F ²	1.039	1.088
Final R indexes [I ≥ 2σ (I)]	R ₁ = 0.0613	R ₁ = 0.0424
Final R indexes [all data]	R ₁ = 0.1232, wR ₂ = 0.1390	R ₁ = 0.0510, wR ₂ = 0.0931
Largest diff. peak/hole / e Å ⁻³	0.52/-0.55	0.41/-0.33

e. Acknowledgements

I am grateful to Laura Allen who lent her organic expertise to the synthesis of mesitylterpy, to Julio Palma for very thorough computational work and to Bob Crabtree for many helpful and memorable discussions in regard to this work. Lastly, I am indebted to Will Stratton who started off the project (and kept a great lab note book!). Of course it all came down to thermobronamics.

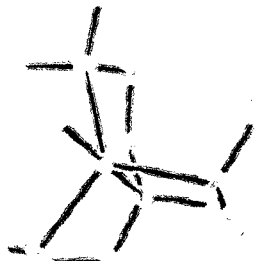
V. References

- (1) Guard, L. M.; Palma, J. L.; Stratton, W. P.; Allen, L. J.; Brudvig, G. W.; Crabtree, R. H.; Batista, V. S.; Hazari, N. *Dalton Trans.* **2012**, *41*, 8098.
- (2) Morgan, G. T.; Burstall, F. H. *J. Chem. Soc.* **1932**, 20.
- (3) Morgan, G. T.; Burstall, F. H. *J. Chem. Soc.* **1934**, 1498.
- (4) Morgan, G. T.; Burstall, F. H. *J. Chem. Soc.* **1937**, 1649.
- (5) Morgan, G. T.; Burstall, F. H. *J. Chem. Soc.* **1938**, 1675.
- (6) Morgan, G. T.; Davies, G. R. *J. Chem. Soc.* **1938**, 1858.
- (7) Constable, E. C. *Adv. Inorg. Chem.* **1986**, *30*, 69.
- (8) 'Terpyridine, oligopyridine, and polypridine ligands'. R. P. Thummel in *Comprehensive Coordination Chemistry II*, Eds. J. A. McCleverty and T. J. Meyer, Elsevier, New York, 2004, Volume 1, 41-53.
- (9) Cummings, S. D. *Coord. Chem. Rev.* **2009**, *253*, 449.
- (10) Nazeeruddin, M. K.; Péchy, P.; Renouard, T.; Zakeeruddin, S. M.; Humphry-Baker, R.; Comte, P.; Liska, P.; Cevey, L.; Costa, E.; Shklover, V.; Spiccia, L.; Deacon, G. B.; Bignozzi, C. A.; Grätzel, M. *J. Am. Chem. Soc.* **2001**, *123*, 1613.
- (11) Limburg, J.; Vrettos, J. S.; Liable-Sands, L. M.; Rheingold, A. L.; Crabtree, R. H.; Brudvig, G. W. *Science* **1999**, *283*, 1524.
- (12) Constable, E. C. *Prog. Inorg. Chem.* **1994**, *42*, 67.
- (13) Winter, A.; Hoepfener, S.; Newkome, G. R.; Schubert, U. S. *Adv. Mater.* **2011**, *23*, 3484.
- (14) Juris, A.; Balzani, V.; Barigelletti, F.; Campagna, S.; Belser, P.; von Zelewsky, A. *Coord. Chem. Rev.* **1988**, *84*, 85.
- (15) Langen, R.; Chang, I. J.; Germanas, J. P.; Richards, J. H.; Winkler, J. R.; Gray, H. B. *Science* **1995**, *268*, 1733.
- (16) Baranoff, E.; Collin, J.-P.; Flamigni, L.; Sauvage, J.-P. *Chem. Soc. Rev.* **2004**, *33*, 147.
- (17) Wong, K. M.-C.; Yam, V. W.-W. *Acc. Chem. Res.* **2011**, *44*, 424.
- (18) Harriman, A.; Ziessel, R. *Chem. Commun.* **1996**, 1707.
- (19) Flores-Torres, S.; Hutchison, G. R.; Soltzberg, L. J.; Abruña, H. D. *J. Am. Chem. Soc.* **2006**, *128*, 1513.
- (20) Constable, E. C.; Doyle, M. J.; Healy, J.; Raithby, P. R. *Chem. Commun.* **1988**, 1262.
- (21) Constable, E. C.; Healy, J.; Drew, M. G. B. *Polyhedron* **1991**, *10*, 1883.
- (22) Skelton, B. W.; Waters, A. F.; White, A. H. *Aust. J. Chem.* **1996**, *49*, 137.
- (23) Waters, A. F.; White, A. H. *Aust. J. Chem.* **1996**, *49*, 147.
- (24) Bell, T. W.; Cragg, P. J.; Drew, M. G. B.; Firestone, A.; Kwok, D.-I. A. *Angew. Chem. Int. Ed.* **1992**, *31*, 345.

- (25) H. G. Richey, Jr. (Ed), *Grignard Reagents: New Developments*, Wiley, Chichester, 2000.
- (26) B. J. Wakefield, *Organomagnesium Methods in Organic Synthesis*, Academic Press, London, 1995.
- (27) Viebrock, H.; Weiss, E. *J. Organomet. Chem.* **1994**, *464*, 121.
- (28) Yousef, R. I.; Walfort, B.; Ruffer, T.; Wagner, C.; Schmidt, H.; Herzog, R.; Steinborn, D. *J. Organomet. Chem.* **2005**, *690*, 1178.
- (29) Han, R.; Looney, A.; Parkin, G. *J. Am. Chem. Soc.* **1989**, *111*, 7276.
- (30) Han, R.; Bachrach, M.; Parkin, G. *Polyhedron* **1990**, *9*, 1775.
- (31) Han, R.; Parkin, G. *J. Am. Chem. Soc.* **1990**, *112*, 3662.
- (32) Han, R.; Parkin, G. *Organometallics* **1991**, *10*, 1010.
- (33) Han, R.; Parkin, G. *J. Am. Chem. Soc.* **1992**, *114*, 748.
- (34) Constable, E. C.; Lewis, J.; Liptrot, M. C.; Raithby, P. R. *Inorg. Chim. Acta* **1990**, *178*, 47.
- (35) Noller, C. R.; White, W. R. *J. Am. Chem. Soc.* **1937**, *59*, 1354.
- (36) Addison, A. W.; Rao, T. N.; Reedijk, J.; Vanrijn, J.; Verschoor, G. C. *J Chem Soc Dalton* **1984**, 1349.
- (37) Fletcher, D. A.; McMeeking, R. F.; Parkin, D. *J. Chem. Inf. Comput. Sci.* **1996**, *36*, 746.
- (38) Farrugia, L. J. *J. Appl. Crystallogr.* **1997**, *30*, 565.
- (39) Göller, A. H.; Grummt, U.-W. *Chem. Phys. Lett.* **2000**, *321*, 399.
- (40) Göller, A. H.; Grummt, U.-W. *Chem. Phys. Lett.* **2002**, *354*, 233.
- (41) Mori, T.; Kato, S. *J. Phys. Chem. A* **2009**, *113*, 6158.
- (42) Wheeler, S. E.; Moran, A.; Pieniazek, S. N.; Houk, K. *J. Phys. Chem. A* **2009**, *113*, 10376.
- (43) Moya, S. A.; Pastene, R.; Bozec, H. L.; Baricelli, P. J.; Pardey, A. J.; Gimeno, J. *Inorg. Chim. Acta* **2001**, *312*, 7.

TREN STRIKES AGAIN!

Known
trapped amine
trix: amine
ammonium
inc. who often
and by the
also Me₆tren
has claimed



NEW YORK (AP) — A new complex of the metal magnesium and the organic compound tren has been reported by chemists at the University of California, San Diego.

The complex, called Me₆tren, is a hexamethyltren complex of magnesium. It is the first of a series of complexes that the researchers expect to develop.

Novel Mg
Complexes
of Me₆tren

2.8 2.7
2.9 ppm
3.0
3.1
3.2

282

Synthesis and Reactivity of Magnesium Complexes Supported by Tris(2-dimethylaminoethyl)amine (Me₆tren)

This work has been previously published.¹

I. Introduction

Tren (tris(2-aminoethyl)amine, H₆tren, Figure 2.01) was the first tripodal tetraamine ligand to be reported² and since its initial preparation in 1896 more than fifty derivatives have been synthesized.³ It has been demonstrated that tren and related ligands coordinate to almost all transition metals⁴⁻⁶ and a variety of different properties of H₆tren-supported complexes have been explored. These include in-depth studies of the thermodynamics and kinetics of H₆tren binding,⁷ magnetism and conductivity measurements,⁵ and structural studies on how the H₆tren ligand effects crystal field splitting and geometry.^{5,6} Furthermore, H₆tren-containing compounds have found utility as catalysts for a number of processes such as C-O bond formation,⁸ the living radical polymerization of vinyl chlorides⁹ and the synthesis of thioesters from thiols and aryl halides.¹⁰ A H₆tren-containing complex has even been used as a structure directing agent in the synthesis of zeolites.¹¹ A common derivative of H₆tren is tris(2-dimethylaminoethyl)amine (Me₆tren, Figure 2.01), which provides reactive metals centers with increased steric protection and also results in complexes with greater solubility in organic solvents. Transition metal complexes incorporating the Me₆tren ligand have been used for the reduction of nitrile

ions,¹² the modeling of cytochrome c oxidase,^{13,14} in aliphatic C-H bond activation,¹⁵ and as catalysts for atom transfer radical addition reactions.¹⁶

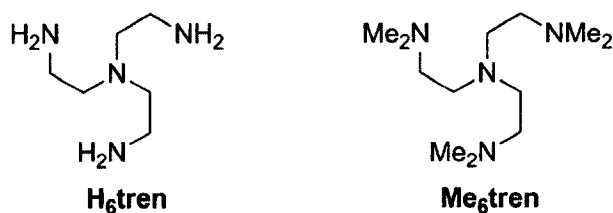


Figure 2.01: Tris(aminoethyl)amine (H₆tren) and tris(2-dimethylaminoethyl)amine (Me₆tren).

Although very frequently used to support transition metals,³ tren and derivatives have rarely been used to stabilize s-block compounds. The only H₆tren compounds of s-block elements were reported by White *et al.* who prepared and structurally characterized complexes of the type [(H₆tren)M]⁺ (M = Li, Na) (Figure 2.02, a).¹⁷ Using the Me₆tren ligand, Davidson and co-workers synthesized the amido complex (Me₆tren)Li(HMDS) (HMDS = hexamethyldisilazide) and the alkoxide species (Me₆tren)Na(OR)(HOR) (R = 2,4,6-trimethylphenoxide) and (Me₆tren)Na(OR') (R' = 2,6-di-*tert*-butyl-4-methylphenoxide) (Figure 2.02, b).¹⁸ Subsequently, in collaboration with Mulvey and Robertson, Davidson reported (Me₆tren)M(PhCH₂) (M = Li, Na, K), where the benzyl ligand was found to bind in a different mode depending on the metal (Figure 2.02, c). These are the only examples of monomeric s-block *organometallic* compounds supported by tren or a related ligand.¹⁹ Overall, group I compounds supported by tren or derivatives are far more prevalent than group II species. In fact, to date the only reported X-ray crystal structure of tren, or a derivative bound to a group II element, was (H₆tren)Sr(thd)₂ (thd = 2,2,6,6-tetramethyl-3,5-heptanedionate), prepared by Koo and co-workers (Figure 2.02, d).²⁰

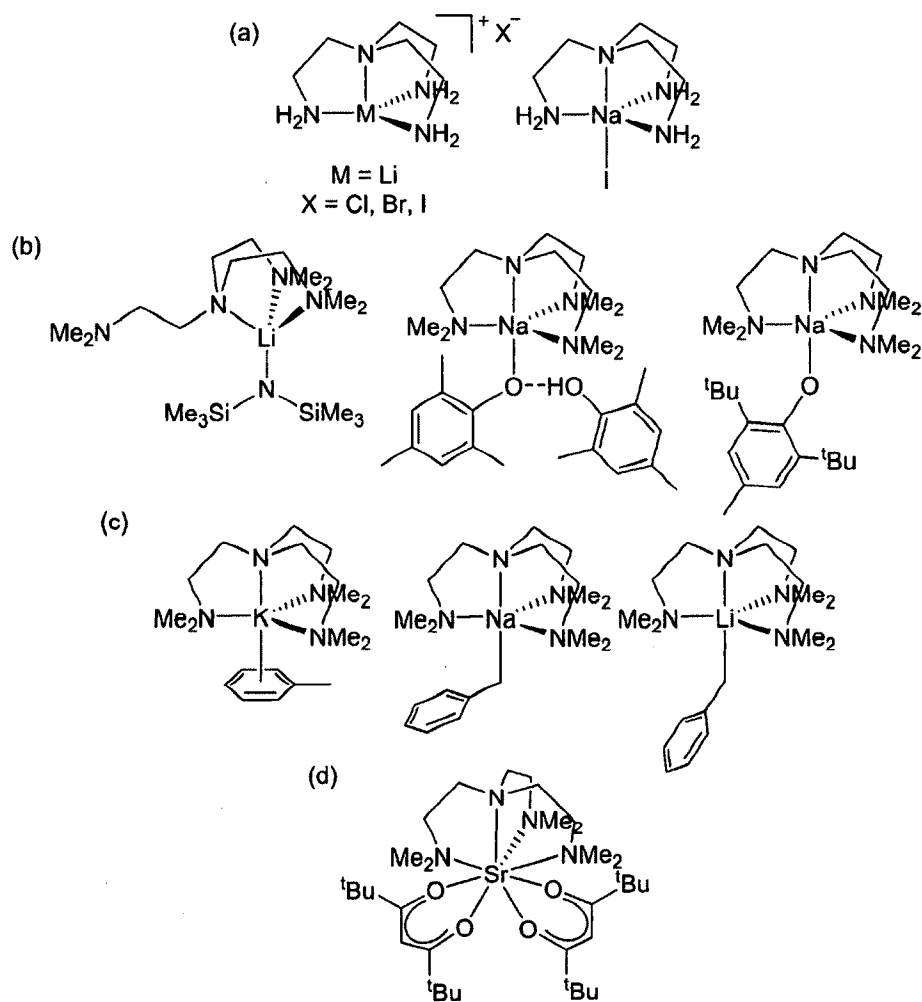


Figure 2.02: Group I and II complexes of H₆tren and Me₆tren.¹⁷⁻²⁰

Here, the synthesis of both coordination and organometallic complexes of Mg, supported by Me₆tren, are reported, the first Mg complexes containing any form of the tren ligand. In particular, using Me₆tren, rare examples of mono-methyl and dimethyl Mg species supported by the same ligand set have been isolated. Preliminary reactivity studies of the dimethyl Mg species are described.

II. Results and Discussion

a. Synthesis and Characterization of Mg Compounds

The reaction of Me₆tren with one equivalent of PhMgBr in diethyl ether resulted in the instant formation of a precipitate. The solid was isolated by filtration, and NMR spectroscopy and X-ray crystallography (*vide infra*) were used to establish its identity as [(Me₆tren)MgBr]Br (**1**), which had formed in approximately 50% yield based on Me₆tren (Figure 2.03). The filtrate from the reaction mixture contained half an equivalent of unreacted Me₆tren and presumably half an equivalent of Ph₂Mg or a related decomposition product, which had formed through the disproportionation of PhMgBr. There was no evidence to indicate that the diphenyl species (Me₆tren)MgPh₂ or the mono-phenyl, mono-halide species [(Me₆tren)MgPh]Br formed in the reaction.

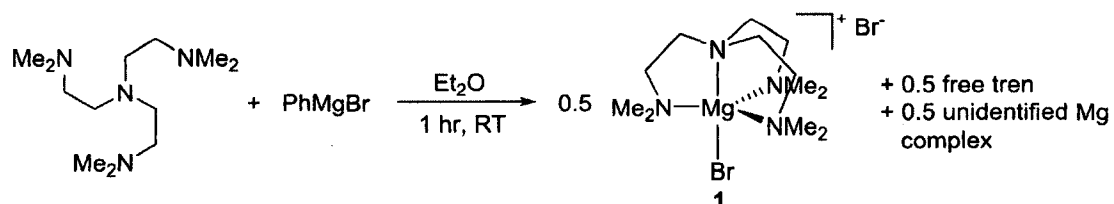


Figure 2.03: The reaction of Me₆tren with one equiv. PhMgBr.

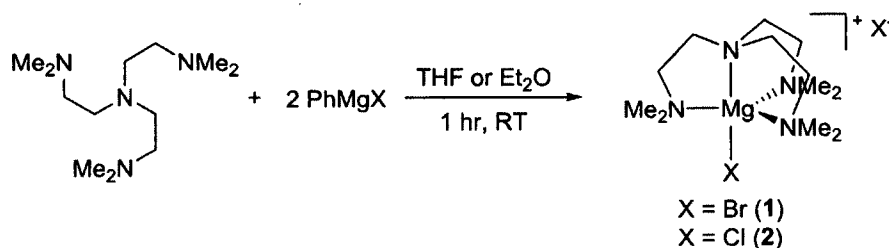


Figure 2.04: The reaction of Me₆tren with two equiv. PhMgX.

The reaction of Me₆tren with two equivalents of PhMgBr afforded **1** in near quantitative yield, with no unreacted ligand (Figure 2.04). The analogous reaction between two equivalents of PhMgCl and Me₆tren generated [(Me₆tren)MgCl]Cl (**2**) in 84% yield. The parent ions corresponding to both **1** and **2** were observed using ESI-MS (data for **1** shown

in Figure 2.05), although in the case of **1**, the parent ion was also accompanied by a small ion corresponding to **2**, which most likely forms due to the reaction of **1** with dichloromethane (the solvent for the ESI-MS experiment).

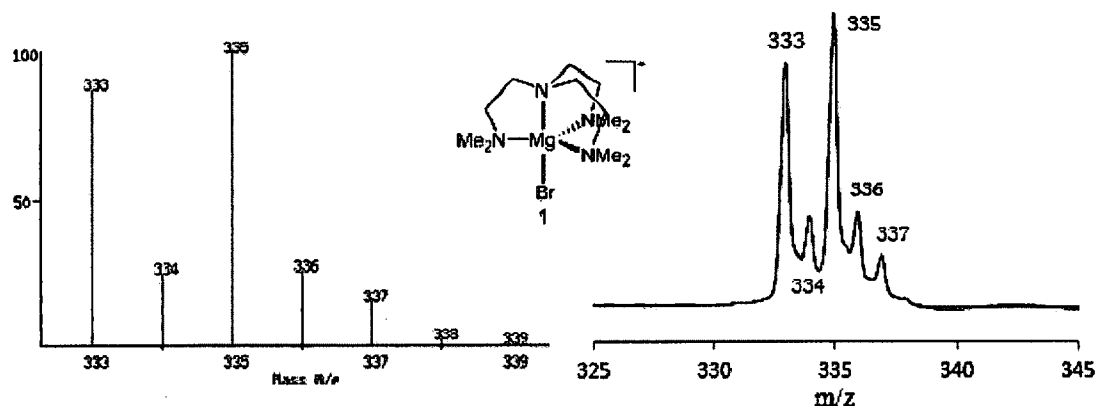


Figure 2.05: Simulated (left) and recorded (right) ESI-MS spectra of compound **1**. Spectra were simulated using the Isotope Distribution Calculator and Mass Spec Plotter²¹ and the appropriate molecular formula.

Both **1** and **2** are indefinitely stable when stored as solids in a nitrogen filled glove box but slowly decompose in dichloromethane and acetonitrile solutions at room temperature. Results for the reaction of PhMgX (X = Cl or Br) with tetradentate Me₆tren ligand are consistent with those reported for the reaction of PhMgX with tridentate terpy ligands, where only dihalide species were observed.²² To the best of our knowledge, **1** and **2** represent the first time the tren ligand or any other neutral tetradentate non planar nitrogen ligand has been coordinated to Mg.

Compound **1** was characterized by X-ray crystallography (Figure 2.06), which clearly indicates that the coordination number around Mg is five, with an outersphere bromide counterion. Presumably, steric factors prevent the outersphere bromide from coordinating and forming a six coordinate Mg center. The geometry around Mg is trigonal bipyramidal with the tren ligand occupying three equatorial and one axial site, and the

coordinated bromide occupying the second axial site. There is a C_3 rotation axis along the N(1)-Mg(1)-Br(1) bond and the angle formed between any of the equatorial nitrogens, the Mg center, and the bromide ligand (for example N(2)-Mg(1)-Br(1) is $98.25(12)^\circ$) is larger than the expected 90° for an idealized trigonal bipyramidal structure. This distortion occurs because the Mg atom sits slightly out of the plane (0.316\AA) formed by the three equatorial nitrogen atoms. As a result, the bond angles between any two of the equatorial nitrogen atoms and Mg (for example N(2)-Mg(1)-N(2') is $117.98(6)^\circ$) are not 120° . The distances between the Mg center and the axial and equatorial nitrogens are $2.193(8)\text{\AA}$ and $2.193(5)\text{\AA}$, respectively, both unremarkable for Mg-N bonds.²³ Previously, transition metal compounds of the type $[(\text{Me}_6\text{tren})\text{MBr}]\text{Br}$ ($\text{M} = \text{Co},^{24} \text{Cu},^{25} \text{Ni},^{25} \text{Mn},^{26} \text{Fe},^{26}$ and Zn^{26}) were prepared and crystallized by Orioli and co-workers. The bond lengths and angles around the metal centers in those species are comparable to those observed in **1**.

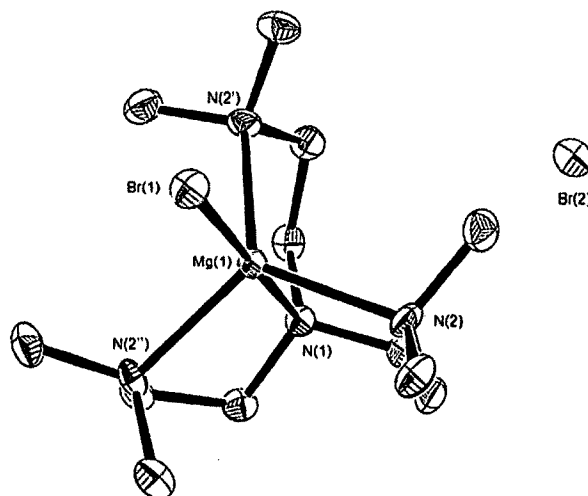


Figure 2.06: ORTEP²⁷ of **1** at 30% probability (hydrogen atoms have been omitted for clarity). A C_3 axis is present along the N(1)-Mg(1)-Br(1) bond. Selected bond lengths (\AA) and angles ($^\circ$): Mg(1)-N(1) $2.193(8)$, Mg(1)-N(2) $2.193(5)$, Mg(1)-Br(1) $2.503(4)$, N(1)-Mg(1)-N(2) $81.75(12)$, N(1)-Mg(1)-Br(1) $180.00(11)$, N(2)-Mg(1)-Br(1) $98.25(12)$, N(2)-Mg(1)-N(2') $117.98(6)$.

In contrast to the reaction between Me_6tren and PhMgBr , a mixture containing two products was isolated when one equivalent of MeMgBr was treated with Me_6tren (Figure 2.07). One of these products was compound **1**, while the second product contained a peak integrating to three protons (relative to the Me_6tren ligand) at -1.69 ppm in the ^1H NMR spectrum at 25°C . This second product was too unstable to record a $^{13}\text{C}\{^1\text{H}\}$ NMR spectrum at room temperature but at -40°C , a peak at -19.2 ppm was visible in the $^{13}\text{C}\{^1\text{H}\}$ NMR spectrum. On the basis of the ^1H and $^{13}\text{C}\{^1\text{H}\}$ NMR data, the second product is assigned as $[(\text{Me}_6\text{tren})\text{MgMe}]\text{Br}$ (**3**). We believe that the bromide ligand is outersphere by analogy to compound **1**. In order to balance the stoichiometry in Figure 2.07, a third product is required. Although there was no evidence for the formation of $(\text{Me}_6\text{tren})\text{MgMe}_2$, a significant amount of free Me_6tren and a small Mg side product were observed. These could be separated from **1** and **3** by filtration, as **1** and **3** precipitated from the reaction mixture. The relative ratio of **1** to **3** was 1.4:1. The addition of 2,6-lutidine·HBr to a CD_2Cl_2 solution of a mixture of **1** and **3** resulted in the quantitative conversion of **3** to **1**. Furthermore, the evolution of methane (identified by ^1H NMR spectroscopy) in a quantity consistent with the initial amount of **3** present in solution was observed. This provides further evidence for the assignment of **3** as the second component of the mixture. Unfortunately, **3** could not be separated from **1** as the solubilities of both compounds were similar in solvents in which they were stable (THF) and **3** was unstable when dissolved in dichloromethane or acetonitrile for periods of time greater than five minutes. To the best of our knowledge the only other examples of Me_6tren supported organometallic complexes were reported by Vacca and co-workers who prepared $[(\text{Me}_6\text{tren})\text{HgR}][\text{CF}_3\text{SO}_3]$ ($\text{R} = \text{Me}, \text{Ph}$),²⁸ though

only the later was characterized by X-ray crystallography, and Mulvey, Robertson and Davidson who synthesized $(\text{Me}_6\text{tren})\text{M}(\text{PhCH}_2)$ ($\text{M} = \text{Li}, \text{Na}, \text{K}$).¹⁷

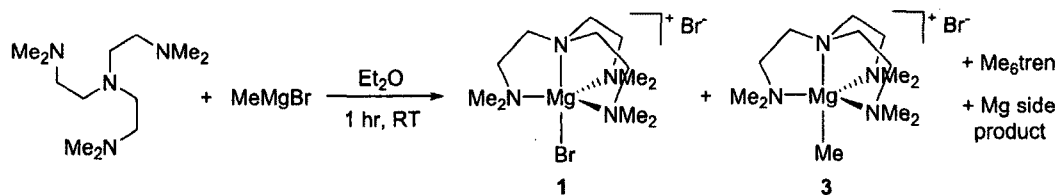


Figure 2.07: The reaction of Me₆tren with 1 equiv. MeMgBr.

The relative ratio of **1** and **3** could be changed by varying the number of equivalents of Grignard reagent used and though neither could be formed exclusively, one equivalent of Grignard reagent produced a higher proportion of **3** (1.4:1 ratio of **1** to **3**) compared with two equivalents (3:1 ratio of **1** to **3**). A similar trend was observed when MeMgCl was used as the Grignard reagent, where **2** was observed as the product. Again, the two components could not be separated as their solubilities in a range of common solvents were similar. The results from the reaction of Me₆tren and MeMgBr or MeMgCl are different from those observed in reactions between terpy and the same Grignard reagents. In the terpy systems there was no evidence for the formation of a ligated mixed Mg methyl/halide species and only the ligated Mg dihalide, Me₂Mg, and an unidentified terpy containing species from disproportionation of the Grignard reagent were observed.²² The κ⁴ Me₆tren ligand may assist in thermodynamically stabilizing the mixed methyl/halide species towards disproportionation compared with terpy. Previous work has demonstrated that disproportionation is more favorable for phenyl species compared with methyl species, and current results for the reactions of MeMgX and PhMgX with Me₆tren are consistent with this trend.²²

The reaction of Me₆tren with 4 equivalents or greater of MeMgBr resulted in the formation of a new tren-containing product. X-ray crystallography revealed that the new product was [(Me₆tren)MgBr]₂[MgBr₄] (**4**) (Figure 2.08), an analog of **1** with a different counterion. This was also confirmed by ESI-MS, where the single peak observed was attributed to the cationic fragment of **4**. The change in counterion caused a very slight perturbation in the ¹H NMR shifts (Figure 2.09). In **4** the most downfield triplet from the methylene protons appears at 3.06 ppm, whereas in **1** it is seen at 3.08 ppm. Similarly, the NMe₂ protons are at 2.56 ppm in **1** and 2.53 ppm in **4**. X-ray crystallography demonstrates that both cations in the structure are slightly distorted trigonal bipyramids with lengths and angles comparable to those in **1**. As in **1**, the metal center is positioned just below the plane formed by the three terminal nitrogen atoms and N(1)-Mg(1)-Br(1) is 98.55(7)Å and N(5)-Mg(2)-Br(2) is 97.20(7)Å. The ligand is bound in a κ⁴ manner which is supported by the distances between the tripodal nitrogen, where Mg (Mg(1)-N(4) is 2.197(2)Å and Mg(2)-N(8) is 2.205(2)Å). Using MeMgI and observing the reaction by ¹H NMR spectroscopy, an analogous product to **4** was formed, though the corresponding chloride product has not been observed, even when 10 equivalents of MeMgCl were used. Crystallization of **4** by layering of toluene onto a saturated solution of dichloromethane yielded the same cationic unit, but with an alternative chloride containing counterion, [(Me₆tren)MgBr]₂[Br₂Mg(μ-Cl)]₂ (**5**) (Figure 2.09). The lengths and angles are unremarkable in comparison with **1** and **4**, though this is the first time the [Br₂Mg(μ-Cl)]₂²⁻ counterion has been described in the literature although a similar compound, [Cd(Me₆tren)I]₂[Cd₂I₆], was previously reported by Ciampolini and co-workers.²⁹

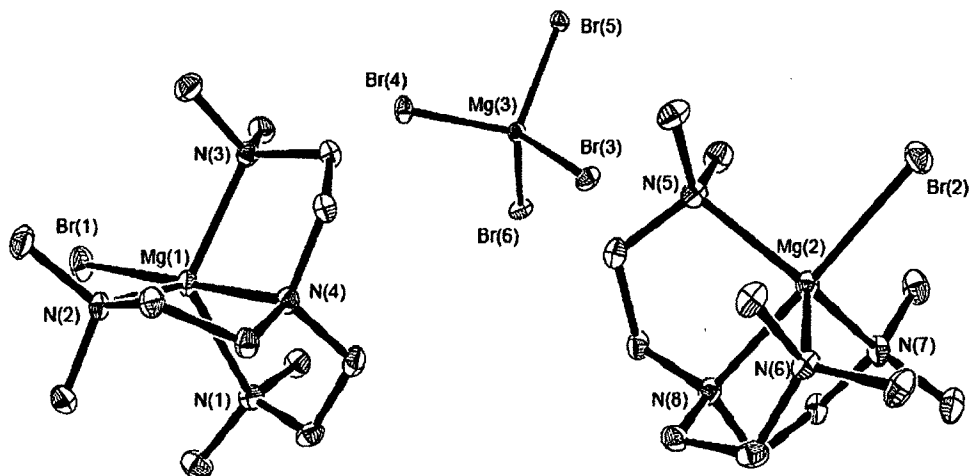


Figure 2.08: ORTEP²⁷ of **4** at 30% probability (hydrogen atoms and toluene of crystallization have been omitted for clarity). Selected bond lengths (Å) and angles (°): Molecule A (left) Mg(1)-N(1) 2.197(2), Mg(1)-N(2) 2.177(2), Mg(1)-N(3) 2.182(2), Mg(1)-N(4) 2.197(2), Mg(1)-Br(1) 2.4970(9), N(1)-Mg(1)-N(2) 117.42(9), N(1)-Mg(1)-N(3) 118.98(9), N(1)-Mg(1)-Br(1) 98.55(7), N(2)-Mg(1)-N(3) 117.11(9), N(2)-Mg(1)-Br(1) 99.39(7), N(3)-Mg(1)-Br(1) 97.68(7), N(4)-Mg(1)-Br(1) 179.06(7). Molecule B (right) Mg(2)-N(5) 2.213(2), Mg(2)-N(6) 2.193(3), Mg(2)-N(7) 2.196(2), Mg(2)-N(8) 2.205(2), Mg(2)-Br(2) 2.4787(9), N(5)-Mg(2)-N(6) 118.72(9), N(6)-Mg(2)-N(7) 115.89(10), N(5)-Mg(2)-Br(2) 97.20(7), N(7)-Mg(2)-N(5) 118.38(10), N(6)-Mg(2)-Br(2) 100.28(7), N(7)-Mg(2)-Br(2) 99.19(7), N(8)-Mg(2)-Br(2) 178.37(7).

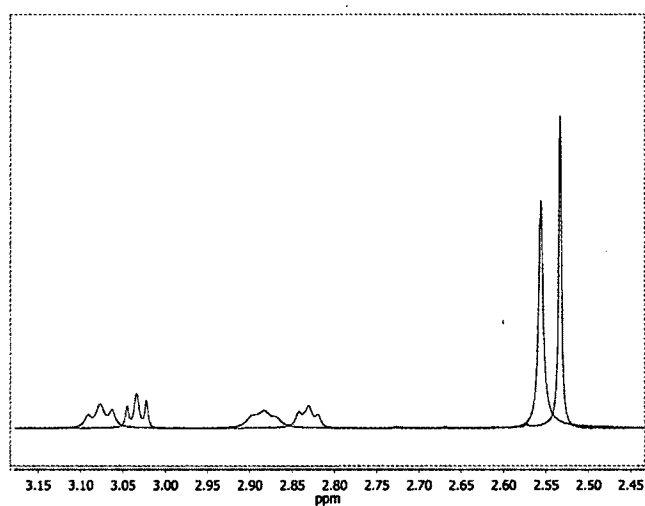


Figure 2.09: Overlaid ¹H NMR spectra of **1** (blue) and **4** (red).

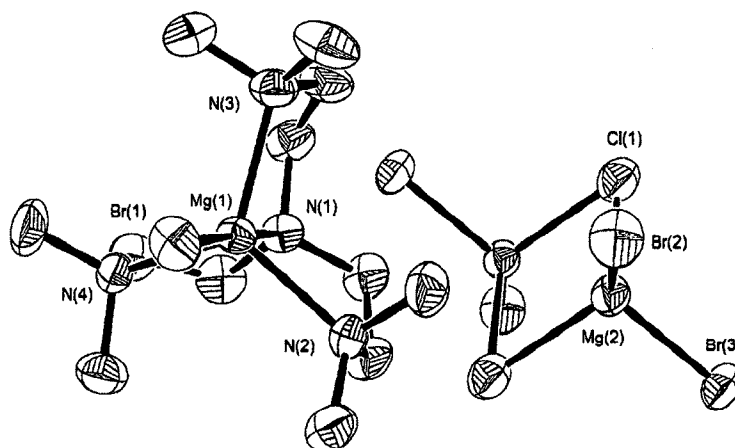


Figure 2.10: ORTEP²⁷ of **5** at 30% probability (hydrogen atoms have been omitted for clarity, There is only half a counter ion per asymmetric unit, whole ion is depicted here for clarity). Selected bond lengths (Å) and angles (°): Mg(1)-N(1) 2.159(5), Mg(1)-N(2) 2.177(6), Mg(1)-N(3) 2.162(5), Mg(1)-N(4) 2.169(5), Mg(1)-Br(1) 2.457(3), N(2)-Mg(1)-N(3) 116.22(19), N(3)-Mg(1)-N(4) 115.8(2), N(4)-Mg(1)-N(2) 120.84(18) N(1)-Mg(1)-Br(1) 178.45(14), N(2)-Mg(1)-Br(1) 98.48(13), N(3)-Mg(1)-Br(1) 100.31(13), N(4)-Mg(1)-Br(1) 98.12(14).

In an attempt to isolate a pure sample of an organometallic Mg complex, Me₆tren was treated with dimethyl magnesium (Me₂Mg) in diethyl ether. Filtration and storage at -80°C for 24 hours, generated a precipitate. The solid was isolated and characterized by NMR spectroscopy and X-ray crystallography (Figures 2.11 and 2.12) as (Me₆tren)MgMe₂ (**6**). Compound **6** is thermally unstable and needed to be stored at -30°C in a nitrogen filled glove box. This thermal instability is presumably why **6** was not observed as a disproportionation product in the reaction between MeMgBr and Me₆tren (Figure 2.07).

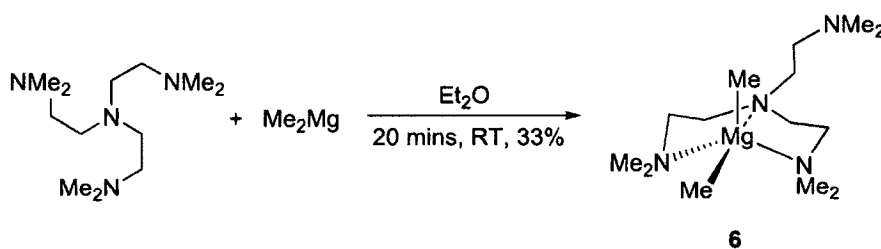


Figure 2.11: The reaction of Me₆tren with 1 equiv. Me₂Mg.

Interestingly, the solid state structure of **6** displays an unusual binding mode of Me₆tren, where the third arm of the ligand is free and is not coordinated to Mg. In addition, the bond length between the axial nitrogen of Me₆tren and the Mg center is extremely long (2.4814(13)Å). A survey of all Mg-N bonds in the Cambridge Structural Database^{23,30} revealed that this distance is significantly longer than the mean Mg-N distance of 2.120Å. The sum of van der Waals radii of Mg and N is 3.28Å³¹ which suggests that a bonding interaction between the central nitrogen in Me₆tren and the Mg center is present, but weak. Previously, κ³ coordination of Me₆tren has been observed in transition metal complexes containing Pd,³² Ru,³³ and Cu.¹⁶ However, the only other example for an s-block element was reported by Davidson *et al.*, who prepared (Me₆tren)Li(HMDS).¹⁸ Though not crystallographically confirmed, Macbeth and co-workers used IR spectroscopy to postulate that [(Me₆tren)Cu(CO)]PF₆ featured a κ³ bound ligand.³⁴ More recently, the Me₆tren ligand has been observed to bind κ² to zinc and bridge three gallium centers, with each metal bound to one arm.³⁵

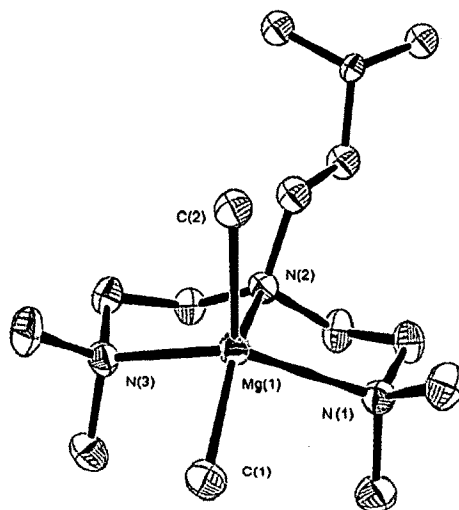


Figure 2.12: ORTEP²⁷ of **6** at 30% probability (hydrogen atoms have been omitted for clarity; only one site of disordered Me₆tren arm shown). Selected bond lengths (Å) and angles (°): Mg(1)-N(1) 2.3148(11), Mg(1)-N(2) 2.4814(11), Mg(1)-N(3) 2.2959(12), Mg(1)-C(1) 2.2042(14), Mg(1)-C(2) 2.1710(13), N(1)-Mg(1)-N(2) 73.98(4), N(1)-Mg(1)-N(3) 131.76(4), N(1)-Mg(1)-C(1) 94.14(5), N(1)-Mg(1)-C(2) 112.64(5), N(2)-Mg(1)-N(3) 74.27(4), N(2)-Mg(1)-C(1) 149.33(5), N(2)-Mg(1)-C(2) 97.84(4), N(3)-Mg(1)-C(1) 95.09(5), N(3)-Mg(1)-C(2) 106.87(5), C(1)-Mg(1)-C(2) 112.82(6).

Comparison of the structure of **6** with (PMDTA)MgMe₂ (PMDTA = *N,N,N',N',N''*-pentamethyldiethylenetriamine), one of only three other crystallographically characterized monomers to feature two terminal methyl groups bound to Mg,³⁶⁻³⁸ reveals significant lengthening of the Mg(1)-N(2) bond of **6**. In (PMDTA)MgMe₂, which features a κ³ PMDTA ligand, the corresponding Mg-N bond length is 2.424(2)Å.³⁷ This suggests stronger binding for the tridentate PMDTA ligand, than for Me₆tren, once one arm of the Me₆tren is no longer coordinated. The overall geometry around Mg in **6** is square pyramidal. One of the methyl groups is *trans* to the apical nitrogen of the Me₆tren ligand and the strong *trans* influence of the methyl ligand is presumably partially responsible for the elongated Mg(1)-N(2) bond distance. The other methyl ligand is *trans* to a vacant site and as a result, the Mg(1)-C(2) bond distance is significantly shorter (2.1710(13)Å)

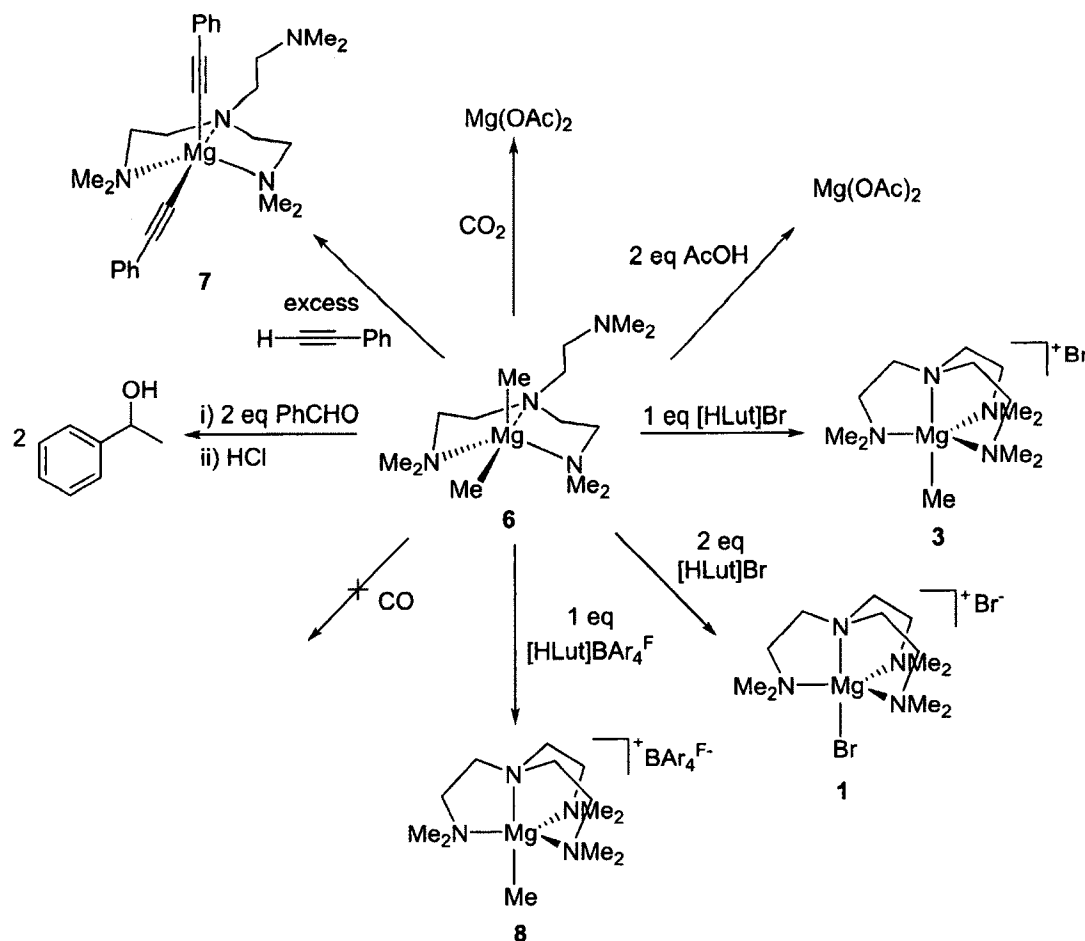
compared to the Mg(1)-C(1) bond distance (2.2042(14) Å). The bond distances between Mg and the Me₆tren ligands are significantly longer in **6** compared to those observed in **1**. For example, the Mg(1)-N(1) and Mg(1)-N(3) bond distances in **6** are 2.3148(11) and 2.2959(12)Å, respectively, while the corresponding distance in **1** is 2.193(5)Å (due to symmetry requirements the two Mg-N distances are identical). The longer distances in **5** probably occur because the compound is neutral, whereas **1** is cationic.

Although the solid state structure of **6** shows one of the ligand arms to be chemically non-equivalent, the ¹H NMR spectrum in toluene-*d*₈ displays only one environment for the ligand methylene protons between -90°C and 25°C. This NMR behavior is comparable to that observed in transition metal complexes containing κ³ coordinated tren, which also only show one signal for the methylene protons at low temperature.^{16,18} Consistent with the observation of only one methylene environment, only one Mg-Me resonance (at -0.99 ppm), integrating to six protons, is observed in the ¹H NMR spectrum of **6**, even at low temperature. The ¹³C{¹H} NMR spectrum of **6** features a resonance at -12.53 ppm, which is assigned to the Mg bound Me groups.

b. Reactivity of Mg Complexes

Given the relative paucity of ligated bis(alkyl) Mg species, we were interested in exploring the reactivity of **6**. The reaction of **6** in C₆D₆ with a variety of substrates with O-H and N-H bonds such as aniline, benzyl amine, 4-*tert*-butylcatechol, benzyl alcohol, and 4-*tert*-butylphenol all resulted in the liberation of Me₆tren and no Mg containing products were isolated. In all cases a precipitate formed which could not be easily dissolved. The observation of free Me₆tren suggests that even the tetradentate Me₆tren ligand is not tightly bound to Mg. The addition of 10 equivalents of phenyl acetylene to a solution of **6** in

benzene formed $(\text{Me}_6\text{tren})\text{Mg}(\text{CCPh})_2$ (**7**), which was thermally unstable (Scheme 2.01). In analogous fashion to **6**, **7** displays a different signal pattern in its ^1H NMR spectrum than **1-4**. In **7**, a resonance associated with one of the methylene proton triplets appears furthest upfield, while in **1-4**, the signal associated with the nitrogen methyl groups appears the furthest upfield. In lieu of an X-ray crystal structure, this could indicate that **7** also features a κ^3 bound Me_6tren .



Scheme 2.01: Summary of the reactivity of $(\text{Me}_6\text{tren})\text{MgMe}_2$ (**6**).

The reaction of **6** with carbon dioxide in C_6D_6 led to the instant formation of a white precipitate and free Me_6tren was present in the 1H NMR spectrum. The same white precipitate was formed when two equivalents of acetic acid were added to a solution of **6** in C_6D_6 . In this experiment two equivalents of methane were also observed by 1H NMR spectroscopy. On this basis and by comparison with an authentic sample, we believe that the white precipitate is $Mg(OAc)_2$. It is probable that this reaction occurs by nucleophilic attack of the methyl group on electrophilic carbon dioxide but other mechanisms cannot be ruled out at this stage. Further evidence of the nucleophilic character of the methyl ligands was provided by the reaction of **6** with two equivalents of benzaldehyde which yielded two equivalents of 1-phenylethanol, the product of nucleophilic attack, after an acidic workup. Compound **6** did not react with carbon monoxide. The weak binding of $tren$ displayed in these reactions is in direct contrast to the findings of Parkin and co-workers who were able to isolate a wide range of ligated Mg products from the reactions of {tris(pyrazolyl)hydroborato} Mg alkyl derivatives with substrates such as carbon dioxide, alcohols, terminal alkynes and ketones among others.³⁹⁻⁴¹ It appears that the use of an anionic ligand vastly improves the stability of Mg complexes supported by nitrogen-based ligands compared with our tripodal neutral nitrogen donor set.

The reaction of **6** with two equivalents of 2,6-lutidine·HBr in CD_2Cl_2 formed **1**, while reaction with one equivalent generated the mono-methyl species **3**, which was observed by 1H NMR spectroscopy, though the previously mentioned instability led to swift decomposition. In an attempt to isolate a solution-stable Me_6tren -ligated Mg mono-methyl species, **6** was reacted with 2,6-lutidine· $HBAr_4^F$ (BAr_4^F = tetrakis(3,5-bis(trifluoromethyl)phenyl)borate) in diethyl ether. On the basis of NMR spectroscopy and

ESI-MS, the resulting product is proposed to be $[(\text{Me}_6\text{tren})\text{MgMe}]\text{BAr}_4^{\text{F}}$ (**8**). NMR spectroscopy showed ligand resonances that are nearly identical to those observed for **3** and Mg-Me resonances were observed at -1.65 and -19.38 ppm in the ^1H and $^{13}\text{C}\{^1\text{H}\}$ spectra respectively. A single peak at 62.86 ppm in the ^{19}F NMR spectrum confirms the presence of the BAr_4^{F} counterion in **8**. The compound is stable for at least one hour in CD_2Cl_2 at room temperature, which is in vast contrast to **3**, where decomposition is observed almost instantly. Addition of 2,6-lutidine·HBr to a solution of **8** in CD_2Cl_2 results in the liberation of methane (detected by ^1H NMR spectroscopy) and the formation of a new tren-containing product. This new compound displays more downfield ^1H NMR shifts when compared to **8**, and the disappearance of the Mg-Me peak are consistent with the formation of $[(\text{Me}_6\text{tren})\text{MgBr}]\text{BAr}_4^{\text{F}}$. Though Mg mono-methyls ligated by anionic nitrogen ligands are comparatively plentiful,⁴²⁻⁴⁵ **8** is only the second example of a compound containing a Mg-Me supported only by a neutral nitrogen donor set. The other example, $[\text{MeMg}(14\text{N}4)]\text{Cp}$ (14N4 = 1,4,8,11-tetramethyl-1,4,8,11-tetraazacyclotetradecane; Cp = C_5H_5^-), features a planar nitrogen containing macrocycle.⁴⁶ Compound **8** is considerably less stable than either $[\text{MeMg}(14\text{N}4)]\text{Cp}$ or examples of mono-methyls with anionic ligands.

III. Conclusions

The reaction of various Grignard reagents with Me_6tren has been shown to yield a series of Mg compounds where the type and quantity of the Grignard has a pronounced effect on the identity of the product. For RMgX (R = Ph, X = Cl, Br) only $[(\text{Me}_6\text{tren})\text{MgX}]\text{X}$ was isolated, whereas when R = Me, a mixture containing both $[(\text{Me}_6\text{tren})\text{MgMe}]\text{X}$ and

$[(\text{Me}_6\text{tren})\text{MgX}]_2$ was observed. These compounds represent the first time Mg has been coordinated to any type of tren ligand. The tren ligand was also able to support the unusual Mg dimethyl species, $(\text{Me}_6\text{tren})\text{MgMe}_2$, which was formed through the reaction of Me_6tren with Me_2Mg . $(\text{Me}_6\text{tren})\text{MgMe}_2$ has an atypical structure in the solid state, where one of the ligand arms is not coordinated to the Mg center. When $(\text{Me}_6\text{tren})\text{MgMe}_2$ and phenyl acetylene were mixed, $(\text{Me}_6\text{tren})\text{Mg}(\text{CCPh})_2$ formed, but the use of aniline, benzyl amine, 4-*tert*-butylphenol and 4-*tert*-butylcatechol all resulted in decomposition. Insertion into both Mg-Me bonds was observed when $(\text{Me}_6\text{tren})\text{MgMe}_2$ was placed under 1 atm of carbon dioxide, though no reaction was observed with CO. Reaction with benzaldehyde produced 1-phenylethanol after acidic workup, further confirming the nucleophilic nature of the methyl group in this complex. The reaction of $(\text{Me}_6\text{tren})\text{MgMe}_2$ with one equivalent of 2,6-lutidine· HBAr^{F} forms $[(\text{Me}_6\text{tren})\text{MgMe}]\text{BAr}^{\text{F}}$ which is more stable in solution than the analogous compound with a halide counterion. Our previous work on the binding of κ^3 terpy to Mg was hindered by both ligand dissociation and an inability to observe any organometallic products. The use of a κ^4 ligand appears to have stabilized organometallic compounds and allowed us to prepare relatively rare examples of well-defined Mg methyl species.

IV. Experimental

a. General Methods

Experiments were performed under a dinitrogen atmosphere in an M-Braun dry box or using standard Schlenk techniques, unless otherwise noted. (Under standard glovebox conditions, purging was not performed between uses of pentane, diethyl ether, benzene,

toluene and THF; thus, when any of these solvents were used, traces of all these solvents were in the atmosphere and could be found intermixed in the solvent bottles.) Moisture- and air-sensitive liquids were transferred by stainless steel cannula on a Schlenk line or in a dry box. Solvents were dried by passage through a column of activated alumina followed by storage under dinitrogen. All commercial chemicals were used as received, except where noted. MeMgBr, MeMgCl, PhMgCl (all in THF), MeMgI in diethyl ether and PhMgBr in both diethyl ether and THF were purchased from Acros Organics and titrated using salicylaldehyde phenylhydrazone.⁴⁷ 2,2',2''-Triaminotriethylamine (tren) was purchased from Strem Chemicals. Trimethoxybenzene and 1-phenylethanol were purchased from Sigma Aldrich, as were phenyl acetylene, aniline, benzaldehyde, benzyl alcohol and benzyl amine which were all distilled prior to use. 4-*tert*-butylphenol and 4-*tert*-butylcatechol were sublimed before use and were purchased from Sigma Aldrich and Acros Organics, respectively. Deuterated solvents were obtained from Cambridge Isotope Laboratories. CD₂Cl₂ and CD₃CN were dried using CaH₂ and C₆D₆ and toluene-*d*₈ were dried using sodium metal. All deuterated solvents were vacuum-transferred prior to use. NMR spectra were recorded on Bruker AMX-400, -500 or Varian-300 spectrometers at ambient probe temperatures unless otherwise stated. Chemical shifts are reported in ppm with respect to residual internal protio solvent for ¹H and ¹³C{¹H} NMR spectra and to an external standard for ¹⁹F{¹H} spectra (CFCl₃ at 0.0 ppm). NMR coupling constants (*J*) are given in Hz. IR spectra were measured using a diamond Smart Orbit ATR on a Nicolet 6700 FT-IR instrument. Elemental analysis was not performed due to extreme instability of almost all compounds studied in this work. Literature procedures were utilized to

synthesize Me_2Mg ,³⁷ 2,6-lutidine·HCl⁴⁸ and Me_6tren ,⁴⁹ while 2,6-lutidine·HBr and 2,6-lutidine·HBAr^F were prepared via an adapted literature procedure.⁴⁸

b. X-ray Crystallography

X-ray diffraction experiments were carried out on either a Rigaku Mercury 275R CCD (SCX mini) diffractometer using graphite-monochromated Mo $K\alpha$ radiation ($\lambda = 0.71073\text{\AA}$) at -50°C , a Rigaku R-AXIS RAPID diffractometer coupled to a R-AXIS RAPID imaging plate detector with graphite-monochromated Mo $K\alpha$ radiation ($\lambda = 0.71073\text{\AA}$) at -180°C or a Rigaku MicroMax-007HF diffractometer coupled to a Saturn994+ CCD detector with Cu $K\alpha$ radiation ($\lambda = 1.54178\text{\AA}$) at -180°C . The crystals were mounted on MiTeGen polyimide loops with immersion oil. The data frames were processed using Rigaku CrystalClear and corrected for Lorentz and polarization effects. Using Olex2,⁵⁰ the structure was solved with the XS⁵¹ structure solution program using direct methods and refined with the XL⁵¹ refinement package using least squares minimisation. The non-hydrogen atoms were refined anisotropically. Hydrogen atoms were refined using the riding model.

c. ESI-MS

Mass spectra were collected using the home-built cryogenic ion mass spectrometer of Johnson and co-workers.^{52,53} Briefly, millimolar solutions of each species were prepared and drawn into the electrospray syringe under inert atmosphere. The syringe was then quickly transported into a nitrogen-purged enclosure attached to the inlet capillary of the mass spectrometer and the solutions were electrosprayed through a $30\ \mu\text{m}$ fused silica capillary tip. The generated ions were guided through four differentially pumped stages using two RF-only quadrupole guides and an octopole guide. The ions were then directed

90° with a DC quadropole bender through a second octopole and einzel lens, which guide the ions into a Paul trap (Jordan) cooled to 10 K with a closed-cycle helium cryostat. He buffer gas was introduced into the trap with a pulsed-valve allowing for collisional cooling of the ions. After equilibrating in the trap for about 90 ms, the ions were extracted by applying +/- 90 V push/pull to the entrance and exit lenses of the trap, respectively. The ejected ions next entered the extraction region of a Wiley-McLaren TOF mass spectrometer, accelerating the ions through a field-free flight tube, and finally detected with a MCP detector.

d. Synthesis and Characterization of Compounds

[(Me₆tren)MgBr]Br (1)

15 ml diethyl ether was transferred by cannula to a Schlenk flask containing PhMgBr (2.71 M in diethyl ether, 0.64 ml, 1.74 mmol) and subsequently added to solution of Me₆tren in toluene (50 mg/ml, 4.00 ml, 0.87 mmol) diluted with 15 ml diethyl ether. The immediate formation of a light brown precipitate was observed and the mixture was stirred for one hour at RT. The reaction mixture was filtered and the off white solid collected. The crude product was washed with 2 x 15 ml toluene and dried under reduced pressure to yield **1** as a white powder. Yield: 0.35 g (97%). X-ray diffraction quality crystals were grown by layering toluene on a saturated acetonitrile solution of **1** at -30°C.

¹H NMR (CD₂Cl₂, 400.0 MHz): δ 3.08 (6H, t, CH₂, J = 5.51 Hz), 2.88 (6H, t, CH₂, J = 5.20 Hz), 2.56 (18 H, s, N(CH₃)₂). ¹³C NMR (CD₂Cl₂, 100 MHz): δ 56.48, 50.20, 46.53. ESI-MS (CH₂Cl₂): 334 (M⁺). IR (ATR, Smart Orbit diamond plate, cm⁻¹): 2979.3, 2874.6, 1642.0, 1590.7, 1484.0, 1474.7, 1457.5, 1293.9, 1170.8, 1096.7, 1018.7, 1000.2, 938.2, 930.7, 904.7, 798.5, 769.3, 698.1.

[(Me₆tren)MgCl]Cl (2)

Me₆tren in toluene (50 mg/ml, 3.00 ml, 0.65 mmol) was diluted with 20 ml diethyl ether and added to a Schlenk flask containing PhMgCl (1.73 M in THF, 753 μ l, 1.30 mmol) in 20 ml diethyl ether at RT. A white precipitate formed instantly, and the mixture was stirred for one hour. The crude product was isolated by filtration and purified by addition of pentane to a concentrated THF solution to give **2** as a white powder. Yield: 0.18 g (84%).

¹H NMR (CD₂Cl₂, 300.0 MHz): δ 3.06 (6H, t, CH₂, *J* = 4.92 Hz), 2.82 (6H, t, CH₂, *J* = 4.69 Hz), 2.51 (18 H, s, N(CH₃)₂). ¹³C {¹H} NMR CD₂Cl₂, 75 MHz): δ 56.44, 50.15, 46.27. ESI-MS (CH₂Cl₂): 290 (M⁺). IR (ATR, Smart Orbit diamond plate, cm⁻¹): 2968.0, 2845.0, 1472.9, 1293.9, 1173.3, 1101.6, 1039.9, 1023.1, 1010.4, 945.0, 933.2, 904.5, 801.9, 771.8.

[(Me₆tren)MgMe]Br (3)

Me₆tren in toluene (50 mg/ml, 3.00 ml, 0.65 mmol) was diluted with 30 ml diethyl ether and MeMgBr (1.24 M in diethyl ether, 525 μ l, 0.65 mmol) was added. A white precipitate formed instantly and the mixture was stirred for one hour at RT. Filtration of the reaction mixture yielded a white powder containing a mixture of **1** and **3** in a ratio of 1:0.7. The combined yield was 253 mg. Although both crystallization and extraction were attempted to separate **1** and **3**, these attempts were unsuccessful due to similar solubility of the compounds and the thermal instability of **3** in solution. The NMR line listing for **3** is given below.

¹H NMR (CD₂Cl₂, 400.0 MHz): δ 2.85 (6H, t, CH₂, *J* = 5.51 Hz), 2.67 (6H, t, CH₂, *J* = 4.54 Hz), 2.33 (18 H, s, N(CH₃)₂), -1.76 (3H, s, MgCH₃) ¹³C {¹H} NMR (CD₂Cl₂, 125 MHz, 233 K): δ 55.10, 49.48, 47.50, 42.66, -19.19.

[(Me₆tren)MgBr]₂[MgBr₄] (4)

Me₆tren in toluene (50 mg/ml, 2.00 ml, 0.44 mmol) was placed in a Schlenk flask containing 30 ml diethyl ether. MeMgBr (1.36 M in diethyl ether, 6.40 ml, 8.72 mmol) was added and a white precipitate formed. The mixture was stirred for eighty minutes and then filtered. The resulting precipitate was purified by dissolution in THF and precipitation by addition of pentane. The solid was collected and dried under reduced pressure to give **4** as a white powder. Yield: 189 mg (86%). Diffraction quality crystals were grown by layering toluene onto a saturated acetonitrile solution of **4** at -30°C.

¹H NMR (CD₂Cl₂, 300.0 MHz): δ 3.05 (6H, t, CH₂, J = 5.64 Hz), 2.86 (6H, t, CH₂, J = 5.86 Hz), 2.53 (18 H, s, N(CH₃)₂). ¹³C{¹H} NMR (CD₂Cl₂, 75 MHz): δ 56.52, 50.26, 46.52. ESI-MS (CH₂Cl₂): 334 (M⁺). IR (ATR, Smart Orbit diamond plate, cm⁻¹): 2972.5, 2874.0, 1471.5, 1457.5, 1354.8, 1293.6, 1171.1, 1097.8, 1019.5, 1000.8, 931.4, 903.8, 873.3, 799.4, 770.3.

(Me₆tren)MgMe₂ (5)

Me₆tren in toluene (45 mg/ml, 5 ml, 0.98 mmol) was placed in a Schlenk flask and the toluene removed *in vacuo*. To the resulting yellow oil, diethyl ether (30 mL) and Me₂Mg (53 mg, 0.98 mmol) were added and a cloudy solution with an off-white precipitate formed. The mixture was stirred for twenty minutes and then filtered into a Schlenk flask in a -78°C bath. The volume of the filtrate was reduced to ~4 ml and placed in a -80°C freezer. After twenty four hours, a white precipitate was present which was separated from the solvent by filtration. After washing the precipitate with pentane (2 x 5 ml), **5** was isolated as a thermally sensitive white powder which was stored in a -30°C freezer in a nitrogen filled

glovebox. Yield: 91 mg (33%). Diffraction quality crystals were grown by layering diethyl ether and pentane at -30°C.

^1H NMR (C_6D_6 , 400.0 MHz): δ 2.41 (6H, t, $\text{NCH}_2\text{CH}_2\text{N}$, $J = 5.66$ Hz), 2.06 (6H, t, $\text{NCH}_2\text{CH}_2\text{N}$, $J = 5.67$ Hz), 1.98 (18H, s, $\text{N}(\text{CH}_3)_2$), -0.99 (6H, s, MgCH_3). $^{13}\text{C}\{^1\text{H}\}$ NMR (C_6D_6 , 100 MHz): δ 55.29, 49.73, 46.88, -12.53.

(Me₆tren)Mg(CCP_h)₂ (6)

Compound **5** (20 mg, 0.07 mmol) was weighed into a vial and 2 ml benzene was added. Phenyl acetylene (77 μl , 0.70 mmol) was added to the solution. The mixture was agitated for three minutes and all the volatiles removed under reduced pressure to yield **6** as a white powder. Compound **6** is thermally unstable and was stored in a -30°C freezer in a nitrogen filled glovebox. Yield: 31 mg (97%).

^1H NMR (C_6D_6 , 400.0 MHz): δ 7.76 (4H, app. d, ArH, $J = 8.28$ Hz), 7.14 (4H, t, ArH, $J = 7.77$ Hz), 7.00 (2H, tt, ArH, $J = 7.41, 1.21$ Hz), 2.45 (6H, t, $\text{NCH}_2\text{CH}_2\text{N}$, $J = 5.41$ Hz), 2.25 (18H, s, $\text{N}(\text{CH}_3)_2$), 1.97 (6H, t, $\text{NCH}_2\text{CH}_2\text{N}$, $J = 5.63$ Hz). $^{13}\text{C}\{^1\text{H}\}$ NMR (C_6D_6 , 125 MHz): δ 131.90, 130.04, 129.83, 128.35, 125.11, 110.10, 54.98, 49.98, 46.15.

Reaction between 5 and CO₂ and CO

Compound **5** (5 mg, 0.02 mmol) was dissolved in C_6D_6 in a J. Young NMR tube. The mixture was degassed using three freeze-pump-thaw cycles and carbon dioxide introduced into the tube using a dual-manifold Schlenk line at RT. A ^1H NMR spectrum recorded less than ten minutes after carbon dioxide addition showed that free Me₆tren was present in solution along with a precipitate. The solvent was removed under vacuum and the resulting white precipitate dissolved in D_2O . The ^1H NMR spectrum of the precipitate was consistent

with an authentic sample of $\text{Mg}(\text{OAc})_2$. The reaction with CO was carried out in an analogous fashion, but only **5** was observed in the ^1H NMR spectrum after mixing.

Reaction between 5 and acetic acid

Compound **5** (5 mg, 0.02 mmol) was dissolved in C_6D_6 in a screw cap NMR tube. Acetic acid (0.083 M in THF, 500 μl , 0.042 mmol) was then added via a micro pipette and the tube quickly capped. Both Me_6tren and methane were visible in the ^1H NMR spectrum. The solvent was removed under reduced pressure and the residue dissolved in D_2O . The ^1H NMR spectrum indicated the formation of $\text{Mg}(\text{OAc})_2$ which, as above, was compared with a spectrum of an authentic sample.

Reaction of 5 with 2,6-lutidine·HBr

2,6-lutidine·HBr (3.3 mg, 0.02 mmol) was dissolved in CD_2Cl_2 in a screw cap NMR tube containing **5** (5 mg, 0.02 mmol) and the sample frozen in liquid nitrogen. A ^1H NMR spectrum recorded at RT indicated that the sample contained 92% **3** and 8% **1**. The same procedure was followed for the reaction with two equivalents of 2,6-lutidine·HBr (6.6 mg, 0.04 mmol). In this case only **1** was observed in the ^1H NMR spectrum.

Reaction of 5 with benzaldehyde

Compound **5** (5 mg, 0.02 mmol) was weighed into a vial and dissolved in 1 ml benzene to form a colorless solution. Benzaldehyde (3.6 μl , 0.04 mmol) was added by micropipette, with no visible change in the appearance of the solution. After agitating the solution for two minutes, HCl (0.147 M in diethyl ether, 238 μl , 0.04 mmol) was added, resulting in the formation of a white precipitate. The reaction mixture was filtered and the solvent removed from the filtrate by the passage of dinitrogen over the reaction vessel. A ^1H NMR

spectrum of the residue in CDCl_3 showed 1-phenylethanol to be the major product. This assignment was confirmed by comparison with an authentic sample.

[(Me₆tren)MgMe]BAr^F (7)

2,6-lutidine·HBAr^F (12.2 mg, 0.01 mmol) was dissolved in 2 ml diethyl ether and added dropwise to an agitated solution of **5** (4 mg, 0.01 mmol) in 3 ml diethyl ether. The colorless solution was stirred for one minute and all volatiles removed *in vacuo*. The residue was washed with 2 ml toluene and dried to yield **7** as a white solid. Yield: 14 mg (98%).

¹H NMR (CD_2Cl_2 , 400.0 MHz): δ 7.72 (8H, app t, ArH, J = 2.37), 7.56 (4H, br s, ArH), 2.72 (6H, t, CH₂, J = 5.26 Hz), 2.62 (6H, t, CH₂, J = 6.34 Hz), 2.38 (18 H, s, N(CH₃)₂), -1.65 (3H, s, MgCH₃). ¹³C{¹H} NMR (CD_2Cl_2 , 125 MHz, 233 K): δ 161.73 (q, J = 49.9), 134.62, 128.61 (q, J = 31.1), 124.42 (q, J = 272.6), 117.52, 54.91, 49.50, 47.58, 42.45, -19.38. ¹⁹F{¹H} NMR (CD_2Cl_2 , 376 MHz): δ 62.86. ESI-MS (CH_2Cl_2): 270 (M⁺).

Table 2.01: Crystallographic data for 1, 4, 5 and 6.

	1	4	5	6
Empirical formula	C ₁₂ H ₃₀ Br ₂ MgN ₄	C ₅₅ H ₁₂₈ Br ₁₂ Mg ₆ N ₁₆	C ₁₂ H ₃₀ Br ₃ ClMg ₂ N ₄	MgN ₄ C ₁₄ H ₃₀
Formula weight	414.53	2118.51	554.20	278.73
Temperature/K	223	93.15	223	93.15
Crystal system	cubic	monoclinic	triclinic	monoclinic
Space group	P2 ₁ 3	P2 ₁ /c	P-1	P2 ₁ /n
a/Å	12.193(17)	15.1927(3)	7.945(7)	8.3141(3)
b/Å	12.193(17)	19.9755(4)	9.961(8)	11.5776(5)
c/Å	12.193(17)	15.9698(11)	14.237(12)	19.5193(14)
α/°	90.00	90.00	104.590(14)	90.00
β/°	90.00	113.437(8)	95.656(16)	99.555(7)
γ/°	90.00	90.00	92.374(17)	90.00
Volume/Å ³	1813(4)	4446.7(3)	1082.4(16)	1852.80(16)
Z	4	2	2	4
ρ _{calc} /mg/mm ³	1.519	1.582	1.700	0.999
m/mm ⁻¹	4.502	7.154	5.773	0.091
F(000)	848.0	2124.0	552.0	616.0
Crystal size/mm ³	0.08 × 0.08 × 0.03	0.1 × 0.1 × 0.05	0.2 × 0.2 × 0.2	0.2 × 0.2 × 0.2
2θ range for data collection	6.68 to 50.48°	6.34 to 131.72°	6.24 to 49.42°	6.08 to 56.56°
Index ranges	-14 ≤ h ≤ 14, - 14 ≤ k ≤ 14, -14 ≤ l ≤ 14	-17 ≤ h ≤ 17, -23 ≤ k ≤ 21, -18 ≤ l ≤ 18	-9 ≤ h ≤ 9, -11 ≤ k ≤ 11, -16 ≤ l ≤ 16	-10 ≤ h ≤ 11, -15 ≤ k ≤ 15, -26 ≤ l ≤ 26
Reflections collected	15533	72247	8439	36292
Independent reflections	1108[R(int) = 0.0666]	7629[R(int) = 0.0364]	3682[R(int) = 0.0463]	4566[R(int) = 0.0643]
Data/restraints/parameters	1108/0/60	7629/63/446	3682/0/205	4566/170/22 7
Goodness-of-fit on F ²	0.876	1.085	1.109	1.059
Final R indexes [I ≥ 2σ(I)]	R ₁ = 0.0366, wR ₂ = 0.1054	R ₁ = 0.0280, wR ₂ = 0.0699	R ₁ = 0.0408, wR ₂ = 0.0952	R ₁ = 0.0458, wR ₂ = 0.1004
Final R indexes [all data]	R ₁ = 0.0407, wR ₂ = 0.1091	R ₁ = 0.0290, wR ₂ = 0.0705	R ₁ = 0.0651, wR ₂ = 0.1271	R ₁ = 0.0622, wR ₂ = 0.1081
Largest diff. peak/hole / e Å ⁻³	0.50/-0.28	1.16/-0.96	0.65/-0.61	0.26/-0.20

e. Acknowledgements

I am incredibly grateful to Joe Fournier (Johnson Group, Yale University) who performed all of the ESI-MS experiments and Dr. Mike Takase for assistance with X-ray crystallography.

V. References

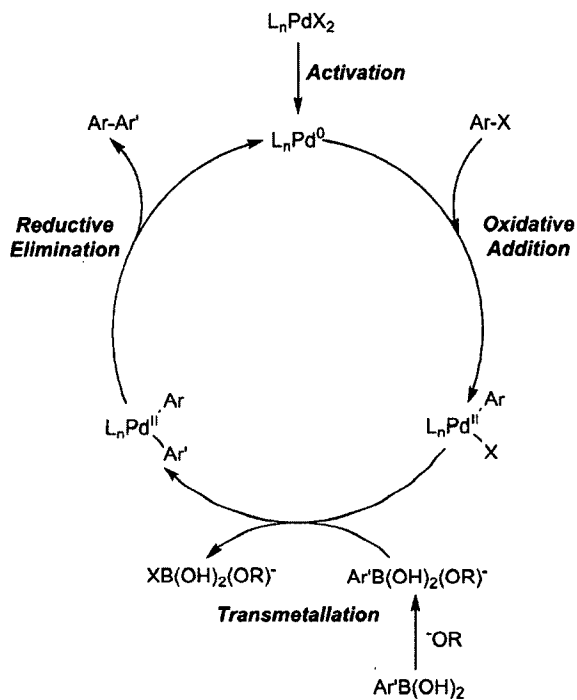
- (1) Guard, L. M.; Hazari, N. *Organometallics* **2013**, *32*, 2787.
- (2) Ristenpart, E. *Berichte* **1896**, *29*, 2526.
- (3) Blackman, A. G. *Polyhedron* **2005**, *24*, 1.
- (4) Zipp, S. G.; Zipp, A. P.; Madan, S. K. *J. Indian Chem. Soc.* **1977**, *54*, 149.
- (5) Ciampolini, M.; Nardi, N.; Speroni, G. P. *Coord. Chem. Rev.* **1966**, *1*, 222.
- (6) Morassi, R.; Bertini, I.; Sacconi, L. *Coord. Chem. Rev.* **1973**, *11*, 343.
- (7) Zipp, S. G.; Zipp, A. P.; Madan, S. K. *Coord. Chem. Rev.* **1974**, *14*, 29.
- (8) Jogdand, N. R.; Shingate, B. B.; Shingare, M. S. *Tetrahedron Lett.* **2009**, *50*, 4019.
- (9) Percec, V.; Popov, A. V.; Ramirez-Castillo, E.; Monteiro, M.; Barboiu, B.; Weichold, O.; Asandei, A. D.; Mitchell, C. M. *J. Am. Chem. Soc.* **2002**, *124*, 4940.
- (10) Jogdand, N. R.; Shingate, B. B.; Shingare, M. S. *Tetrahedron Lett.* **2009**, *50*, 6092.
- (11) Zhou, Y. M.; Zhu, H. G.; Chen, Z. X.; Chen, M. Q.; Xu, Y.; Zhang, H. Y.; Zhao, D. Y. *Angew. Chem. Int. Ed.* **2001**, *40*, 2166.
- (12) Woollard-Shore, J. G.; Holland, J. P.; Jones, M. W.; Dilworth, J. R. *Dalton Trans.* **2010**, *39*, 1576.
- (13) Lee, S. C.; Holm, R. H. *J. Am. Chem. Soc.* **1993**, *115*, 5833.
- (14) Scott, M. J.; Lee, S. C.; Holm, R. H. *Inorg. Chem.* **1994**, *33*, 4651.
- (15) Wurtele, C.; Sander, O.; Lutz, V.; Waitz, T.; Tuzcek, F.; Schindler, S. *J. Am. Chem. Soc.* **2009**, *131*, 7544.
- (16) Eckenhoff, W. T.; Pintauer, T. *Dalton Trans.* **2011**, *40*, 4909.
- (17) BATTERY, J. H. N.; PLACKETT, N. C.; SKELTON, B. W.; WHITAKER, C. R.; WHITE, A. H. *Z. Anorg. Allg. Chem.* **2006**, *632*, 1856.
- (18) Cousins, D. M.; Davidson, M. G.; Frankis, C. J.; Garcia-Vivo, D.; Mahon, M. F. *Dalton Trans.* **2010**, *39*, 8278.
- (19) Davidson, M. G.; Garcia-Vivo, D.; Kennedy, A. R.; Mulvey, R. E.; Robertson, S. D. *Chem. Eur. J.* **2011**, *17*, 3364.
- (20) Park, J. W.; Kim, J. T.; Koo, S. M.; Kim, C. G.; Kim, Y. S. *Polyhedron* **2000**, *19*, 2547.
- (21) Manura, J. J.; Manura, D. J. <http://www.sisweb.com/mstools/isotope.htm>, 2012.
- (22) Guard, L. M.; Palma, J. L.; Stratton, W. P.; Allen, L. J.; Brudvig, G. W.; Crabtree, R. H.; Batista, V. S.; Hazari, N. *Dalton Trans.* **2012**, *41*, 8098.
- (23) Allen, F. H. *Acta Crystallogr., Sect. B: Struct. Sci.* **2002**, *B58*, 380.
- (24) Divaira, M.; Orioli, P. L. *Inorg. Chem.* **1967**, *6*, 955.
- (25) Divaira, M.; Orioli, P. L. *Acta Crystallogr., Sect. B: Struct. Sci.* **1968**, *B 24*, 595.
- (26) Divaira, M.; Orioli, P. L. *Acta Crystallogr., Sect. B: Struct. Sci.* **1968**, *B 24*, 1269.
- (27) Farrugia, L. J. *J. Appl. Crystallogr.* **1997**, *30*, 565.
- (28) Ghilardi, C. A.; Midollini, S.; Orlandini, A.; Vacca, A. *J. Organomet. Chem.* **1994**, *471*, 29.
- (29) Orioli, P. L.; Ciampolini, M. *J. Chem. Soc., Chem. Commun.* **1972**, 1280.

- (30) Bruno, I. J.; Cole, J. C.; Edgington, P. R.; Kessler, M.; Macrae, C. F.; McCabe, P.; Pearson, J.; Taylor, R. *Acta Crystallogr., Sect. B: Struct. Sci.* **2002**, *B* 58, 389.
- (31) Bondi, A. *J. Phys. Chem.* **1964**, *68*, 441.
- (32) Ferguson, G.; Parvez, M. *Acta Crystallogr., Sect. B: Struct. Sci.* **1979**, *35*, 2207.
- (33) Slugovc, C.; Gemel, C.; Shen, J. Y.; Doberer, D.; Schmid, R.; Kirchner, K.; Mereiter, K. *Monatsh. Chem.* **1999**, *130*, 363.
- (34) Chu, L.; Hardcastle, K. I.; MacBeth, C. E. *Inorg. Chem.* **2010**, *49*, 7521.
- (35) Cadenbach, T.; Hevia, E.; Kennedy, A. R.; Mulvey, R. E.; Pickrell, J. A.; Robertson, S. D. *Dalton Trans.* **2012**, *41*, 10141.
- (36) Greiser, T.; Kopf, J.; Thoennes, D.; Weiss, E. *J. Organomet. Chem.* **1980**, *191*, 1.
- (37) Yousef, R. I.; Walfort, B.; Ruffer, T.; Wagner, C.; Schmidt, H.; Herzog, R.; Steinborn, D. *J. Organomet. Chem.* **2005**, *690*, 1178.
- (38) Toney, J.; Stucky, G. D. *J. Organomet. Chem.* **1970**, *22*, 241.
- (39) Han, R.; Looney, A.; Parkin, G. *J. Am. Chem. Soc.* **1989**, *111*, 7276.
- (40) Han, R.; Parkin, G. *J. Am. Chem. Soc.* **1992**, *114*, 748.
- (41) Han, R.; Parkin, G. *J. Am. Chem. Soc.* **1990**, *112*, 3662.
- (42) Han, R.; Parkin, G. *Organometallics* **1991**, *10*, 1010.
- (43) Gibson, V. C.; Segal, J. A.; White, A. J. P.; Williams, D. J. *J. Am. Chem. Soc.* **2000**, *122*, 7120.
- (44) Bailey, P. J.; Lorono-Gonzalez, D.; Parsons, S. *Chem. Commun.* **2003**, 1426.
- (45) Chivers, T.; Fedorchuk, C.; Parvez, M. *Organometallics* **2005**, *24*, 580.
- (46) Pajerski, A. D.; Squiller, E. P.; Parvez, M.; Whittle, R. R.; Richey, H. G. *Organometallics* **2005**, *24*, 809.
- (47) Love, B. E.; Jones, E. G. *J. Org. Chem.* **1999**, *64*, 3755.
- (48) Gronberg, K. L. C.; Henderson, R. A.; Oglieve, K. E. *J. Chem. Soc., Dalton Trans.* **1998**, 3093.
- (49) Britovsek, G. J. P.; England, J.; White, A. J. P. *Inorg. Chem.* **2005**, *44*, 8125.
- (50) Dolomanov, O. V.; Bourhis, L. J.; Gildea, R. J.; Howard, J. A. K.; Puschmann, H. *J. Appl. Crystallogr.* **2009**, *42*, 339.
- (51) Sheldrick, G. M. *Acta Crystallogr., Sect. A: Found. Crystallogr.* **2008**, *A64*, 112.
- (52) Kamrath, M. Z.; Relph, R. A.; Guasco, T. L.; Leavitt, C. M.; Johnson, M. A. *Int. J. Mass Spectrom.* **2011**, *300*, 91.
- (53) Robertson, W.; Kelley, J.; Johnson, M. A. *Rev. Sci. Instrum.* **2000**, *71*, 4431.

Comparison of a Series of dppf Supported Ni Precatalysts for the Suzuki-Miyaura Reaction: The Importance of Ni(I)

I. Introduction

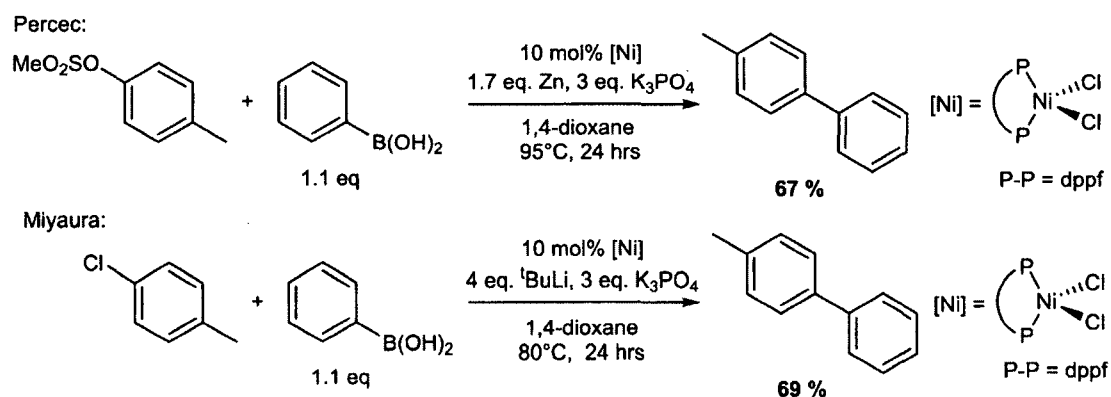
Cross coupling has become a powerful and ubiquitous tool for the formation of carbon-carbon bonds.¹⁻⁵ Commonly, catalysts based on Pd are used to perform cross coupling reactions, and despite the cost associated with Pd, these systems are used industrially to catalyze the key steps in the preparation of many pharmaceuticals and agrochemicals, where they are often utilized in ppm quantities.⁵ In particular, the Suzuki-Miyaura reaction is one of the most general methods for the formation of new C-C bonds, as a wide variety of boronic acids can readily be prepared.³ Over 50 years of research on Pd based catalysts for the Suzuki-Miyaura reaction has led to the development of sophisticated ligand sets, which have been designed specifically to both speed up the elementary reaction steps and stabilize L-Pd(0), which is widely regarded as the active species in reactions of this type.^{2-4,6} These results have been complemented by in depth mechanistic studies and the reaction is widely accepted to occur via a Pd(0)/(II) cycle (Scheme 4.01).^{3,6-10}



Scheme 4.01: Diagram depicting a generic catalytic cycle for the Pd catalyzed Suzuki-Miyaura reaction.

There are, however, economic and chemical advantages to using Ni based catalysts for the Suzuki-Miyaura reaction. Owing to the smaller size and increased nucleophilicity of Ni, systems incorporating Ni can couple challenging substrates, such as deactivated aryl halides, carbamates, carbonates, sulfamates and coordinating substrates, for example heterocycles.¹¹ In addition, the ligands used to support Ni catalysts are typically low cost and commercially available phosphines rather than the complicated and synthetically challenging ligands typically used to stabilize Pd based systems.^{3,4,11} Furthermore, Ni is considerably less expensive than Pd.

The Ni catalyzed Suzuki-Miyaura reaction was first reported by Percec and co-workers in 1995. Initially, they discovered a reaction in which *in situ* generated Ni(0) could homo-couple aryl sulfonates.¹² If a similar system was utilized with phenyl boronic acid, then unsymmetrical biaryls could be synthesized in moderate yields from aryl sulfonates (Scheme 4.02).¹³



Scheme 4.02: First reports of Ni catalysts for the Suzuki-Miyaura reaction.

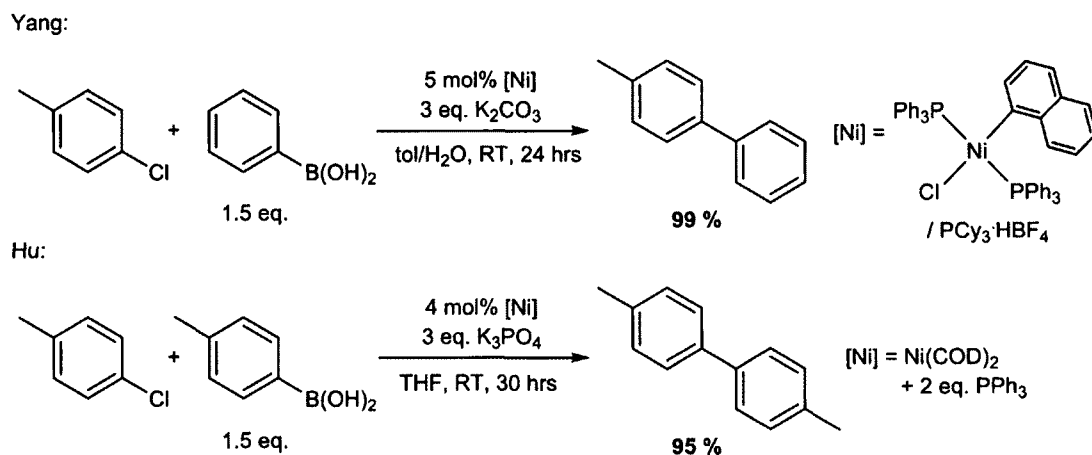
A year later, it was demonstrated that a similar transformation could be affected using an aryl halide in place of an aryl sulfonate. Again, a Ni(II) complex was reduced *in situ* to generate the proposed catalytically active Ni(0) species (Scheme 4.01).¹⁴ These initial reports have subsequently been followed by much research aimed at using Ni to perform this transformation under milder conditions.^{11,15}

The next major improvement was reported by Indolese,¹⁶ who found that the reaction was catalyzed by simple Ni(P-P)(Cl)₂ complexes (P-P = dppf (1,1'-bis(diphenylphosphino)ferrocene), dppb (1,4-bis(diphenylphosphino)butane), dppp ((1,4-bis(diphenylphosphino)propane), dppe (1,4-bis(diphenylphosphino)ethane)) without using an external reductant. This was a significant advance as it meant that reactive alkyl lithium reagents were no longer required, which greatly increased the range of functional groups that could be utilized. In fact, performing reactions of this type without a reductant has now

become commonplace. Another benefit of the Indolese system was that a catalyst loading of 1 mol % could be used, and in the case of activated (electron deficient) aryl chlorides this could be reduced even further to 0.5 mol %. Overall this study marked a significant improvement on previous systems; turnover numbers (TON) of up to 200 were achieved compared to previous reports with TON of 10.^{13,14,16}

After Indolese's seminal work further incremental improvements to the catalytic conditions were made; often a higher yield is obtained when excess ligand, either PR_3 ($R = Ph$,¹⁷⁻²⁰ Cy ,¹⁷⁻¹⁹ OMe ²¹) or P-P ($P-P = dppf$,^{19,22} $dppe$,¹⁹ $dppb$ ¹⁹), is added to reactions. Much like in Pd cases,⁶ this is postulated to stabilize the Ni active species. Additionally, increased yields are observed when the number of equivalents of boronic acid present is increased from 1.1 eq. to greater than 1.5 eq. in most systems,^{17,18,23,24} although there is still no consensus explanation for this phenomenon.

Currently, there are limited examples of Ni based precatalysts that are effective at temperatures lower than 50°C, and to the best of our knowledge, there are only two Ni precatalysts that are competent for the coupling of aryl halides and boronic acids at room temperature (Scheme 4.03).^{17,18} Although both systems only require a weak base, reaction times are long, the Ni loading high and substrate scope limited.



Scheme 4.03: Previously reported room temperature Ni precatalysts for the coupling of aryl halides and boronic acids.

At this stage despite 20 years of research, nearly all Ni precatalysts for the Suzuki-Miyaura reaction use simple mono- and bidentate phosphines as ancillary ligands and are based on 4 structural motifs (Figure 4.01) which are closely related to the initial Ni based systems. Furthermore, there are relatively few studies on the mechanism of Ni catalyzed C-C bond forming reactions, and the nature of the active species during catalysis is often unknown, although a Ni(0)/Ni(II) cycle is most commonly invoked.^{11,13} In general, Ni catalyzed Suzuki Miyaura reactions require high temperatures, high catalyst loading, long reaction times and have limited substrate scope. Frequently, the cost benefit of using an abundant, first row transition metal over Pd is offset by one or more of these problems.

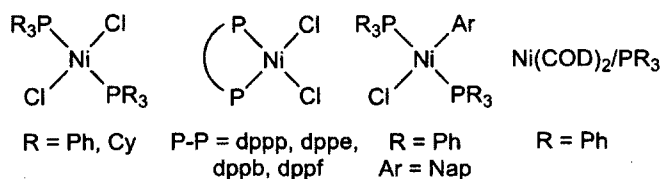
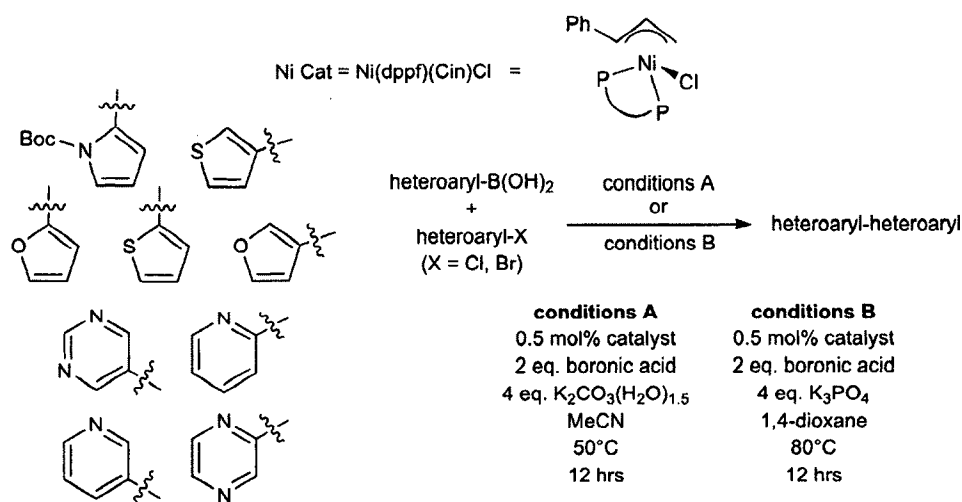


Figure 4.01: Common Ni precatalysts.

Against this background a remarkable advance was made in 2012, when Hartwig and co-workers reported the highly active Ni precatalyst, Ni(dppf)(Cin)(Cl), which addressed the majority of these issues. Using 0.5 mol% precatalyst at either 50 or 80°C, a variety of heteroaryl halides and heteroaryl boronic acids, containing O, S and N atoms, were coupled in high yield (Scheme 4.04). Interestingly, the cinnamyl supported precatalyst is structurally distinct from previously reported precatalysts and it is unclear what made this complex so active.

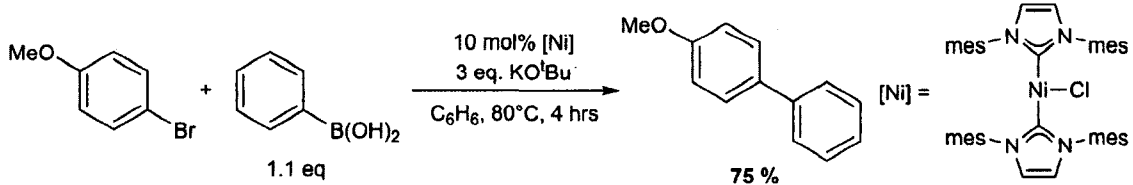


Scheme 4.04: Substrate scope and conditions for the Suzuki-Miyaura reaction using Ni(dppf)(Cin)(Cl)²⁴

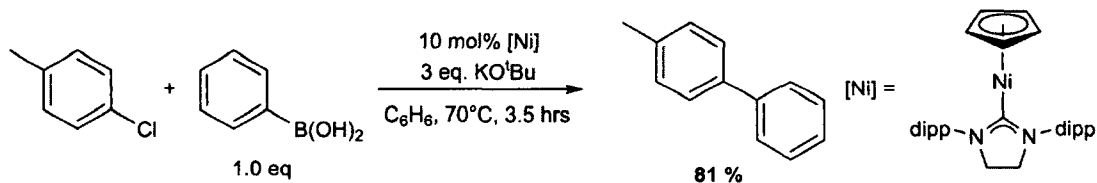
As part of studies in our group on Pd catalyzed Suzuki-Miyaura reactions, we previously studied the precatalyst Pd(IPr)(Cin)(Cl) (IPr = 1,3-bis(2,6-diisopropylphenyl)imidazol-2-ylidene) in detail. We observed significant amounts of Pd(I) both during and at the end of catalysis when Pd(IPr)(Cin)(Cl) and related complexes were used as precatalysts.^{7,25,26} Given the close structural similarity of Hartwig's complex and the compounds we have previously investigated, we were interested in whether Ni(I) was relevant in catalysis using Ni(dppf)(Cin)(Cl).

Ni(I) complexes have previously been implicated in a variety of catalytic reactions including alkene polymerization,²⁷⁻²⁹ linear polymerization, the cyclotrimerization of phenyl acetylene^{30,31} and the cyclodimerization of cyclic alkenes.^{32,33} In general, they give poor activity for a variety of cross coupling reactions, including the Buchwald-Hartwig,³⁴ Kumada³⁴⁻³⁸ and Negishi³⁹ transformations. There are only two reports of Ni(I) compounds which are competent for the Suzuki-Miyaura reaction (Scheme 4.05) and both require high catalyst loading (10 mol%), 3 equivalents of a strong base (KO^tBu) and elevated temperatures (70-80°C). In addition, neither reaction reached completion.^{38,40}

Louie:



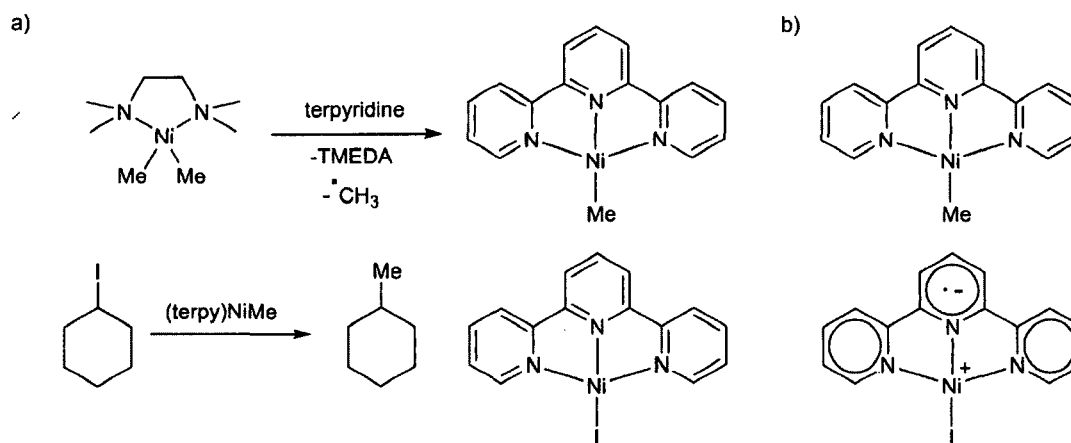
Our Group:



Scheme 4.05: Previously reported Ni(I) precatalysts for the Suzuki-Miyaura reaction.

Although no well-defined Ni(I) complexes have been highly active for cross coupling, Ni(I) has, of late, been postulated to participate directly in a number of cross coupling reactions and related Ni(I)/(III) cycles have been proposed. Vicic^{39,41} and co-workers suggested that a Ni(I) complex was a catalytically active species in the Negishi reaction. A series of stoichiometric reactions were conducted to demonstrate that the product forming step in alkyl-alkyl cross coupling did not result from reductive elimination from a Ni(II) dialkyl species, but that an alkyl fragment was transferred from a Ni(I) complex to an alkyl halide generating a Ni(I) halide as the inorganic product (Scheme 4.06, a). Further

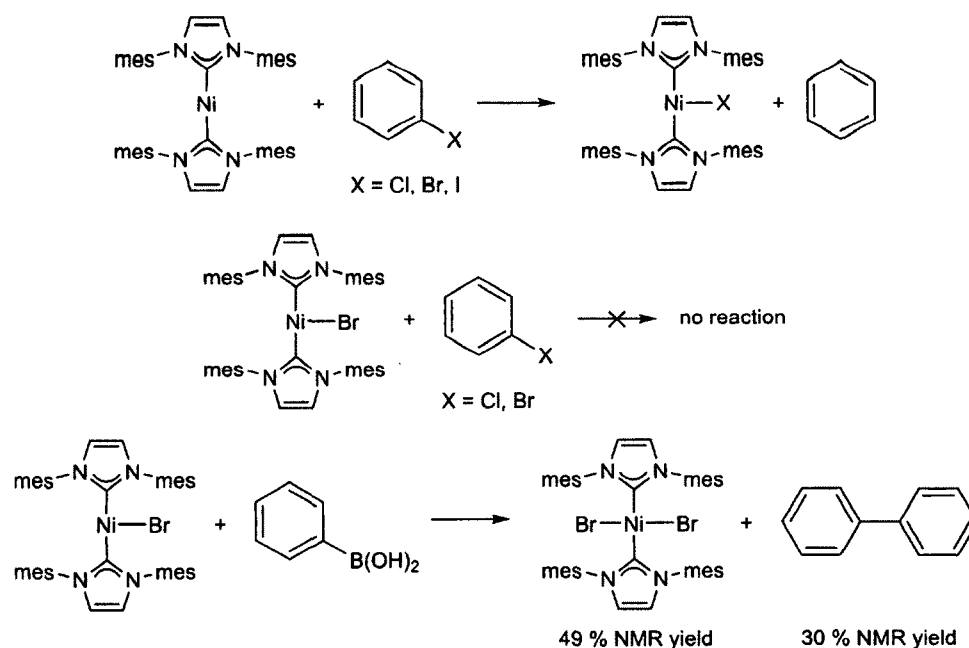
investigation showed that a related Ni(II) alkyl halide complex did not transmetallate with an alkylzinc reagent to give a cross coupled product in high yield. Instead addition of an alkyl halide to a Ni(I) alkyl complex produced the cross coupled product in high yield. Interestingly, a later EPR and computational analysis of the key Ni(I) complex in Vici's study revealed that it is better described as a Ni(II) alkyl cation, where the radical is largely ligand centered (Scheme 4.06, b).⁴² This could imply that these observations might not be valid for systems without a redox active ligand.



Scheme 4.06: a) Stoichiometric reactions to test Ni(I) viability and b) Ni(I) methyl complex, top, and Ni(II) alkyl cation, bottom.

The only recent mechanistic study on Ni catalyzed Suzuki-Miyaura reactions was conducted by Louie and co-workers.³⁸ After noticing that Ni(IMes)₂ reacted with PhX (X = Cl, Br, I) to form Ni(IMes)₂X, these complexes, as well as Ni(IMes)₂X₂ were screened for a simple Suzuki-Miyaura reaction, and found to have very similar activity. In a series of stoichiometric reactions between Ni(IMes)₂Br, they found that no reaction was observed with either PhBr or PhCl, but that reaction with phenylboronic acid gave Ni(IMes)₂Br₂ (in ~50 % yield) and biphenyl (in ~30 % yield) (Scheme 4.07). This prompted the proposal that a Ni(I)/(III) cycle was operative, in which the first step was transmetalation, followed

by oxidative addition and reductive elimination of the organic product. At this stage, it is unclear whether Ni(I) is the active species in all cases, if it is present during the reaction or if it is activated under the reaction conditions into Ni(0) or Ni(II). As a result we were interested in performing a study on phosphine ligated precatalysts, as they are more commonly used in Ni catalyzed cross coupling compared with NHC ligands. Though Percec and co-workers have performed a comprehensive study in which Ni-phosphine complexes, ligands, solvents and bases were all varied,¹⁹ our studies represent the first time a series of precatalysts supported by the same ligand has been rigorously investigated.



Scheme 4.07: The reaction of Ni(0) and Ni(I) precatalysts with aryl halides and/or boronic acids.

II. Results and Discussion

a. Synthesis

A series of Ni(0) and Ni(II) complexes with the potential to be active precatalysts for the Suzuki-Miyaura reaction were prepared. As previously mentioned, these reactions are often proposed to involve Ni(0)/(II) cycles and as a result Ni(dppf)(C₂H₄) (**1**) and Ni(dppf)₂ (**2**) were synthesized as representative Ni(0) species. The Ni(II) species Ni(dppf)(*o*-tol)(Cl) (**3**) was prepared as a representative example from the commonly used Suzuki-Miyaura precatalyst motif (Ni(PR₃)₂(Ar)(Cl)), as well as Ni(dppf)(Cin)(Cl) (**4**), which is one of the most active Ni precatalysts reported to date (Figure 4.02). All of these complexes have been previously reported in the literature.^{24,43-45} We were particularly interested in **3** due to its air stability and ease of synthesis compared to the other complexes.^{24,43-45} Specifically, its synthesis avoids the use of Ni(COD)₂ (an expensive and air sensitive reagent) and costly and reactive reducing agents.

The crystal structures of **2** and **3** have been previously published,^{46,47} and as part of this study **1** was crystallographically characterized (Figure 4.03). The X-ray structure displays a distorted trigonal planar geometry where the dppf ligand has a bite angle of 108.26(5)°. This is a wide angle for dppf, which has a natural bite angle of 99°. ^{48,49} The C-C bond in the coordinated ethylene is elongated compared to free ethylene (1.362(8) versus 1.3391(13) Å in free ethylene⁵⁰) but the lengthening is not as large as observed in Ni(dippf)(C₂H₄) (dippf = 1,1'-bis(di-*iso*-propylphosphino)ferrocene, 1.416(3) Å),⁴⁶ Ni(dtbpf)(C₂H₄) (dtbpf = 1,1'-bis(di-*tert*-butylphosphino)ferrocene, 1.399(4) Å),⁴⁶ Ni(PPh₃)₂(C₂H₄) (1.391(5) Å),⁵¹ Ni(P^{*i*}Pr)₂(C₂H₄) (1.386(3) Å),⁵² or Ni(dtbp)(C₂H₄) (dtbp = 1,2-bis(di-*tert*-butylphosphino)ethane, 1.4189(6) Å)⁵³ where presumably

increased backbonding from the ligand, compared to dppf, leads to a longer C-C bond distance.

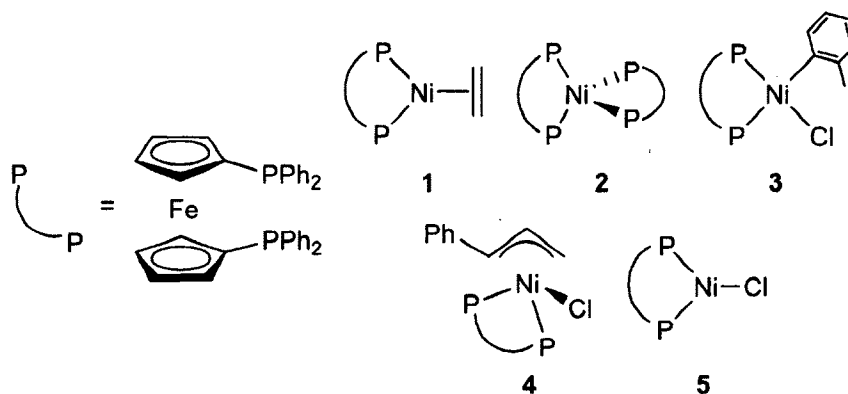


Figure 4.02: Ni precatalysts studied in this work.

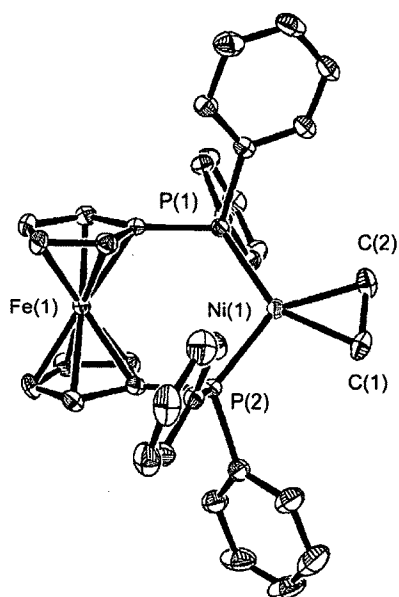


Figure 4.03: ORTEP⁵⁴ of **1** (ellipsoids at 30% probability, hydrogen atoms have been omitted for clarity). Selected bond lengths (Å) and angles (°): P(1)-Ni(1) 2.1483(14), P(2)-Ni(1) 2.1590(14), Ni(1)-C(1) 1.979(6), Ni(1)-C(2) 1.963(5), C(1)-C(2) 1.362(8), P(1)-Ni(1)-P(2) 108.26(5), P(1)-Ni(1)-C(2) 103.11(17), P(2)-Ni(1)-C(1) 108.19(15).

Attempts to crystalize **4** resulted in the crystallographic characterization of the Ni(I) complex, Ni(dppf)(Cl) (**5**) (Figure 4.04). As with **1**, the solid state structure shows a distorted trigonal planar geometry. The bite angle of the dppf ligand is $105.56(9)^\circ$ (P(1)-Ni(1)-P(2)) which is slightly more obtuse than in Ni(dippf)(Cl) ($104.49(3)^\circ$)⁵⁵ and contracted compared to Ni(PPh₃)₂(Cl) ($114.94(2)^\circ$).^{52,56} However, these angles are all far smaller than that of Ni(PⁱPr₃)₂(Cl), where P-Ni-P is $119.44(2)^\circ$.⁵² Crystallization of two complexes related to **4** (Ni(dppf)(allyl)(X), (X = Cl, BF₄)) revealed the allyl ligand was bound in an η^3 fashion, and we therefore assume that the cinnamyl ligand is bound in an η^3 coordination mode in **4**.⁵⁷

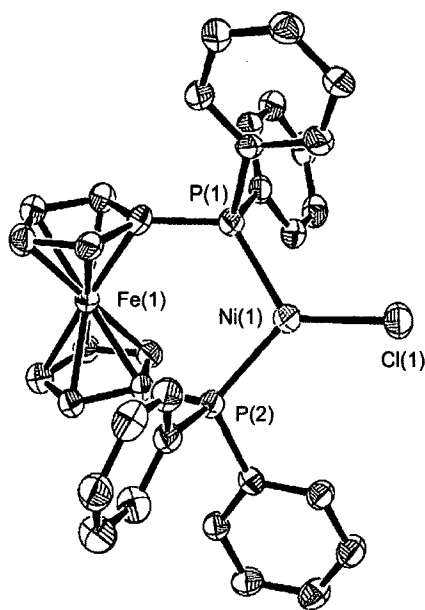


Figure 4.04: ORTEP⁵⁴ of **5** (ellipsoids at 30% probability, hydrogen atoms and solvent in crystal lattice have been omitted for clarity). Selected bond lengths (Å) and angles ($^\circ$): P(1)-Ni(1) 2.196(3), P(2)-Ni(1) 2.205(2), Ni(1)-Cl(1) 2.150(3), P(1)-Ni(1)-P(2) $105.56(9)$, P(1)-Ni(1)-Cl(1) $122.99(10)$, P(2)-Ni(1)-Cl(1) $131.30(11)$.

Assuming there was a facile pathway to form **5** from **4**, we decided to independently synthesize **5** and screen it against the Ni(0) and Ni(II) precatalysts in this study. Complex **5** has previously been implicated as an inactive species present in catalytic annulation reactions using Ni(COD)₂/dppf.⁵⁸

By adapting the literature procedure used to prepare Ni(PⁱPr₃)₂(Cl),⁵² **5** was isolated in good yield (78%) from the comproportionation of **1** with Ni(dppf)(Cl)₂ (**6**) in diethyl ether (Figure 4.05). Comproportionation is a commonly utilized route for the preparation of Ni(I) compounds.^{35,52,59} Complex **5** was characterized by paramagnetic ¹H NMR spectroscopy and displayed three resonances at 12.59, 4.58 and 1.61 ppm in C₆D₆. Characterization by UV-Vis spectroscopy, electrochemistry and EPR spectroscopy was also completed. The complex was found to have a μ_{eff} of 2.18 BM,⁶⁰⁻⁶² which is consistent with one unpaired electron on Ni and is within the range of those recorded for other Ni(I) complexes of similar structure.^{52,55,62-64}

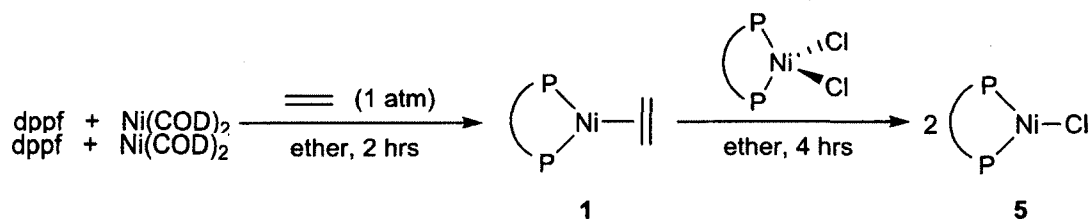
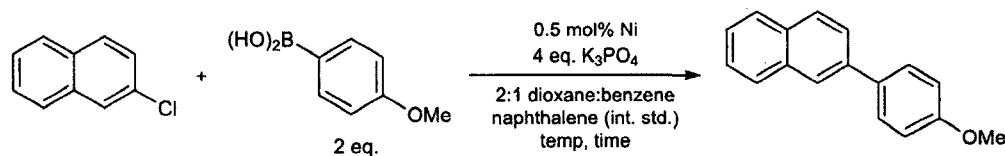


Figure 4.05: Synthesis of **5**.

b. Catalysis

With these complexes in hand, we compared their catalytic performance at a range of temperatures, using 2-chloronaphthalene and 4-methoxyphenylboronic acid as representative coupling partners (Table 4.01). The conditions utilized are related to those used by Hartwig and co-workers,²⁴ although we found that using 2:1 1,4-dioxane:benzene solvent mixture gave improved catalytic performance compared with neat ethereal solvent.

Table 4.01: Yields^a of product for the Suzuki–Miyaura reaction^b catalyzed by complexes **1**-**5**.



Temp (°C)	Time (hours)	% yield for precatalysts				
		1	2	3	4	5
80	0.5	81	>99	66	94	69
	1	>99	-	95	>99	>99
	1.5	-	-	>99	-	-
60	0.5	55	66	20	28	30
	1	67	80	42	63	65
	1.5	82	>99	62	>99	>99
	2	>99	-	>99	-	-
40	4	30	42	76	65	>99
	8	90	>99	>99	>99	-
RT ^a	16	-	-	>99	-	>99

^aYields were calculated using gas chromatography and are the average of two runs. ^bReaction conditions: 0.2 mmol 2-chloronaphthalene, 0.4 mmol 4-methoxyphenylboronic acid, 0.8 mmol K₃PO₄, 0.2 mmol naphthalene, 0.001 mmol precatalyst, 340 μL 1,4-dioxane and 160 μL benzene.

At all temperatures, **2** outperforms **1**. In both cases the generation of the proposed catalytically active (dppf)Ni(0) species presumably occurs via ligand dissociation. A control experiment under catalytically relevant conditions (i.e. no ethylene overpressure) between **1** and dppf indicates that the equilibrium constant for the formation of **2** and ethylene is 0.1 (Figure 4.06). This implies that the coordinated ethylene in **1** is more tightly bound than the second dppf ligand in **2**, which is consistent with the relative performance of **2** and **1**, as **2** presumably activates faster than **1** via ligand dissociation.

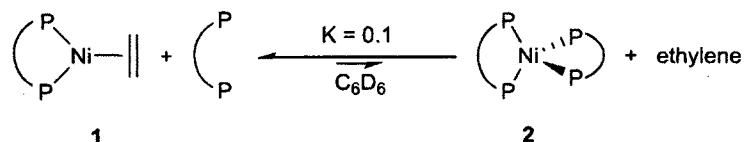


Figure 4.06: Equilibrium between **1** and **2**.

Whereas activation of **1** and **2** is proposed to occur via ligand dissociation, we believe that, in agreement with previous reports in the literature,^{24,65} activation of the Ni(II) precatalysts **3** and **4** occurs via transmetallation and reductive elimination as shown in Figure 4.07. At higher temperatures (80 and 60°C) **2** gives slightly better catalytic performance than **4**, suggesting that it is activated more efficiently. However, at lower temperature (40°C) **4** is a better precatalyst than **2**, suggesting that it is activated more efficiently at lower temperature.

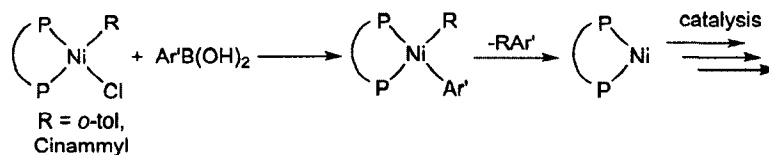


Figure 4.07: Activation pathway for Ni(II) precatalysts.

Although both **3** and **4** are proposed to be activated via transmetallation, there is a large disparity in their catalytic performance at 80°C (at 30 min, **3** is 66 % complete and **4** 94 %). This is almost certainly related to the relative stability of **3** and **4** at elevated temperature. Indeed, it has been previously noted that **3** is unstable in solution⁴⁴ and decomposition of **3** at 80°C could explain its lesser catalytic performance. This is supported by data recorded at 40°C, where after 4 hours **3** and **4** are comparable (76% yield for **3** vs 65% yield for **4**).

Interestingly, the Ni(I) complex **5** performs well compared to the Ni(0) and Ni(II) precatalysts. There are only two reports of Ni(I) precatalysts showing activity for the Suzuki-Miyaura reaction^{38,40} and to the best of our knowledge, this is the first report showing that a Ni(I) complex gives comparable reactivity to Ni(0) or Ni(II) precatalysts.

At 80°C, **5** gives slightly inferior performance to all precatalysts except **3**, but upon cooling to 60°C the catalytic activity of **4** and **5** is near identical. The trend continues upon cooling to 40°C, where **5** is a more efficient precatalyst than **4**. A similar relationship was observed between the catalytic performance of **5** and the Ni(0) complexes **1** and **2**. At

higher temperatures ($>60^{\circ}\text{C}$) they show superior performance to **5**, but at 40°C their 4 hour yields are 30 % and 42% respectively compared to $>99\%$ for **5**.

After discovering the surprising efficiency of **5** at 40° , we tested its performance at room temperature. Complex **3** was also screened at room temperature owing to its good performance at 40°C and its simple synthesis⁴⁴ and air stability. Both complexes were found to give complete conversion after 12 hours at room temperature using 2.5 mol% catalyst. To the best of our knowledge, there are only two Ni precatalysts that are competent for the coupling of aryl halides and boronic acids at room temperature but both require significantly higher catalyst loadings and longer reaction times than our systems.^{17,18}

After observing that **1-5** were all highly active for the Suzuki-Miyaura reaction, we were interested in determining why they performed so well at low catalyst loading and temperature. We hoped that determining the speciation of Ni under the catalytic conditions would provide an indication as to why these compounds were such efficient precatalysts.

c. Speciation of Ni during catalysis

Initially, a catalytic reaction using **1** was tracked by ^{31}P NMR spectroscopy. In order to observe a signal in the spectra, the catalyst loading was increased to 4 mol% (8 times the loading of a typical reaction) (Figure 4.08). At room temperature, only resonances pertaining to **1** and the internal standard (PPh_3 in a capillary) were observed. After heating the sample for 1 hour at 80°C , a time at which complete conversion of the substrate can be assumed (Figure 4.08, a) there were no peaks present in the $^{31}\text{P}\{^1\text{H}\}$ spectrum indicating that no diamagnetic phosphorus containing species were present in any appreciable concentration.

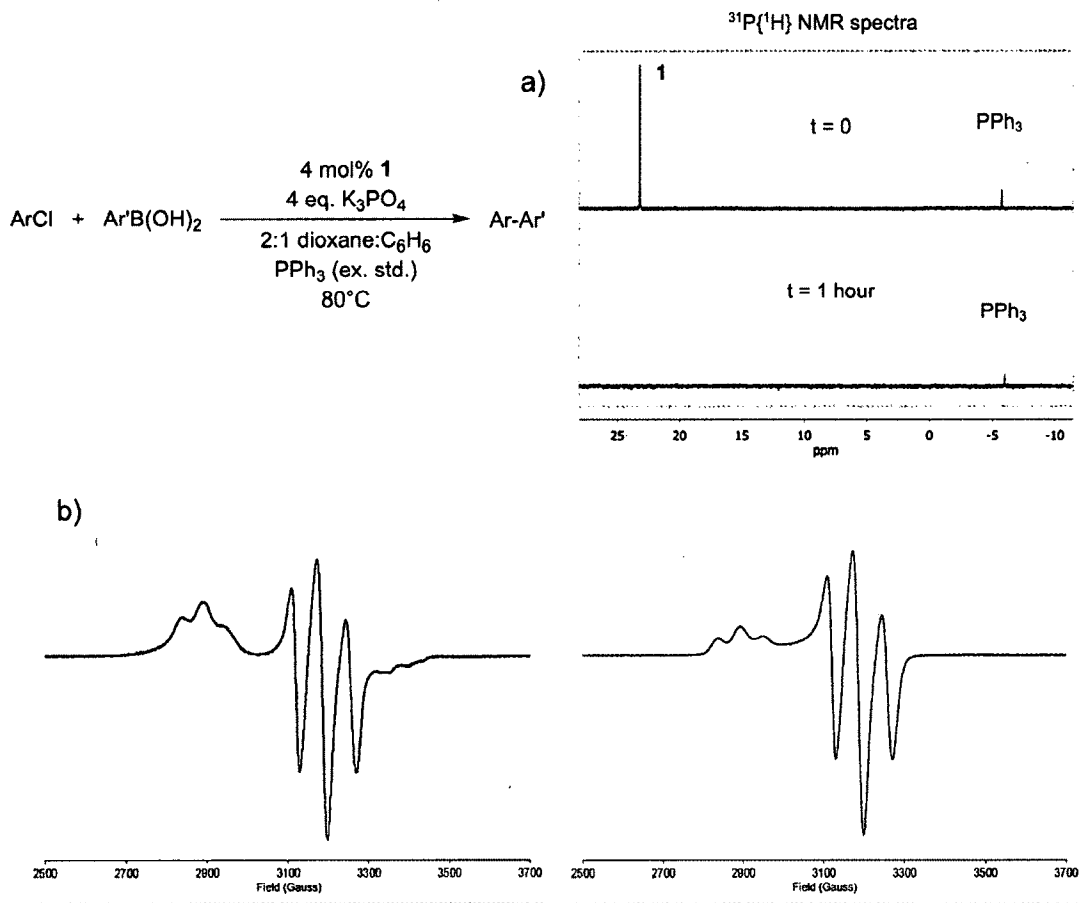
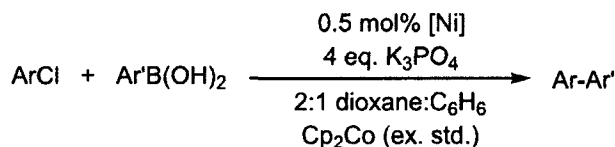


Figure 4.08: (a) ³¹P{¹H} NMR spectra taken before and after a catalytic reaction using **1** as the precatalyst. (b) EPR spectra of a catalytic reaction mixture (left, black) and a pure sample of **5** (blue, right).

To ascertain whether paramagnetic Ni species were present in the reaction mixture, an aliquot was taken after catalysis using **1** was complete and an EPR spectrum obtained. Comparison with an authentic sample revealed that the main species present was **5** (Figure 4.08, b)

Next we sought to quantify the percentage of Ni that exists in the paramagnetic state both during and after catalysis and establish whether other Ni precatalysts were also forming Ni(I) species. A typical catalytic reaction was performed (using 0.5 mol% [Ni]), and the amount of **5** was determined using ¹H NMR spectroscopy (Table 4.02).

Table 4.02: Percentage **5** formed at various time points during catalysis.

Temp (°C)	Time (hours)	% yield of 5				
		1	2*	3	4	5
80	0.25	51	41	>99	26	>99
	0.5	63	85	>99	23	>99
	Completion (hrs)	62 (1)	85 (0.5)	>99 (1.5)	68 (1)	96 (1)
60	Completion (hrs)	16 (2)	19 (1.5)	55 (2)	31 (1.5)	>99 (1.5)

^aYields were calculated using paramagnetic ¹H NMR integrations of **5** against a standardized capillary containing Cp₂Co.

^bReaction conditions 0.6 mmol 2-chloronaphthalene, 1.2 mmol 4-methoxyphenylboronic acid, 2.4 mmol K₃PO₄, 0.003 mmol precatalyst, 1020 μL 1,4-dioxane and 480 μL benzene. 750 μL reaction mixture removed, evaporated and dissolved in 500 μL C₆D₆. ***2** formed a different Ni(I) complex, [Ni(dppf)(Cl)]₂(μ-dppf) (**6**). Capillaries were standardized accordingly.

In all cases at the end of the reactions using Ni(0) and Ni(II) precatalysts, the majority of the total Ni is in the form of **5**. Furthermore in catalytic reaction using **5**, 100% of the Ni was in the form of **5** at the end of the reaction. Earlier aliquots taken at 15 and 30 minutes also show significant amounts of **5**. Interestingly, complex **3** appears to have been converted completely to complex **5** very early in the reaction, and this could explain the near identical catalytic performances of **3** and **5**. This also implies that the conversion occurs during precatalyst activation. If comproportionation is faster than transmetallation, then Ni(dppf)(Ar)(X) will be converted into Ni(I) faster than into Ni(dppf)(Ar)(Ar'). The inverse case seems to hold for **4**, where little **5** is formed in precatalyst activation and the concentration of **5** rises drastically at complete catalytic conversion. These results suggest that **1-4** all have a facile pathway to form **5** under catalytic conditions, but that **5** does not form appreciable quantities of Ni(0) or Ni(II) species. Furthermore, they indicate that Ni(I) is formed throughout the reaction and not just once catalysis is complete. To the best of

our knowledge, this is the first time that Ni(I) has been observed and quantified during a Ni catalyzed Suzuki-Miyaura reaction and the speciation of the Ni at the end of the reaction determined.

d. Stoichiometric Experiments

In order to determine how Ni(I) forms during catalytic reactions, a series of stoichiometric reactions were performed. Complex **1** was found to be unreactive towards 2-methoxyboronic acid and/or K₃PO₄, but Ni(I) formed quantitatively upon addition of 1 eq. 2-chloronaphthalene to a 2:1 1,4-dioxane-*d*₈/C₆D₆ solution of **1** (Figure 4.09). The related biaryl (in this case 2,2'-binaphthalene) was also observed by GC-MS and quantified (~100%). At this point it is unclear how the reaction is proceeding, though a bimetallic oxidative addition,^{66,67} a comproportionation,⁵² or a radical mechanism^{66,68,69} are among the possibilities. Consistent with this being the pathway for Ni(I) formation during catalysis, a small amount of the biaryl 2,2'-binaphthalene is also detected in catalytic reactions.

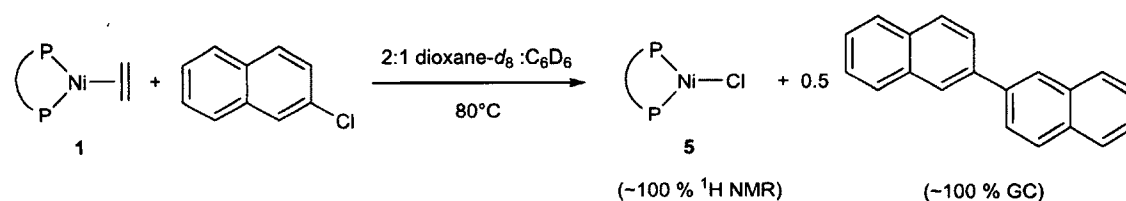


Figure 4.09: Stoichiometric reactivity of **1**.

The stoichiometric reactions of **2** were similar to those for **1**, where no reaction was observed between the Ni complex and 4-methoxyphenylboronic acid and/or K₃PO₄, but the reaction with 2-chloronaphthalene proceeded smoothly at 80°C. Interestingly, the paramagnetic product differed from **5** though still displayed three similarly shifted peaks in the ¹H NMR spectrum in C₆D₆ at room temperature. Upon cooling a sample in toluene

to -80°C , the peaks split and the new complex was crystallographically characterized as $[\text{Ni}(\text{dppf})(\text{Cl})]_2(\mu\text{-dppf})$ (**6**) (Figure 4.11). As with **1**, the organic product was identified as 2,2'-binaphthalene, which was formed in 100% yield (Figure 4.10).

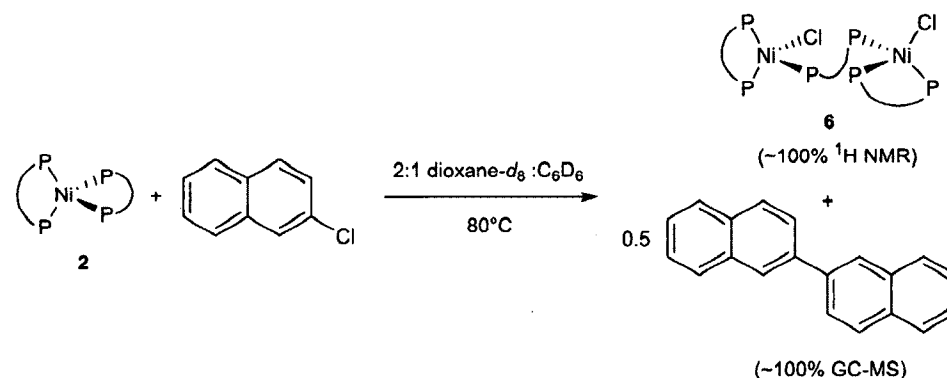


Figure 4.10: Stoichiometric reactivity of **2**.

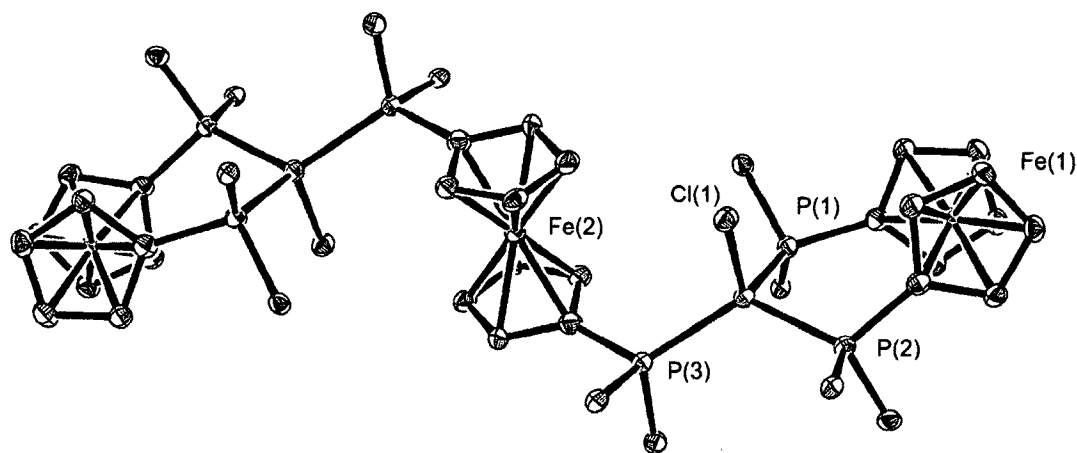


Figure 4.11: ORTEP⁵⁴ of $[\text{Ni}(\text{dppf})(\text{Cl})]_2(\mu\text{-dppf})$ at 30% probability (hydrogen atoms, phenyl groups of dppf and THF of crystallization removed for clarity). Half a molecule per asymmetric unit, contains an inversion centre at Fe(2). Selected bond lengths (Å) and angles ($^{\circ}$): Ni(1) – Cl(1) 2.3025(13), Ni(1)–P(1) 2.2710(12), Ni(1)–P(2) 2.2525(12), Ni(1)–P(3) 2.3107(12), P(1)–Ni(1)–P(2) 100.71(14), P(2)–Ni(1)–P(3) 122.05(5), P(3)–Ni(1)–P(1) 116.45(5), P(1)–Ni(1)–Cl(1) 116.22(5), P(2)–Ni(1)–Cl(1) 93.31(4), P(3)–Ni(1)–Cl(1) 106.42(5).

These results are in line with those reported by Hartwig and co-workers who noted that Ni(dppf)(COD) (COD = 1, 5 cyclooctadiene) did not react with aryl halides at room temperature, but at elevated temperature formed **5** and the related biaryl.⁵⁸ The reaction of Ni(NHC)₂ (NHC = IPr,³⁷ IMes³⁸) with various aryl halides has also been shown to generate Ni(I) products and biaryl (in the case of IPr) and aryl (in the case of IMes), indicating that this observation could be broadly applicable to other ligand sets.

This is in contrast to observations made by Kochi, where the formation of Ni(PEt₃)₃X and free PEt₃ from the reaction of Ni(PEt₃)₄ and ArX was observed only when X = I or Br for a wide range of Ar groups including 1,4-MeC₆H₄X, 1,4-MeOC₆H₄X, 1,4-ClC₆H₄X, and C₆H₅X.^{70,71} Additionally, abstraction of a hydrogen from the solvent by the Ar radical was observed to yield ArH.⁷⁰ A similar study was also conducted by Fahey who found very low yields (<20 %) of Ni(II) could be obtained from the reaction of Ni(PEt₃)₂(C₂H₄) with various aryl halides.⁷² It is possible that the low Ni(II) yield was due to the formation of significant amounts of Ni(I).

In contrast is the reactivity observed with **3**, where no reaction occurred with 2-chloronaphthalene, but when one equivalent of 4-methoxyphenylboronic acid and K₃PO₄ was used, **5** was observed in 50 % yield by paramagnetic ¹H NMR spectroscopy. Additionally, the biaryl product of transmetalation and reductive elimination (4'-methoxy-2-methyl-1,1'-biphenyl) was also observed in 50 % yield (Figure 4.12).

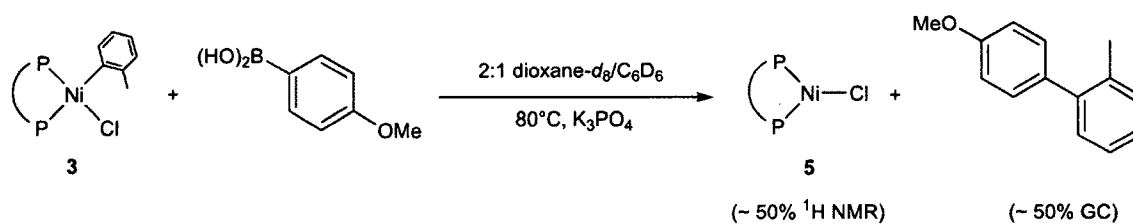


Figure 4.12: Stoichiometric reactivity of **3**.

Presumably, this reaction proceeds by half an equivalent of **3** undergoing transmetallation and reductive elimination to yield Ni(dppf), which then comproportionates with the remaining half equivalent of **3** to give **5** and most likely Ni(dppf)(Ar) (Figure 4.13). Though the latter was not detected in the ^1H NMR spectrum, decomposition was observed, which is expected as Ni(dppf)(Ar) is assumed to be highly unstable. Further support for this hypothesis is the reaction of **3** with **1** in C_6D_6 forming **5** and decomposition products at both ambient temperature and 80°C (Figure 4.14). Additionally, when catalysis is performed using **3** a small peak correlating to 4'-methoxy-2-methyl-1,1'-biphenyl is observed in the GC spectrum, which is consistent with this pathway of activation (transmetallation-reductive elimination).

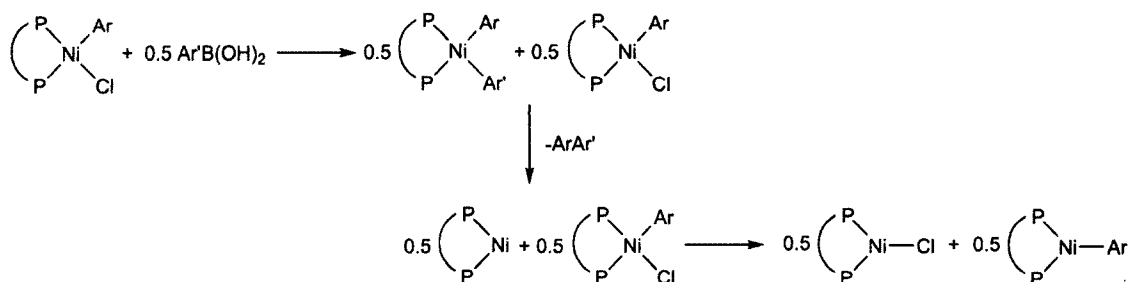


Figure 4.13: Transmetallation-reductive elimination pathway for the formation of **5** and Ni(dppf)(Ar) from **3**.

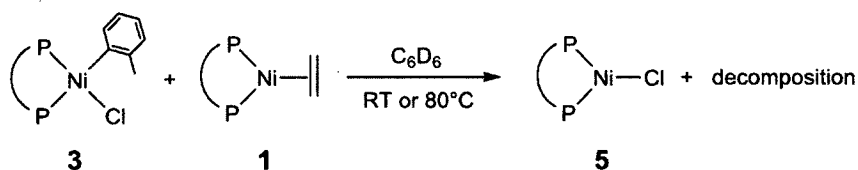


Figure 4.14: Comproportionation of **3** and **1** to form **5**.

The stoichiometric reactivity of **4** was determined to be similar to **3** where reaction was observed with 4-methoxyphenylboronic acid and K_3PO_4 (Figure 4.15). Complex **5** was detected in ~50 % yield by paramagnetic 1H NMR spectroscopy. The detection of the related organic fragment was more complicated; there were numerous species observed in both the GC and the GC-MS spectra, though a peak at $m/z = 224$ could correspond to 1-cinnamyl-4-methoxybenzene (the product of transmetalation and reductive elimination, or an isomer thereof). As with **3**, the reaction of **4** with **1** generated **5** and decomposition.

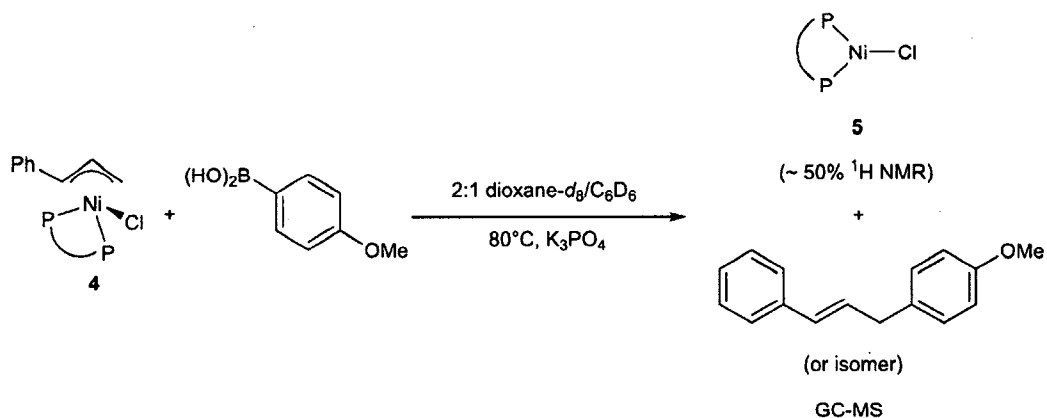
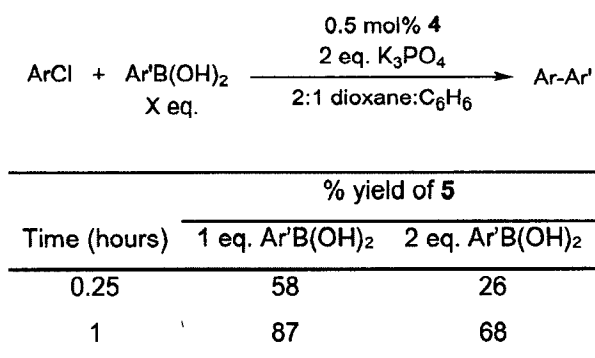


Figure 4.15: Stoichiometric reactivity of **4**

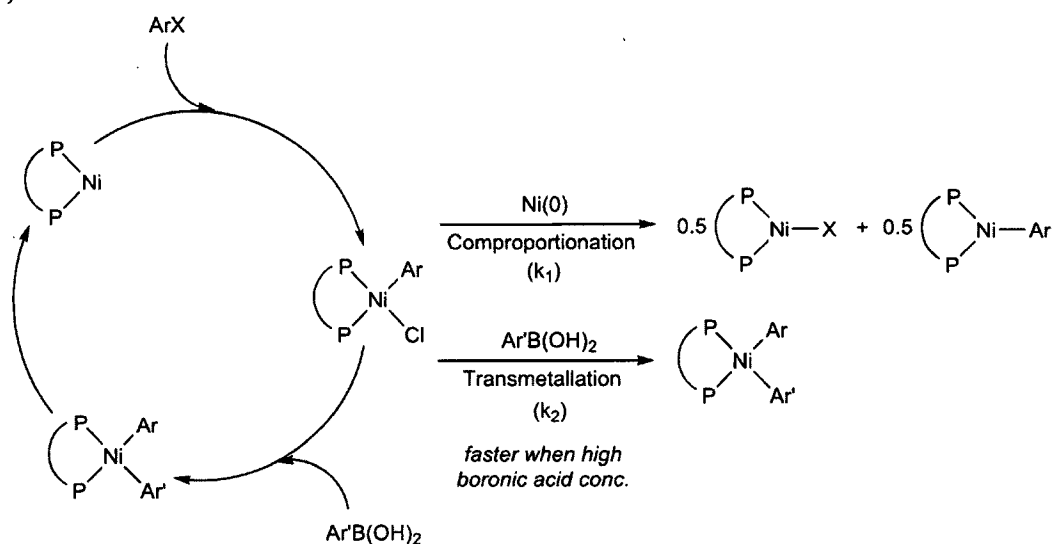
If our proposed pathway for the formation of Ni(I) from **3** and **4** is correct, then the amount of Ni(I) formed in catalysis could be effected by the concentration of the boronic acid. It is plausible that by reducing the effective concentration of boronic acid, the starting material will undergo slower transmetalation and as a result is more likely to comproportionate with Ni(0) that has been formed via transmetalation and reductive elimination ($k_1 > k_2$) (Scheme 4.08,b). When only 1 eq. 4-methoxyphenylboronic acid was used in catalysis with **4**, the amount of Ni(I) produced after 15 minutes was approximately double than when 2 eq. boronic acid was used. (Scheme 4.08, a). The total amount of Ni(I) after the reaction was complete (1 hour) was also elevated in the 1 eq case vs the 2 eq. case. This could have

wider implications in future catalytic design; in systems where Ni(I) complexes are formed and are active, then perhaps the amount of boronic acid used can be reduced without an overall decline in activity. Conversely, in systems where Ni(I) is less active, both increasing the equivalency of boronic acid and ensuring it is fully soluble in the reaction mixture could result in more effective catalysis.

a)



b)



Scheme 4.08: Quantification of Ni(I) with varying boronic acid equivalents.

Surprisingly, no reaction was observed when either 2-chloronaphthalene or 4-methoxyphenylboronic acid and K₃PO were added to a benzene solution of **5** and heated

at 80°C for 2 hours, though having all catalytic components present resulted in the formation of biaryl and regeneration of **5**. It was confirmed by EPR spectroscopy that the yield of Ni(I) was 100%.

Here we have demonstrated that precatalysts **1**, **2**, **3** and **4** all form **5** from reactions with the catalytic components. We next sought to investigate pathways in which **5** could form from Ni(0) and Ni(II). This is highly relevant to any mechanistic proposal concerning bidentate phosphine Ni complexes.

e. Disproportionation/Comproportionation of Ni(0)/Ni(II) and Ni(I)

Since **5** has been determined to be an excellent precatalyst, we investigated if there was a facile pathway from which Ni(I) could form Ni(0) and enter a traditional Ni(0)/Ni(II) catalytic cycle. Initially, we exposed **5** to an atmosphere of CO in a C₆D₆ solution.⁷⁰ An instantaneous color change from orange to green was observed and the formation of Ni(dppf)(CO)₂ and Ni(dppf)(Cl)₂ was confirmed by comparison with literature values⁷³ and an authentic sample, respectively (Figure 4.16).

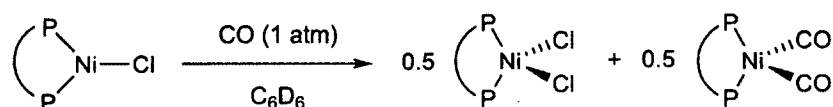


Figure 4.16: Reaction of **5** with CO.

Knowing disproportionation was possible with a very strong ligand, we attempted to reproduce these results with a weaker ligand. The reaction of **5** with 0.5 eq. dppf in C₆D₆ gave no evidence for any diamagnetic Ni(0) or Ni(II) containing species. We instead observe the formation of **6**. (Figure 4.17). This is in stark contrast to reports on Ni(PⁱPr₃)₂(X) (X= Cl, Br, I) by Johnson and co-workers who noted that, upon standing, C₆D₆ solutions of their Ni(I) complexes underwent disproportionation into Ni(PⁱPr₃)₂(X)₂

and a nickel mirror within 24 hours, though solutions of the complexes in pentane were significantly more stable.⁵²

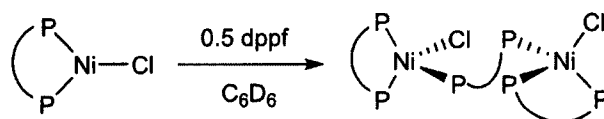
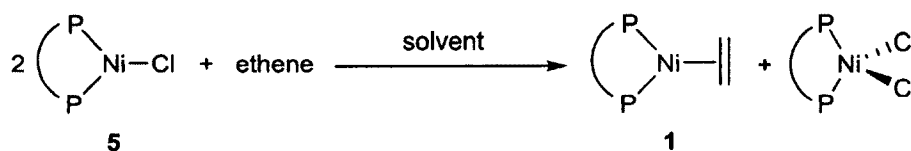


Figure 4.17: Reaction of **5** with 0.5 equivalents of dppf

Given the experimental difficulty in Ni(I) disproportionation, we sought to computationally investigate the problem. DFT calculations were performed on complexes containing both the full dppf ligand and a simplified ligand (dmpf, 1,1'-bis(dimethylphosphinoferrocene). Initially the disproportionation of **5** to form **1** and Ni(dppf)(Cl)₂ was modelled, along with the reduced ligand analogue (Table 4.03) in both diethyl ether (the solvent for the synthesis of **5**) and 1,4-dioxane (the main component of the catalytic solvent mixture).

Table 4.03: Computational results for the disproportionation of **5** with ethene as the L ligand

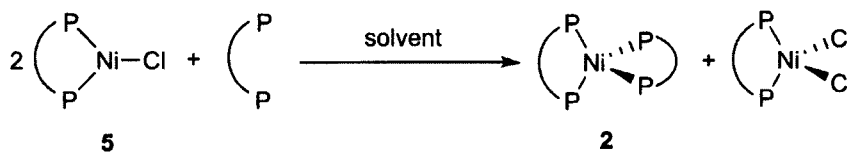


Ligand (solvent)	$\Delta G^{\circ}_{\text{com}}$ (Kcal mol ⁻¹)
dmpf (1,4-dioxane)	1.8
dmpf (diethyl ether)	3.2
dppf (1,4-dioxane)	5.0
dppf (diethyl ether)	5.9

For all 4 scenarios, we found that the disproportionation of Ni(I) was significantly thermodynamically uphill. The unfavorable nature of this reaction was increased by the addition of steric bulk to the ligand. In order to rule out the possibility of significant

computational error due to the components being in different states, we also performed a calculation using the dmpf version of **2** (Table 4.04).

Table 4.04: Computational results for the disproportionation of **5** with dmpf as the L type ligand



Ligand (solvent)	$\Delta G^\circ_{\text{com}}$ (Kcal mol ⁻¹)
dmpf (1,4-dioxane)	3.5
dmpf (diethyl ether)	5.5

Again, the disproportionation is energetically uphill, and this would presumably be more accentuated with the full ligand. This is consistent with experimental observation, where the comproportionation of **2** with Ni(dppf)(Cl)₂ in C₆D₆ was complete in under ten minutes at room temperature (Figure 4.18). Interestingly, the μ -dppf bridging complex is formed, presumably from the reaction with the displaced dppf ligand in **2** and **5**. The thermodynamic stability of Ni(I) formed by comproportionation has been documented previously in other systems.^{31,38,74,75}

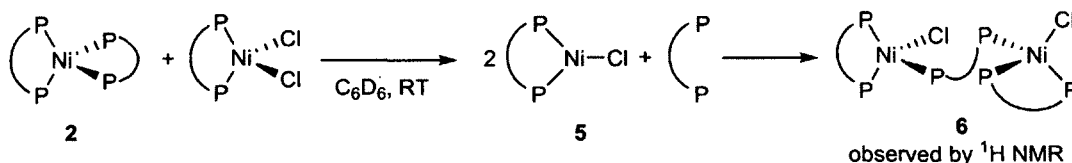


Figure 4.18: Comproportionation of **2** with Ni(dppf)(Cl)₂.

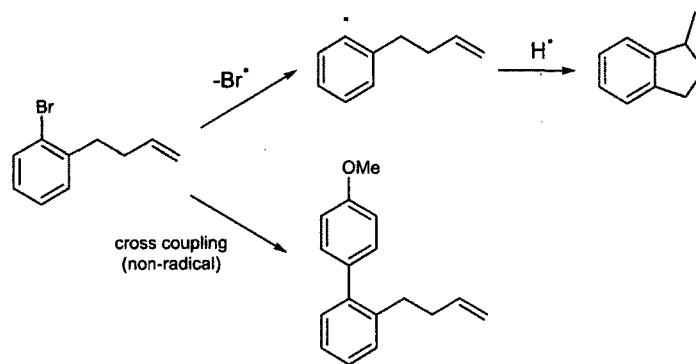
f. Catalytic Implications

Based on our previously described experimental and computational work, it seems unlikely that once **5** forms in the catalytic mixture, there is any accessible pathway for it to be converted to Ni(0) or Ni(II). This, in conjunction with the fact that at 80°C Ni(0) and Ni(II) outcompetes Ni(I) would indicate that two cycles are operative. Presumably **1-4** can

participate in a traditional Ni(0)/Ni(II) cycle, but upon comproportionation can form Ni(I). Support for a Ni(0)/Ni(II) cycle is supplied by the apparent lack of induction period for catalysis using **1-4**, and the absence of correlation between Ni(I) formation and product formation; Ni(I) does not need to form for turnover to occur.

Since Ni(I) cannot form Ni(0) or Ni(II) and **5** is highly active for the Suzuki-Miyaura reaction, there is strong evidence that Ni(I) is active in a cycle independent from Ni(0)/Ni(II). Additional credence is given in catalytic reactions using **5** where 100% Ni is present as **5** at the end of catalysis. The regeneration of **5** suggests that **5** is either directly on a cycle or easily converted to an active species under catalytic conditions. Since Ni(0) or Ni(II) formation has been ruled out, this would likely be an odd electron species. Finally, in reactions using Ni(0) and Ni(II), the fact that at the end of catalysis the majority of Ni is in the form of Ni(I), and that Ni(I) begins to accumulate in fewer than 15 minutes at 80°C without apparent loss of activity, lend support for a Ni(I) containing cycle.

We also wanted to investigate the nature of the catalytic reaction i.e. whether a radical-mediated mechanism was operative. To probe this, catalysis was performed using *o*-(3-butenyl)bromobenzene, which has previously been used to investigate potential radical mechanisms.⁷⁶ The aryl radical that could form has been shown to undergo cyclization and abstract H[•] from solvent to form 1-methylindane on the scale of 5×10^8 s⁻¹.⁷⁷ After conducting catalytic reactions using **1-5** under previously optimized conditions (0.5 mol% Ni, 80°C, 1 hr), we observed no evidence for 1-methylindane⁷⁸ by ¹H NMR spectroscopy or GC-MS which is evidence against a radical mechanism. The cross coupling product (Scheme 4.10), however, was observed.⁷⁹



Scheme 4.09: Possible products of catalysis when a radical clock substrate is used.

III. Conclusions

In conclusion, we have prepared a series of Ni complexes and demonstrated that they are highly active for the Suzuki-Miyaura reaction at low catalyst loadings. Ni(dppf)(Cl) is a rare example of a Ni(I) complex which is active for the Suzuki-Miyaura reaction and this is the first time a Ni(I) precatalyst has shown comparable activity to Ni(0) or Ni(II) precatalysts. Additionally we have shown that Ni(dppf)(Cl) and Ni(dppf)(*o*-tol)(Cl) are highly active at room temperature and moderate catalyst loading, the mildest conditions reported to date for Ni catalyzed Suzuki-Miyaura reactions. Using ^1H NMR and EPR spectroscopy, we have shown that after termination of catalysis, the majority of Ni is in the form of Ni(I) in all cases at 80°C and is a significant component of the metal containing species at 60°C. Early time points in the reactions also show that Ni(I) is unequivocally forming during the catalysis, and not just as a byproduct at the end. Additionally, we have shown that the amount of boronic acid used has a dramatic effect on the amount of Ni(I) formed at early reaction times. Using stoichiometric reactions, it has been plausibly shown how Ni(I) can form from Ni(0) and Ni(II) and it has been demonstrated both experimentally

and computationally that the disproportionation of Ni(I) into Ni(0) and Ni(II) is thermodynamically uphill. Based on these data, we propose that two cycles are operative during catalysis, a Ni(0)/(II) system, and one in which Ni(I) is a component catalyst. As our Ni(I) complex is catalytically active, the formation of Ni(I) is not problematic, but based on our results it seems that in cases where odd electron complexes are not active, then the minimization of comproportionation could drastically improve catalytic performance.

IV. Experimental

a. General Methods

Experiments were performed under a dinitrogen atmosphere in an M-Braun dry box or using standard Schlenk techniques, unless otherwise noted. (Under standard glovebox conditions, purging was not performed between uses of pentane, diethyl ether, benzene, toluene and THF; thus, when any of these solvents were used, traces of all these solvents were in the atmosphere and could be found intermixed in the solvent bottles.) Moisture- and air-sensitive liquids were transferred by stainless steel cannula on a Schlenk line or in a dry box. Solvents were dried by passage through a column of activated alumina followed by storage under dinitrogen. All commercial chemicals were used as received, except where noted. 4-methoxyphenylboronic acid, 2-chloronaphthalene and anhydrous 1,4-dioxane were purchased from Acros Organics. Cobaltocene, naphthalene and sodium were purchased from Sigma Aldrich, as was K_3PO_4 which was ground and stored in an oven prior to use. Dppf was purchased from Strem Chemicals. Deuterated solvents were obtained from Cambridge Isotope Laboratories except dioxane- d_8 , which was purchased

from Santa Cruz Biotechnology. C_6D_6 and toluene- d_8 were dried using sodium metal using benzophenone ketyl radical as an indicator. $CDCl_3$ was dried using CaH_2 . All deuterated solvents were vacuum-transferred prior to use except dioxane- d_8 which was opened in a glovebox and used as received. NMR spectra were recorded on Bruker AMX-400, -500 or Varian-300 spectrometers at ambient probe temperatures unless otherwise stated. Chemical shifts are reported in ppm with respect to residual internal protio solvent for 1H and $^{13}C\{^1H\}$ NMR spectra and to an external standard for $^{19}F\{^1H\}$ spectra ($CFCl_3$ at 0.0 ppm). NMR coupling constants (J) are given in Hz. IR spectra were measured using a diamond Smart Orbit ATR on a Nicolet 6700 FT-IR instrument. Elemental analysis was not performed due to compound instability. Gas chromatography analyses (GC) were performed on a Shimadzu GC-2010 Plus apparatus equipped with a flame ionization detector and a Shimadzu SHRXI-5MS column (30 m, 250 μm inner diameter, film 0.25 μm). The following conditions were utilized for GC analyses: flow rate 1.23 mL/min constant flow, column temperature 50 $^{\circ}C$ (held for 5 min), 20 $^{\circ}C$ /min increase to 300 $^{\circ}C$ (held for 5 min), total time 22.5 min. The response factor used to calculate GC yields was determined using by calibration using the biaryl of interest. Literature procedures were utilized to synthesize $Ni(dppf)(C_2H_4)$,⁴³ $Ni(dppf)_2$,⁴⁵ $Ni(dppf)(o\text{-tol})(Cl)$,⁴⁴ and $Ni(dppf)(Cin)(Cl)$.²⁴ 2,2'-binaphthalene^{80,81} and 2-(4-methoxyphenyl)naphthalene²⁴ were prepared using $Pd(\eta^3\text{-1-BuIndenyl})(IPr)(Cl)$ ²⁶ and compared to literature NMR data.

b. X-ray Crystallography

X-ray diffraction experiments were carried out on either a Rigaku Mercury 275R CCD (SCX mini) diffractometer using graphite-monochromated Mo $K\alpha$ radiation ($\lambda = 0.71073\text{\AA}$) at $-50^{\circ}C$ or a Rigaku MicroMax-007HF diffractometer coupled to a Saturn994+

CCD detector with Cu K α radiation ($\lambda = 1.54178\text{\AA}$) at -180°C . The crystals were mounted on MiTeGen polyimide loops with immersion oil. The data frames were processed using Rigaku CrystalClear and corrected for Lorentz and polarization effects. Using Olex2,⁸² the structure was solved with the XS⁸³ structure solution program using direct methods and refined with the XL⁸³ refinement package using least squares minimisation. The non-hydrogen atoms were refined anisotropically. Hydrogen atoms were refined using the riding model.

c. Computational Details

Density functional calculations were carried out using Gaussian 09 Revision D.01.⁸⁴ Calculations were performed using the BP86 functional. The SDDALL basis set and pseudo potential were used for Ni, Fe and P (augmented with one d polarization function) and the 6-31G++(d,p) basis set was used for all other atoms. Initial geometries were obtained using the coordinates from X-ray structures where available and all optimized structures were verified using frequency calculations. Solvent was modelled using the IEPCM model (benzene, 1,4-dioxane, diethyl ether) as implemented in Gaussian 09. All energies presented are Gibbs Free Energies with solvent corrections.

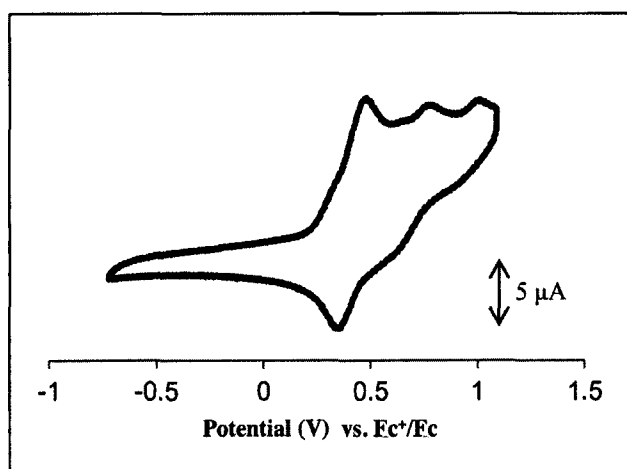
d. Synthesis and Characterization of Compounds

Synthesis of Ni(dppf)(Cl)(5)

20 mL diethyl ether was added to a 100 mL Schlenk flask containing Ni(dppf)(Cl)₂ (298 mg, 0.44 mmol) and Ni(dppf)(C₂H₄) (280 mg, 0.44 mmol). After two hours of stirring at room temperature, a yellow precipitate had formed, which was isolated by filtration at -78°C . The solid was washed with 10 mL pentane and dried under vacuum to yield Ni(dppf)(Cl) (221 mg, 78 %).

^1H NMR (C_6D_6 , 500.0 MHz): δ 12.59 (10 H), 4.58 (8 H), 1.61 (10 H). Magnetic susceptibility (C_6D_6): 2.18 BM. B. UV-Vis λ_{max} (ϵ): 383 nm (3235), 354 nm (4118).

EPR (simulated) (toluene, 4.8K), $g_{\text{para}} = 2.321$, $g_{\text{perp}} = 2.101$, $A(\text{P1}) = [182.56 \ 170.00]$ MHz, $A(\text{P2}) = [222.55 \ 169.81]$ MHz



CV of **5** (1.0 mM) in a 0.10 M $n\text{Bu}_4\text{NPF}_6$ solution of THF under nitrogen at room temperature.

Peak separation = 0.12 V at $E_{1/2} = 0.41$ V vs Fc^+/Fc

Procedure for EPR spectroscopy

Samples for EPR spectroscopy were prepared in a nitrogen filled glovebox by dissolving 3.2 mg $\text{Ni}(\text{dppf})(\text{Cl})$ in 10 mL toluene to give a 0.5 mM solution. 300 μL was pipetted into an EPR tube and the EPR tube was sealed in the glovebox. For spectra from catalysis, 2-chloronaphthalene (32.6 mg 0.2 mmol), 4-methoxyphenylboronic acid (60.8 mg, 0.4 mmol), potassium phosphate (170 mg, 0.8 mmol) and $\text{Ni}(\text{dppf})(\text{C}_2\text{H}_4)$ (**1**) (5.2 mg, 4 mol%) were added to a 1 dram vial in a glovebox. 1,4-dioxane (1.2 mL) and benzene (0.6 mL) were added and the vial tightly capped, removed from the glovebox and heated at 80°C for 30 mins. In a glovebox, 20 μL of the catalytic mixture was removed, evacuated to dryness, dissolved in 200 μL toluene and added to an EPR tube. X-band EPR spectra were acquired on a Bruker ELEXSYS E500 EPR spectrometer equipped with a SHQ resonator and an Oxford ESR-900 helium-flow cryostat. EPR scans were acquired at 4.8 K with the

following instrumental parameters: microwave frequency 9.39 GHz, modulation frequency 100 kHz, modulation amplitude 10 G, and microwave power 0.8 mW.

Procedure for electrochemistry

Electrochemistry voltammetric data were collected using an air tight three-electrode system, which was assembled in a nitrogen filled glovebox. The working electrode was a 2 mm diameter platinum electrode. The reference and counter electrodes were 0.8 mm platinum wires. The electrolyte was 0.10 M ${}^n\text{Bu}_4\text{NPF}_6$ in THF, which was synthesized by the metathesis of Bu_4NBr and HPF_6 , recrystallized from hot ethanol, and dried under vacuum overnight. The THF used in the experiment was HPLC grade and dried before use. Ferrocene was used as internal standard. Cyclic voltammetry data were measured with a Princeton Applied Research VersaSTAT 4 potentiostat.

Representative procedure for catalytic reactions

A 1 dram vial was charged with 2-chloronaphthalene (32.5 mg, 0.2 mmol, 1 eq), 4-methoxyphenylboronic acid (60.8 mg, 0.4 mmol, 2 eq), potassium phosphate (170 mg, 0.8 mmol, 4 eq) and a magnetic stir bar, loosely capped and moved into a glovebox. A 1,4-dioxane solution containing 0.590 M naphthalene (340 μL) and benzene solution containing 0.006 M precatalyst (160 μL) were both added using gas-tight syringes and the vials tightly capped. Upon removal from the glovebox, the vials were heated at the appropriate temperature using an aluminium heating block and thermocouple. Reactions were quenched by exposure to air. ~ 100 μL solution was added to a ~ 1 cm silica plug eluted with ethyl acetate. Yields were determined by gas chromatography, using naphthalene as the internal standard. All reactions were duplicated and yields reported are an average of

at least two runs. All precatalyst stock solutions were frozen after use and re-used, except the Ni(dppf)(*o*-tol)(Cl) stock solution which was freshly prepared before use.

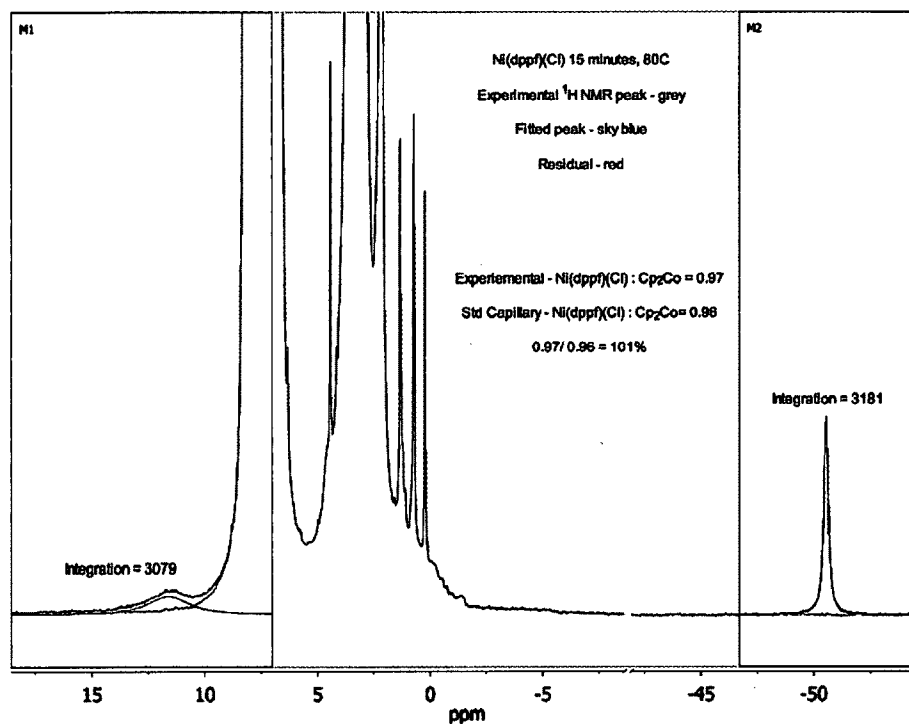
Procedure for the determination of the K value for Ni(dppf)(C₂H₄) + dppf

Dppf (2.6 mg, 0.005 mmol) was weighed out and moved into a glovebox in a loosely capped J. Young tube. The tube was cooled in a liquid nitrogen cooled cold well and Ni(dppf)(C₂H₄) (1) (3 mg, 0.005) in 500 μ L C₆D₆ added and the tube quickly capped. An NMR spectrum was recorded after 30 mins and the relative integrations of the cyclopentadienyl peaks of the dppf ligand in each complex compared. The relative integrations of dppf, Ni(dppf)(C₂H₄) and Ni(dppf)₂ did not change after 16 hours at room temperature.

Representative procedure for Ni(I) quantification

A 1 dram vial was charged with 2-chloronaphthalene (97.5 mg, 0.6 mmol, 1 eq), 4-methoxyphenylboronic acid (182.4 mg, 1.2 mmol, 2 eq), potassium phosphate (509 mg, 2.4 mmol, 4 eq) and a magnetic stir bar in a nitrogen filled glove box. 1020 μ L 1,4-dioxane and a benzene solution containing 0.006M were added, the vial sealed, removed from the glove box and heated at either 60°C or 80°C for the required time. The vial was cooled to room temperature and 750 μ L removed in a glove box. The solvent was removed under reduced pressure, dissolved in 500 μ L C₆D₆, a calibrated Cp₂Co capillary added and an NMR spectrum recorded using the following parameters: nt = 256, d1 = 0.5, at = 1.0 and setsw(-75,75). The spectra were analysed using MestReNova. Apodization-exponential was set to 10 Hz, backfilling LP set to 5 and a Bernstein Polynomial of 3 was applied for a baseline correction. The line fitting tool was used to simulate the product peak, and the

area was compared to that of the external standard (Cp_2Co) to obtain a percentage yield. A representative example of an integrated spectrum is shown below.



Procedure for tracking catalysis using ^{31}P NMR spectroscopy

2-chloronaphthalene (16.3 mg 0.1 mmol), 4-methoxyphenylboronic acid (30.4 mg, 0.2 mmol) and $\text{Ni}(\text{dppf})(\text{C}_2\text{H}_4)$ (2.9 mg, 4 mol%) were added to a 1 dram vial and 300 μL C_6D_6 and 600 μL 1,4-dioxane added. Upon complete dissolution the mixture was transferred to a J. Young tube containing potassium phosphate (85 mg, 0.4 mmol) and a capillary containing a C_6D_6 solution of PPh_3 . ^{31}P spectra were taken at room temperature and after 90 mins at 80°C .

Representative procedure for stoichiometric reactivity of Ni with a boronic acid

A stock solution of 4-methoxyphenylboronic acid was prepared by dissolving 7.6 mg in 1 mL THF. 100 μL (0.76 mg, 0.005 mmol) of this solution was transferred to a vial using a gas-tight syringe and the solvent removed under vacuum. $\text{Ni}(\text{dppf})(o\text{-tol})(\text{Cl})$ (3.7 mg,

0.005 mmol) was added to the vial, with 1,4-dioxane- d_8 (340 μL) and C_6D_6 (160 μL). Upon complete dissolution, the mixture was transferred to a J. Young tube containing potassium phosphate (2.1 mg, 0.01 mmol) and a standardized capillary containing a C_6D_6 solution of Cp_2Co . The tube was heated for 2 hours at 80°C and an NMR spectrum recorded using the following parameters: $nt = 256$, $d1 = 0.5$, $at = 1.0$ and $setsw(-75,75)$. Tubes were then heated for one further hour at 80°C to confirm no change in relative integrations. 1 equivalent naphthalene was then added using a 1,4-dioxane stock solution and the organic component was quantified using Gas Chromatography, with naphthalene as the internal standard.

Representative procedure for stoichiometric reactivity of Ni with an aryl halide

A stock solution of 2-cholonaphthalene was prepared by dissolving 4.8 mg in 1 mL C_6D_6 . 160 μL (0.76 mg, 0.005 mmol) of this solution was transferred to a vial containing $\text{Ni}(\text{dppf})(\text{C}_2\text{H}_4)$ (3.0 mg, 0.005 mmol) and 1,4-dioxane- d_8 (340 μL). Upon complete dissolution, the mixture was transferred to a J. Young tube containing a standardised capillary with a C_6D_6 solution of Cp_2Co . The tube was heated for 2 hours at 80°C and an NMR spectrum recorded using the following parameters: $nt = 256$, $d1 = 0.5$, $at = 1.0$ and $setsw(-75,75)$. Tubes were then heated for one further hour at 80°C to confirm no change in relative integrations. 1 equivalent naphthalene was then added using a 1,4-dioxane stock solution and the organic component was quantified using Gas Chromatography, with naphthalene as the internal standard.

Representative procedure for comproportionation reactions

$\text{Ni}(\text{dppf})(\text{C}_2\text{H}_4)$ (4 mg, 0.006 mmol) and $\text{Ni}(\text{dppf})(\text{otol})(\text{Cl})$ (4.6 mg, 0.006 mmol) were combined in a J. Young NMR tube with 500 μL C_6D_6 . The tube was either left at room

temperature or heated to 80°C until complete consumption of starting materials was observed by ^1H NMR spectroscopy.

Reaction of 5 with CO

A J.Young NMR tube was charged with **5** (5 mg, 0.008 mmol) in 500 μL C_6D_6 . The solution was degassed using three freeze-pump-thaw cycles and one atmosphere of CO introduced at room temperature using a dual manifold Schlenk line. A color change from yellow to green was observed immediately, along with the formation of a green precipitate. The solution was decanted and the precipitate redissolved in CDCl_3 . $\text{Ni}(\text{dppf})(\text{CO})_2$ (agreement with literature shifts ^1H NMR shifts)⁷³ and $\text{Ni}(\text{dppf})(\text{Cl})_2$ (green precipitate, comparison with an authentic sample) were confirmed as the products of the reaction, consistent with disproportionation of Ni(I) to Ni(0) and Ni(II).

Table 4.05: Crystallographic data for **1**, **5** and **6**.

	1	5	6
Empirical formula	C ₄₀ H ₄₂ FeNiOP ₂	C ₃₉ H ₄₀ ClFeNiP ₂	C ₁₁₀ H ₁₀₀ Cl ₂ Fe ₃ Ni ₂ O ₂ P ₆
Formula weight	715.23	720.66	1995.58
Temperature/K	223	93	93
Crystal system	monoclinic	triclinic	triclinic
Space group	P2 ₁ /n	P-1	P-1
a/Å	11.939(2)	9.5571(2)	13.0161(2)
b/Å	24.366(5)	13.8286(3)	13.9427(2)
c/Å	12.474(2)	14.7995(10)	15.9710(11)
α°	90	114.600(8)	69.136(5)
β°	103.822(7)	92.957(7)	72.012(5)
γ°	90	97.094(7)	88.744(6)
Volume/Å ³	3523.7(11)	1753.24(17)	2563.3(2)
Z	4	2	1
ρ _{calc} /mg/mm ³	1.348	1.365	1.293
m/mm ⁻¹	1.067	5.737	5.456
F(000)	1496.0	750.0	1034.0
Crystal size/mm ³	0.2 × 0.05 × 0.01	0.05 × 0.01 × 0.01	0.05 × 0.05 × 0.05
2θ range for data collection	6.04 to 49.428°	6.612 to 122.326°	6.256 to 136.476
Index ranges	-14 ≤ h ≤ 14, -28 ≤ k ≤ 28, -14 ≤ l ≤ 14	-10 ≤ h ≤ 10, -15 ≤ k ≤ 15, -15 ≤ l ≤ 16	-15 ≤ h ≤ 15, -14 ≤ k ≤ 15, - 19 ≤ l ≤ 19
Reflections collected	32876	59044	76263
Independent reflections	5995 [R _{int} = 0.0985, R _{sigma} = 0.0679]	5347 [R _{int} = 0.2155, R _{sigma} = 0.1118]	9195 [R _{int} = 0.0894, R _{sigma} = 0.0494]
Data/restraints/parameters	5995/4/424	5347/31/397	9195/0/565
Goodness-of-fit on F ²	1.114	1.100	1.169
Final R indexes [I ≥ 2σ (I)]	R ₁ = 0.0658, wR ₂ = 0.0898	R ₁ = 0.0829, wR ₂ = 0.2267	R ₁ = 0.0602, wR ₂ = 0.1615
Final R indexes [all data]	R ₁ = 0.1006, wR ₂ = 0.0977	R ₁ = 0.1186, wR ₂ = 0.2549	R ₁ = 0.0683, wR ₂ = 0.1719
Largest diff. peak/hole / e Å ⁻³	0.51/-0.32	1.07/-0.81	0.65/-1.04

e. Acknowledgements

I very grateful for the help of the Brudvig Group in completing this work. Both Gary and David Vinyard have been very helpful in both the running and interpretation of EPR experiments and it was a pleasure working with Alec Durrell to obtain a CV of Ni(dppf)(Cl).

V. References

- (1) Hartwig, J. F. *Acc. Chem. Res.* **2008**, *41*, 1534.
- (2) Marion, N.; Nolan, S. P. *Acc. Chem. Res.* **2008**, *41*, 1440.
- (3) Martin, R.; Buchwald, S. L. *Acc. Chem. Res.* **2008**, *41*, 1461.
- (4) Wurtz, S.; Glorius, F. *Acc. Chem. Res.* **2008**, *41*, 1523.
- (5) Li, H. B.; Seechurn, C. C. C. J.; Colacot, T. J. *ACS Catal.* **2012**, *2*, 1147.
- (6) Christmann, U.; Vilar, R. *Angew. Chem. Int. Ed.* **2005**, *44*, 366.
- (7) Hruszkewycz, D. P.; Balcells, D.; Guard, L. M.; Hazari, N.; Tilset, M. *J. Am. Chem. Soc.* **2014**, *136*, 7300.
- (8) Barrios-Landeros, F.; Hartwig, J. F. *J. Am. Chem. Soc.* **2005**, *127*, 6944.
- (9) Carrow, B. P.; Hartwig, J. F. *J. Am. Chem. Soc.* **2011**, *133*, 2116.
- (10) Amatore, C.; Jutand, A.; Le Duc, G. *Chem. Eur. J.* **2011**, *17*, 2492.
- (11) Han, F. S. *Chem. Soc. Rev.* **2013**, *42*, 5270.
- (12) Percec, V.; Bae, J. Y.; Zhao, M. Y.; Hill, D. H. *J. Org. Chem.* **1995**, *60*, 176.
- (13) Percec, V.; Bae, J. Y.; Hill, D. H. *J. Org. Chem.* **1995**, *60*, 1060.
- (14) Saito, S.; Sakai, M.; Miyaura, N. *Tetrahedron Lett.* **1996**, *37*, 2993.
- (15) Tasker, S. Z.; Standley, E. A.; Jamison, T. F. *Nature* **2014**, 509.
- (16) Indolese, A. F. *Tetrahedron Lett.* **1997**, *38*, 3513.
- (17) Tang, Z. Y.; Hu, Q. S. *J. Org. Chem.* **2006**, *71*, 2167.
- (18) Fan, X. H.; Yang, L. M. *Eur. J. Org. Chem.* **2011**, 1467.
- (19) Percec, V.; Golding, G. M.; Smidrkal, J.; Weichold, O. *J. Org. Chem.* **2004**, *69*, 3447.
- (20) Chen, C.; Yang, L. M. *Tetrahedron Lett.* **2007**, *48*, 2427.
- (21) Griffiths, C.; Leadbeater, N. E. *Tetrahedron Lett.* **2000**, *41*, 2487.
- (22) Moldoveanu, C.; Wilson, D. A.; Wilson, C. J.; Corcoran, P.; Rosen, B. M.; Percec, V. *Org. Lett.* **2009**, *11*, 4974.
- (23) Zhao, Y. L.; Li, Y.; Li, S. M.; Zhou, Y. G.; Sun, F. Y.; Gao, L. X.; Han, F. S. *Adv. Synth. Catal.* **2011**, *353*, 1543.
- (24) Ge, S. Z.; Hartwig, J. F. *Angew. Chem. Int. Ed.* **2012**, *51*, 12837.
- (25) Hruszkewycz, D. P.; Guard, L. M.; Balcells, D.; Feldman, N.; Hazari, N.; Tilset, M. *Organometallics* **2015**, *34*, 381.
- (26) Melvin, P. R.; Nova, A.; Balcells, D.; Dai, W.; Hazari, N.; Hruszkewycz, D. P.; Shah, H. P.; Tudge, M. T. *In Preparation*.
- (27) Meinhard, D.; Reuter, P.; Rieger, B. *Organometallics* **2007**, *26*, 751.
- (28) Wang, H. Y.; Meng, X.; Jin, G. X. *Dalton Trans.* **2006**, 2579.
- (29) Kraikivskii, P. B.; Saraev, V. V.; Bocharova, V. V.; Matveev, D. A.; Petrovskii, S. K.; Gotsko, M. D. *Catal. Commun.* **2011**, *12*, 634.

- (30) Saraev, V. V.; Kraikivskii, P. B.; Vilms, A. I.; Zelinskii, S. N.; Yunda, A. Y.; Danilovtseva, E. N.; Kuzakov, A. S. *Kinet. Catal.* **2007**, *48*, 778.
- (31) Saraev, V. V.; Kraikivskii, P. B.; Bocharova, V. V.; Matveev, D. A. *Kinet. Catal.* **2012**, *53*, 486.
- (32) Saraev, V. V.; Kraikivskii, P. B.; Matveev, D. A.; Bocharova, V. V.; Petrovskii, S. K.; Zelinskii, S. N.; Vilms, A. I.; Klein, H. F. *J. Mol. Catal. A: Chem.* **2010**, *315*, 231.
- (33) Otman, Y. Y.; Manulik, O. S.; Flid, V. R. *Kinet. Catal.* **2008**, *49*, 479.
- (34) Nagao, S.; Matsumoto, T.; Koga, Y.; Matsubara, K. *Chem. Lett.* **2011**, *40*, 1036.
- (35) Page, M. J.; Lu, W. Y.; Poulten, R. C.; Carter, E.; Algarra, A. G.; Kariuki, B. M.; Macgregor, S. A.; Mahon, M. F.; Cavell, K. J.; Murphy, D. M.; Whittlesey, M. K. *Chem. Eur. J.* **2013**, *19*, 2158.
- (36) Marlier, E. E.; Tereniak, S. J.; Ding, K. Y.; Mulliken, J. E.; Lu, C. C. *Inorg. Chem.* **2011**, *50*, 9290.
- (37) Miyazaki, S.; Koga, Y.; Matsumoto, T.; Matsubara, K. *Chem. Commun.* **2010**, *46*, 1932.
- (38) Zhing, K. N.; Conda-Sheridan, M.; Cooke, S. R.; Louie, J. *Organometallics* **2011**, *30*, 2546.
- (39) Anderson, T. J.; Jones, G. D.; Vicic, D. A. *J. Am. Chem. Soc.* **2004**, *126*, 8100.
- (40) Wu, J. G.; Nova, A.; Balcells, D.; Brudvig, G. W.; Dai, W.; Guard, L. M.; Hazari, N.; Lin, P. H.; Pokhrel, R.; Takase, M. K. *Chem. Eur. J.* **2014**, *20*, 5327.
- (41) Jones, G. D.; McFarland, C.; Anderson, T. J.; Vicic, D. A. *Chem. Commun.* **2005**, 4211.
- (42) Jones, G. D.; Martin, J. L.; McFarland, C.; Allen, O. R.; Hall, R. E.; Haley, A. D.; Brandon, R. J.; Konovalova, T.; Desrochers, P. J.; Pulay, P.; Vicic, D. A. *J. Am. Chem. Soc.* **2006**, *128*, 13175.
- (43) Jin, D.; Schmeier, T. J.; Williard, P. G.; Hazari, N.; Bernskoetter, W. H. *Organometallics* **2013**, *32*, 2152.
- (44) Standley, E. A.; Smith, S. J.; Muller, P.; Jamison, T. F. *Organometallics* **2014**, *33*, 2012.
- (45) Pilloni, G.; Toffoletti, A.; Bandoli, G.; Longato, B. *Inorg. Chem.* **2006**, *45*, 10321.
- (46) Langer, J.; Fischer, R.; Gorls, H.; Walther, D. *Eur. J. Inorg. Chem.* **2007**, 2257.
- (47) Park, N. H.; Teverovskiy, G.; Buchwald, S. L. *Org. Lett.* **2014**, *16*, 220.
- (48) Casey, C. P.; Whiteker, G. T. *Isr. J. Chem.* **1990**, *30*, 299.
- (49) Birkholz, M. N.; Freixa, Z.; van Leeuwen, P. W. N. M. *Chem. Soc. Rev.* **2009**, *38*, 1099.
- (50) Karunatilaka, C.; Tackett, B. S.; Washington, J.; Kukolich, S. G. *J. Am. Chem. Soc.* **2007**, *129*, 10522.
- (51) Dreissig, W.; Dietrich, H. *Acta Crystallogr. Sect. B: Struct. Sci.* **1981**, *37*, 931.
- (52) Beck, R.; Shoshani, M.; Krasinkiewicz, J.; Hatnean, J. A.; Johnson, S. A. *Dalton Trans.* **2013**, *42*, 1461.
- (53) Scherer, W.; Eickerling, G.; Shorokhov, D.; Gullo, E.; McGrady, G. S.; Sirsch, P. *New J. Chem.* **2006**, *30*, 309.
- (54) Farrugia, L. J. *J. Appl. Crystallogr.* **1997**, *30*, 565.
- (55) Langer, J.; Fischer, R.; Gorls, H.; Theyssen, N.; Walther, D. *Z. Anorg. Allg. Chem.* **2007**, *633*, 557.
- (56) Norman, N. C.; Orpen, A. G.; Quayle, M. J.; Whittell, G. R. *Acta Crystallogr. Sect. C: Cryst. Struct. Commun.* **2002**, *58*, m160.
- (57) Guard, L. M.; Hazari, N. *Unpublished Results*.
- (58) Ge, S. Z.; Green, R. A.; Hartwig, J. F. *J. Am. Chem. Soc.* **2014**, *136*, 1617.
- (59) Dible, B. R.; Sigman, M. S.; Arif, A. M. *Inorg. Chem.* **2005**, *44*, 3774.
- (60) Evans, D. F. *J. Chem. Soc.* **1957**, 2003.
- (61) Bain, G. A.; Berry, J. F. *J. Chem. Educ.* **2008**, *85*, 532.
- (62) Aresta, M.; Nobile, C. F.; Sacco, A. *Inorg. Chim. Acta* **1975**, *12*, 167.
- (63) Mindiola, D. J.; Waterman, R.; Jenkins, D. M.; Hillhouse, G. L. *Inorg. Chim. Acta* **2003**, *345*, 299.

- (64) Lipschutz, M. I.; Tilley, T. D. *Organometallics* **2014**, *33*, 5566.
- (65) Guan, B. T.; Wang, Y.; Li, B. J.; Yu, D. G.; Shi, Z. J. *J. Am. Chem. Soc.* **2008**, *130*, 14468.
- (66) Breitenfeld, J.; Wodrich, M. D.; Hu, X. L. *Organometallics* **2014**, *33*, 5708.
- (67) Breitenfeld, J.; Ruiz, J.; Wodrich, M. D.; Hu, X. L. *J. Am. Chem. Soc.* **2013**, *135*, 12004.
- (68) Elson, I. H.; Morrell, D. G.; Kochi, J. K. *J. Organomet. Chem.* **1975**, *84*, C7.
- (69) Fahey, D. R.; Mahan, J. E. *J. Am. Chem. Soc.* **1976**, *98*, 4499.
- (70) Tsou, T. T.; Kochi, J. K. *J. Am. Chem. Soc.* **1979**, *101*, 6319.
- (71) Kochi, J. K. *Pure Appl. Chem.* **1980**, *52*, 571.
- (72) Fahey, D. R. *J. Am. Chem. Soc.* **1970**, *92*, 402.
- (73) Hamann, B. C.; Hartwig, J. F. *J. Am. Chem. Soc.* **1998**, *120*, 3694.
- (74) Heimbach, P. *Angew. Chem. Int. Ed.* **1964**, *3*, 648.
- (75) Kraikivskii, P. B.; Frey, M.; Bennour, H. A.; Gembus, A.; Hauptmann, R.; Svoboda, I.; Fuess, H.; Saraev, V. V.; Klein, H. F. *J. Organomet. Chem.* **2009**, *694*, 1869.
- (76) Bose, S. K.; Marder, T. B. *Org. Lett.* **2014**, *16*, 4562.
- (77) Abeywickrema, A. N.; Beckwith, A. L. *J. Chem. Soc., Chem. Commun.* **1986**, 464.
- (78) Parham, W. E.; Bradsher, C. K.; Reames, D. C. *J. Org. Chem.* **1981**, *46*, 4804.
- (79) Manolikakes, G.; Knochel, P. *Angew. Chem. Int. Ed.* **2009**, *48*, 205.
- (80) Cheng, G. J.; Luo, M. M. *Eur. J. Org. Chem.* **2011**, 2519.
- (81) Kirai, N.; Yamamoto, Y. *Eur. J. Org. Chem.* **2009**, 1864.
- (82) Dolomanov, O. V.; Bourhis, L. J.; Gildea, R. J.; Howard, J. A. K.; Puschmann, H. *J. Appl. Crystallogr.* **2009**, *42*, 339.
- (83) Sheldrick, G. M. *Acta Crystallogr. Sect. A: Found. Crystallogr.* **2008**, *A64*, 112.
- (84) Gaussian 09, Revision D.01, Frisch, M. J.; Trucks, G. W.; Schlegel, H. B.; Scuseria, G. E.; Robb, M. A.; Cheeseman, J. R.; Scalmani, G.; Barone, V.; Mennucci, B.; Petersson, G. A.; Nakatsuji, H.; Caricato, M.; Li, X.; Hratchian, H. P.; Izmaylov, A. F.; Bloino, J.; Zheng, G.; Sonnenberg, J. L.; Hada, M.; Ehara, M.; Toyota, K.; Fukuda, R.; Hasegawa, J.; Ishida, M.; Nakajima, T.; Honda, Y.; Kitao, O.; Nakai, H.; Vreven, T.; Montgomery, J. A., Jr.; Peralta, J. E.; Ogliaro, F.; Bearpark, M.; Heyd, J. J.; Brothers, E.; Kudin, K. N.; Staroverov, V. N.; Kobayashi, R.; Normand, J.; Raghavachari, K.; Rendell, A.; Burant, J. C.; Iyengar, S. S.; Tomasi, J.; Cossi, M.; Rega, N.; Millam, M. J.; Klene, M.; Knox, J. E.; Cross, J. B.; Bakken, V.; Adamo, C.; Jaramillo, J.; Gomperts, R.; Stratmann, R. E.; Yazyev, O.; Austin, A. J.; Cammi, R.; Pomelli, C.; Ochterski, J. W.; Martin, R. L.; Morokuma, K.; Zakrzewski, V. G.; Voth, G. A.; Salvador, P.; Dannenberg, J. J.; Dapprich, S.; Daniels, A. D.; Farkas, Ö.; Foresman, J. B.; Ortiz, J. V.; Cioslowski, J.; Fox, D. J. Gaussian, Inc., Wallingford CT, 2009.